B R O A D B A N D, L O W - N O I S E

A N D P O W E R M I C R O W A V E A M P L I F I E R S.

ANDREW D. HALL.

A dissertation submitted to the Faculty of Engineering, University of Cape Town, in fulfilment of the requirements for the degree of Master of Science in Electrical and Electronic Engineering.

CAPE TOWN, 1986.

DECLARATION

I declare that this dissertation is my own unaided work. It is being submitted for the degree of Master of Science in Engineering, at the University of Cape Town. It has not been submitted before for any degree or examination at any other university.

Signed by candidate

ABSTRACT

The design of Broadband, Low-Noise and Power Microwave Amplifiers using microstrip softboard technology is investigated.

The software program TOUCHSTONE(TM) by EEsof is used extensively as a basic design tool.

The characterisation of the GaAs Field Effect Transistors, used for the amplifiers, is carried out. These characterisations are then used by the program in its circuit analysis. A determination of the validity of using the manufacturers data, for the designs, is determined by comparing it to the measured data.

Source-Pull and Load-Pull measurements were performed for the Power GaAs FET characterisation. The noise-parameter device characterisation is carried out in a similar way to that for Load-Pull data.

Each amplifier required final tuning adjustments in order to peak the performances.

The Broadband Maximum Gain Amplifier had a 10 ± 1.5dB gain over a bandwidth from 2- to 6-GHz.

The Low-Noise amplifier achieved 5dB Noise-Figure and 5.4 ± 1.4dB gain over the 2- to 6-GHz band.

The Power amplifier Output Power was 390mW over the 3.7- to 4.2-GHz band.

Techniques of broadband matching are investigated, with Double-Stub matching producing the widest bandwidth.

A literature survey is presented on aspects of broadband microwave amplifiers, as well as a survey on Computer-aided-design at microwave frequencies and techniques of Large-Signal Transistor characterisation.

ACKNOWLEDGEMENTS

The Author wishes to express his gratitude to his supervisor Prof. B.J. Downing for his guidance and support as well as the following co-students in the Microwave Laboratory :- D. Hirson, N.C. Martin, D.M. Rachman and T. Waardenburg.

Lastly, thanks are due to the Council for Scientific and Industrial Research for their financial support and assistance, without which this dissertation would have been impossible.

CONTENTS Page

LIST OF FIGURES

LIST OF FIGURES (continued):-

LIST OF FIGURES (continued):-

LIST OF TABLES

CHAPTER 1. INTRODUCTION.

1.1 CLASSES OF AMPLIFIER OPERATION

Amplifiers can be classified into three basic modes of operation based on the voltage and current conditions existing at the amplifier ports. These classes of operation are: Class-A, Class-B and Class-C as shown in Figure 1.2.1, where the input signal is assumed to be sinusoidal.

If the output current flows for 360° of the input voltage cycle, the amplifier is operated in Class-A mode. If the output current flows for 180° of the input voltage cycle, the amplifier is designated a Class-B amplifier and is biased at cut-off. If the output current flows for less than 180° of the input voltage cycle, the amplifier is called a Class-C amplifier and is biased beyond cut-off. Transistor operation in this mode is highly non-linear. However a Class-C amplifier offers the highest efficiency in terms of d.c. power input versus RF power output. For this reason, Class-C amplifiers are often used in transmitting systems where efficiency is an important consideration [1].

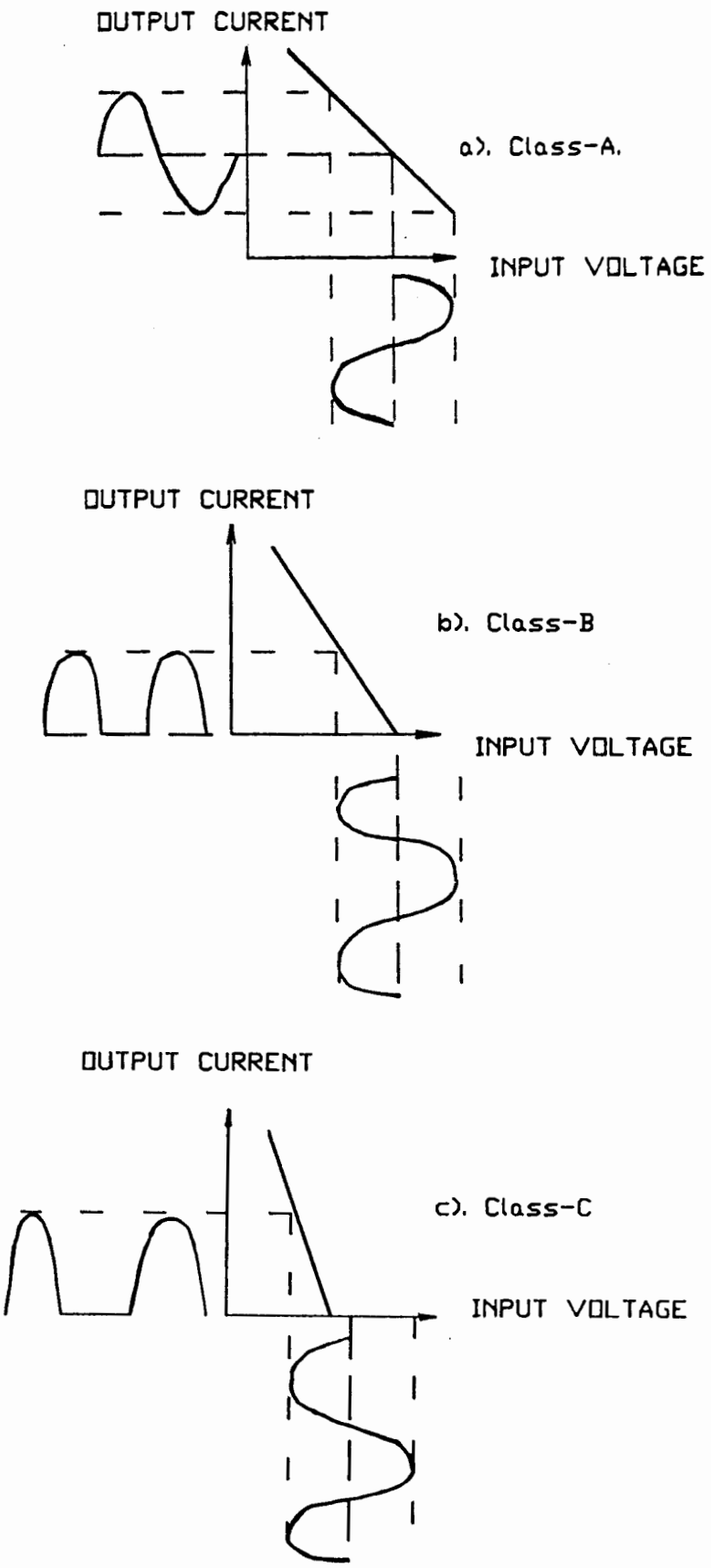

FIGURE 1.2.1: Classes of Amplifier Operation.
a). Class-A b). Class-B c). Class-C.

A drawback is that GaAs FET's cannot be used in Class-C mode, since to bias the fet beyond cut-off requires an increasingly negative voltage on the gate. This will then produce a drain-to-gate voltage which may well be beyond the device limitations and electrical breakdown will occur at the junction. If the bias does not blow the device, it will most certainly blow on the negative voltage swing of the RF input voltage cycle.

The basic limitation of the power FET is that to increase the frequency of operation, the gate-to-drain gap must be minimised and thus, lowers the associated breakdown voltage [2], consequently limiting the maximum output power. To operate transistor amplifiers in the middle- to upper-microwave frequencies requires the use of GaAs FET's, as silicon transistors are limited to the lower microwave region, although they do have higher power handling capabilities due to their favourable structure.

Thus, when the use of GaAs transistor technology is necessary, power amplifiers using field effect transistors are normally operated in a mode called Class-AB. The bias point is set between Class-A and -B with the output current flowing between 180° and 360° of the input voltage cycle. Hence performance is intermediate to the two bounding classes, resulting in more power than in Class-A, and less distortion than in Class-B.

1.2 INTRODUCTION

In the field of microwave engineering, amplifiers are an integral part of microwave systems, as they are the only components which

increase the signal energy to a level which is suitable for further efficient processing. It must be noted, however, that only the design of GaAs FET amplifiers will be considered in this dissertation. The reasons for using GaAs FET's are that for efficient operation bipolar transistors are limited to operation below 6-GHz and GaAs FET's often give superior performance for frequencies as low as 4GHz or even 2GHz. Other amplifier alternatives are ruled out due to the high cost of development (refer to Chapter 2 for a review on microwave amplifiers) and lastly, the amplifiers are developed using a microstrip softboard as this is a relatively inexpensive substrate and allows for mass-production due to the accurate circuit reproduction possible with the etching process. RT DUROID 5880 (E_r = 2.2) will be used, due to its ease of use and higher heat tolerance when soldering, compared to other substrate materials.

There are two fundamental types of microwave amplifiers. They are: low-noise and power amplifiers. However, in practice, there does exist another type of amplifier, commonly called a maximum gain amplifier.

The maximum-gain and low-noise amplifiers are both small-signal, low-power amplifiers and are often used in receiving systems where the signal-level is low enough for distortion to be negligible and efficiency not to be a major concern. Both these amplifiers are therefore operated in Class-A mode.

Maximum-gain amplifiers, as the name suggests, are designed for optimum gain only, using the device small-signal s-parameters,

and thus could utilise either types of GaAs microwave FET, namely low-noise and power transistor's, as the active devices.

This type of amplifier is used in both transmitting and receiving systems, where gain of a signal is required. Examples of this are: Firstly, the preceeding stages of a power amplifier required to drive the actual power amplification stage into saturation and secondly, the stages of amplification after the low-noise amplifier stage in a receiver front-end.

For the Low-Noise amplifier post-amplification stages, the maximum gain amplifiers must utilise low-noise transistors for the active devices so as to minimise the second stage noise-figure in such an amplifier.

This is invariably due to the fact that the low-noise amplifier must drive a mixer with a considerable noise-figure. Therefore, the low-noise amplifier has numerous stages of amplification, the first of which is always designed for low-noise and the rest for maximum gain.

Normally, the low-noise amplifier source impedance gives a poor return loss and would thus cause most of the received signal to be re-transmitted out of the receiving antenna. Thus, some means of isolation is required on the amplifier input. This is normally achieved by using two amplifiers in parallel using two quadrature couplers to split the incoming signal and to present the source (antenna) with a satisfactory return loss or VSWR.

Low-noise amplifiers are used in the extreme case of small-signal amplification where the signal is buried in noise (i.e. the signal power is of the same order of magnitude as that of the atmospheric noise) and thus would be used as the front-end of

microwave receiving systems. ("low-noise" indicates that the amplifiers contribution to the noise-power in the signal is minimised.)

In contrast to receiving systems, transmitting systems require the amplification of high-level signals to furnish considerable signal power to the load such as an antenna. The amplifiers used for these purposes are called Power or Large-signal amplifiers, and since they operate at high drain current levels, their efficiency is of major importance and are thus operated in Class-AB mode (for FETs).

As can be seen from the foregoing discussion, low-noise and power amplifiers perform very different functions in microwave systems but the development procedures are very similar.

The development of low-noise amplifiers involves the optimising of the source-admittance to achieve a minimum in the amplifier noise-figure, whereas power amplifier designs involve the optimisation of the load- admittance for maximum power output and maximum efficiency.

It must be noted that power amplifiers and power pre-amplifiers are operated single-ended and thus require reasonable port return losses or VSWR's to minimise the reflected power at the ports.

Microwave amplifier development, especially broadband amplifiers, is a time-consuming and difficult task due to the unknown losses and the complex equations involved in the designs. Thus, numerous microwave computer-aided-design packages have been

developed to assist the designer in tasks such as, circuit design and optimisation with error correction.

These packages significantly reduce the iterative process, normally involved in amplifier design, by allowing the designer to observe the predicted amplifier response whilst the CAD program optimises the circuit parameters for specified limits in the response. Thus, time consuming and sometimes inaccurate manual calculations are avoided, as well as the many hardware iterations needed in a 'cut-and-try' method of obtaining the desired response. Thus, with CAD techniques, amplifier circuit development costs can be significantly reduced.

1.3 OBJECTIVE

Since 1976, a considerable amount of development has occurred in the United States of America and Europe, in the field of ultra-wideband microwave amplifiers. The purpose of this study is to develop the three basic types of ultra-wideband microwave amplifiers, namely: maximum gain, low-noise and power amplifiers, on low dieletric (Er = 2.2) microstrip softboard (RT Duroid 5880) using Gallium-Arsenide Field Effect Transistors as the active devices. The transistors to be used are manufactured by Mitsubishi Electric Corporation. For low-noise and maximum gain amplification the MGF1403-11-09 will be used (refer to Appendix A for the specification sheets) and lastly for Power amplification, the MGF 2116-01 power transistor will be used.

In practise, there is more demand for receivers designed for ultra-wideband operation than there is for wideband power amplifiers. This is largely due to military requirements of

electronic counter measures (ECC), where enemy transmitters are to be detected at unknown frequencies, thus requiring wide bandwidth receivers rather than transmitters.

All the amplifiers have a common specification in that their frequency of operation is to be wideband, from 2- to 6-GHz for the low-noise amplifier and its associated maximum gain amplifier and from 3.7- to 4.2-GHz for the power amplifier and its associated pre-amplifier. This will necessitate the use of a microwave circuit analysis computer program in order to achieve the required input and output matching networks. The program is run on an IBM Personal Computer and is called TOUCHSTONE (by EEsof Inc. 31194 La Baya Drive, Suite 205, Westlake Village, CA 91362).

The Maximum Gain Amplifiers must have optimal gain, with the minimum ripple over their respective bandwidths.

The Low-Noise Amplifier must have less than 5dB Noise-Figure over the bandwdth and the Power Amplifier must have a minimum Output Power of 400mW over the bandwidth.

1.4 DISSERTATION ORGANISATION

The remainder of this dissertation comprises seven chapters, each dealing with a particular aspect of the amplifier development process, from amplifier fundamental principles to transistor characterisation and amplifier results.

The first, Chapter 2 gives a review of microwave amplifier, transistor, and printed circuit transmission line development since the conception of the first transistor in 1948, to the

development of microwave monolithic integrated circuits in the early 1980's.

Chapter 3 is intended to give the reader an understanding, with regard to amplifier design, of the microwave circuit analysis package - TOUCHSTONE and to give a brief review on microwave computer aided design (CAD) programs in order to set the program Touchstone into its correct perspective.

Chapter 4 involves the device characterisation for the three types of amplifiers - these are: s-parameter measurements, noise parameter measurements and finally "load-pull" measurements, taken at a series of spot frequencies across the bandwidth. This will also involve details of the test-equipment and procedures involved in the parameter measurements.
The manufacturers data will also be discussed with respect to the measured data for the MGF 1403 FET.

In Chapter 5 the various amplifiers will be designed by using the appropriate device parameter measurements. The corresponding broadband source and load impedances will be found using the Smith Chart as the design tool. These designs are then optimised on TOUCHSTONE for: gain, noise-figure or power output, according to the amplifier type.
Details of the artworks used to etch the optimised circuits will also be given.

Chapter 6 deals with the testing of the amplifiers and any possible tuning that may be necessary to achieve the desired amplifier response.

Finally, Chapter 7 will conclude the dissertation by comparing and discussing the responses and characteristics of the amplifiers predicted by TOUCHSTONE, with that achieved with, and without tuning. Similarities in the design of power and low noise amplifiers will be drawn up, as well as a discussion on the use of CAD techniques in amplifier development.

CHAPTER 2. REVIEW OF BROADBAND LOW NOISE AND POWER AMPLIFIERS.

2.1 INTRODUCTION

Present-day, state-of-the-art developments in the field of broadband low-noise and power microwave amplifiers involve the use of Monolithic Microwave Integrated Circuit (MMIC) technology.

Thus, in order to set this thesis into its correct perspective in the microwave scenario, the review will be divided into four sections. Each section will deal with a particular aspect of broadband Low-Noise and broadband Power Amplifiers. In this way, the various amplifiers and amplifying devices history's and developments up to date can be compared. It will also allow the reader to observe how far up the scale of technology that this research project is dealing with.

2.2 DEVELOPMENT OF LOW-NOISE AND POWER AMPLIFIERS.

a). **LOW-NOISE AMPLIFIERS** : Low-noise amplifiers of various types are being used in a wide variety of applications, ranging from terrestrial communication links, satellite communications and highly sensitive radar receivers to radio-astronomy receivers.

Low-Noise amplifiers are particularly important in the microwave region of the frequency spectrum and it is nowadays well known that the overall performance of any receiving system is limited by its front-end noise-figure [3] which in turn is dominated by

the noise-figure of the first receiving device.

The first receivers employed mixers in the front-ends. At the time , communications were little into the UHF band where reciever noise-figures are dominated by the antennae noise temperatures [4]. In the mid-1930's the full potential of low-noise front-ends was realised. During World War 2, mixer noise-figures showed a significant improvement, from 20dB to the 10dB range. In 1945 to the late 1950's further developments in semiconductor technology (diode mixers) revealed noise-figures below 10dB, to the 6dB range. Work was also carried out on cryogenically cooled mixers but this had limited applications.

Today the mixer is still widely used in all microwave systems, but rarely as a low-noise front-end, except in the millimeter wave frequencies where there are no low-noise amplifiers to rival the mixer as a low-noise front-end.

It was realised that reciever performance was determined predominantly by the noise-figure of the front-end [5]. Friis was the first to formulate this relationship of the reciever noise-figure to the noise-figure and gain of each stage of the reciever:

$$F_t = F_1 + (F_2-1)/G_1 + (F_3-1)/G_1G_2 + \ldots\ldots$$

Where F_t is the overall Noise-Figure of the reciever and F_1, G_1, F_2, G_2, F_3, G_3 etc are the noise-figure and gain of the first, second and third stages of the reciever respectively. From this formula it can be seen that the reciever front-end should be an amplifier with as low a noise-figure and as high a

gain as is possible.

Thus, from the mixer 'era' there developed an ultra-low-noise period which was fired by satellite communications (proposed by J.R. Pierce in 1955).

The first of the low-noise amplifiers was the Parametric amplifier developed in 1957 by Wiess. However it required large pump frequency power to operate, and the bandwidth was limited. In the mid to late 1960's the gain-bandwidth problem was alleviated with the use of sophisticated circuit broadbanding techniques and the availability of very high quality GaAs varactors; yielded lower noise-figures in the order of 0.9dB at room temperature and 0.1dB cryogenically cooled [5].

The parametric amplifier had difficulty in keeping up with the MASER, having gain-bandwidth product limitations and non-competitive noise-figure. The Paramp finally took hold in the late 1960's when modern circuit techniques paved the way for Paramp ultra-low-noise performance without the complexities and cost of cryogenics, thus leaving the Paramp as the most successful of all the ultra-low-noise amplifiers.

Next along the line was the MASER (Microwave Amplification by Stimulated Emission of Radiation), suggested by Weber in 1953 [4,5]. The first MASERS were cavity MASERS, being resonant at both the signal and the pump frequencies with the varactor seated in the cavity. Such devices are inherently unstable and had to be used in conjunction with circulators, which resulted in a degradation of the noise performance of the amplifier.

In 1959, De Grasse came up with the travelling wave maser (TWM)

which had the following important properties over the cavity maser:

a) The TWM is intrinsically nonregenerative and therefore does not suffer from the constant gain-bandwidth product restrictions which characterise cavity devices.

b) For a given gain the instantaneous bandwidth is essentially limited only by the effective width of the paramagnetic resonance line.

c) The device can be made completely non-reciprocal.

d) The gain stability is much higher.

Almost all operational masers have been of the TWM type and operated at liquid Helium temperatures, which increases the size and costs significantly. State-of-the-art noise temperatures are 3° (i.e. << 0.1dB) at 1GHz and $5^{\circ}K$ at 4GHz (Equivalent noise temperatures are quoted since the noise figure values are extremely small) [6].

The maser did fall short of the cryogenic parametrics as the bandwidth was limited and it was very costly. It is still being used in the most stringent of radio-astronomy and deep-space requirements where the low noise-figure requirement warrants the cost.

After the maser came the Tunnel Diode Amplifier (TDA), proposed by Esaki in 1958. The TDA was rapidly developed, principally for switching applications. Its advantages being simple construction and therefore cost, and reasonably low noise-figure of 3-6dB, combined with good bandwidth.

The early limitations of the TDA were its low power handling

capabilities and it was very fragile requiring rigid mounting structures. These factors did improve with time however.

The TDA thus found limited application in low complexity, moderately low-noise microwave receivers in the mid 1960's to the early 1970's when the microwave bipolar and FET transistors offered more advantages.

Next to come along the line was the electron beam parametric, proposed in 1958. This never took-off since there were fundamental limitations in its noise performance [5].

Last but not least was the solid-state or transistor amplifiers, in the early 1970's.

State-of-the-art performance is 0.8dB noise figure at 4GHz for uncooled FET amplifiers and 0.6dB for Peltier cooled FET amplifiers [5].

The simplicity of FET amplifiers allows for ease of production and low cost when compared to paramps and masers. This technology allows for Integrated Circuit techniques to be employed thereby reducing size and cost and increasing the reliability of the amplifiers.

b). **POWER AMPLIFIERS** : Traditionally, Travelling Wave Tube amplifiers (TWT's) have been used as the high-power amplifiers in microwave communications and radar applications.

The TWT was invented in 1947 by Kompfner [7] and was the first amplifier to be developed. However, over the past decade, Solid-State amplifiers using GaAs FET's have advanced in both frequency and power to replace TWT amplifiers to a large extent.

The major developments in Solid-State power amplifiers occured

during the mid 1970's when the use of GaAs technology became a reality in the microwave frequencies. The advancements were in improved photolithography, lower device thermal resistance, internally matched devices, higher gate resistance, with small device size to keep the parasitic reactances low and lower current densities.

At first, silicon technology was used, due to shortcomings in the GaAs manufacturing processes.

From the foregoing discussion one can see that by 1979 a single power fet amplifier still fell short of the power obtainable from a TWT amplifier.(typical TWT power outputs were 50W at K-band!!). To solve this problem various power combining techniques were developed such that a complete solid-state power amplifier would consist of numerous single-ended devices, driven in parallel and their outputs combined power-wise. The most efficient of these power combiners/dividers was the radial cavity power combiner.[refer T. Waardenburg M.Sc. Dissertation on power combiners.], [8]. At this stage solid-state power amplifiers were able to replace the TWT amplifiers up to K-band.

This was not the only problem that severely limited the use of solid-state power amplifiers. There was the problem of device input and output impedances being nearly open/short circuit, and therefore difficult to match, for the higher power devices. Thus, in order to improve very high power FET performance, the matching networks required to achieve this would have to be as close to the device as possible. This was overcome by internally matching the power FET's in their packages by the manufacturers thus

easing the designers task of high power FET amplifier design.

The most recent of power FET amplifier developments (as far as the author can determine) are : 1). A K-band FET amplifier with 8.2W output power [8]. 2). An 8GHz, 10W, Solid-State power amplifier. [9]. 3). and a 10W, 10GHz internally matched GaAs Power FET [10].

The next step in the amplifier development was in the field of Microwave Monolithic Integrated Circuits (MMIC) . The first power amplifier of this type was reported by V. Sokolov et al. in 1979 (according to McQuiddy, Jr. [11]). This was a two stage amplifier with 10dB gain at 9.5GHz and an output power of 1.26W. Later, that same year, a four-stage X-band monolithic amplifier was developed with 1W output power, 27dB gain over the 8.6 to 9.2GHz frequency range [11]. Since then little has been reported on the subject that is of any relevance to this review.

2.3 THE DEVELOPMENT OF MICROWAVE LOW-NOISE AND POWER TRANSISTORS.

After World War 2 it was realised that the development of electronic systems was limited by the size of the system. This started a drive toward miniaturising the vacuum tube and their associated circuits. Hand-in-hand with this it was realised that the cost-effectiveness of electronics would have to be improved. This in turn led to the development of the auto-assembly system for electronics.

With the advent of the transistor in 1948 and the Auto-assembly process in 1949 [12] (this was the father of modern-day Print

and Etch Techniques), the miniaturisation process leaped ahead. The first to perceive the idea of Micro-miniaturisation or integrated circuits was G.W.A. Dummer of the Royal Radar Establishment in England in 1952 (according to Kilby [12]). This was finally realised in 1959 by J. Hoerni of Fairchild [12]. It represented the first modern day transistor using photolithographic techniques.

With the advent of GaAs FET's in the microwave region, it was an obvious field to research - GaAs Integrated Circuits (Microwave Monolithic Integrated Circuits, MMIC's). Thus , relying on the already fully developed silicon integrated circuit technology, this technology is fast in extending integrated circuits well into the microwave frequencies.

At first, the market for MMIC's was limited to a few gigabit rate computers and specialised space applications, but now with the development of direct satellite television, the market is large enough to warrant large scale production and thus reduce component costs.

Over the past few years remarkable progress has been made in both low-noise and high power transistors. The great challenge has been to replace the life limited, bulky vacuum tubes with longer life, more compact devices, with improved performance and reliability, simplified operation, relatively maintenance free and cost effective solid-state devices in the microwave region.

Considerable effort has been put into improving the high frequency performance of this device. This has involved the improvement of the manufacturing processes : from point-contact, alloyed, diffused, epitaxial and planar techniques

resulting in transistor operation into the microwave region with practical gain and noise-figure (6GHz is about the maximum frequency for silicon transistors). It took seventeen years from the initial introduction of the bipolar transistor by W. Shockley in 1948 until microwave transistors with practical gain and noise-figure became available [13]. By 1965 Germanium transistors were operating in L-band with noise-figures below 6dB! Since 1968, a significant amount of work has been put into developing X-band bipolar transistors. At 8GHz a silicon npn transistor with 3.9dB noise-figure and 3.8dB associated gain [14] has been reported.

State-of-the-art silicon bipolar transistor amplifiers have noise-figures as low as 2.3dB at 4GHz and 1dB at 1GHz. Above 4GHz the noise figure degrades rapidly to about 5dB at 7GHz. This is due to the large number of noise sources in a bipolar device such as thermal noise, shot noise, generation/recombination noise and flicker noise.

The field-effect transistor, conceptually, is the oldest of transistors having been proposed in 1928 (by Lilenfield), twenty years before the invention of the bipolar transistor [15].

The FET is substantially different from its counterpart since its working current is unipolar as opposed to bipolar, and offers immediate advantages such as: high input impedance, low-noise and simpler, more economical circuit requirements. Also, its frequency of operation is only limited by its gate capacitance as there is no base charge storage time and its noise-figure is inherently lower since it is a unipolar device and suffers only

from a thermal noise contribution. It must be noted though that the gate leakage current does contribute a small amount of shot noise.

By 1976, at 8GHz a silicon npn transistor with 1W CW output power and 6dB power gain was reported [16], at 2GHz a single transistor chip delivered 30W CW output power with 7dB power gain and 32% power added efficiency.

Thus, since the BJT had a poor noise-figure compared to the FET, the FET became the favoured low-noise and power solid-state device. However silicon was limited to operation below about 4GHz since its electron/carrier mobility is at its limit at this frequency. Thus, a large amount of research went into developing high mobility semi-conductor material such as Gallium Arsenide (GaAs) and Indium Phosphide (InP) [17]. Initially Gallium Arsenide (GaAs) was discarded as it had unwanted impurities or crystal imperfections that trap the carriers. Of these, GaAs was the only one to which successful ohmic contacts could be made. This now allowed theoretical transistor operation up to 24GHz (6 times that of silicon), since the GaAs material electron mobility is six times that of silicon. Thus the development of the GaAs FET led to low-noise transistor operation in the upper microwave frequencies. However, the first GaAs transistor was limited to operation below 500MHz [18] due to its physical layout.

In 1966, C. A. Mead of the California Institute of Technology made the first Schottky-barrier MESFET (Metal Semi-conductor Field Effect Transistor) using GaAs material [19]. The geometry of the device was such that microwave operation was not possible.

From this date on, the GaAs FET technology progressed rapidly since it was now able to draw on the photolithographic techniques developed for the microwave silicon transistors.

By 1967 W.W. Hooper and W.I. Lehrer of Fairchild reported the first microwave GaAs FET [20]. This device had a fmax of 3GHz, which was inferior to that obtained in silicon at that time, but this result spurred further development on. A further breakthrough occured when K.E. Drangeid et al of IBM Zurich Research Laboratories reported on a GaAs FET with a 1micrometer gate that had a fmax of 30GHz, and 6dB gain at 10GHz in 1970; performance clearly superior to other transistors of any type [21]. In 1971, breakthroughs in GaAs Field Effect transistors yielded solid-state amplifiers with higher gain, higher power amplification efficiency and lower noise figure, above 4GHz.

The first X-band FET amplifier was reported in 1972 by W. Baechtold, also of IBM Zurich [22]. As far as the author can determine, the present day state-of-the-art is a GaAs FET with a cutoff frequency f_t as high as 45GHz ! This is a High Electron Mobility Transistor (HEMT), [23].

Various types of FET structures are used in GaAs , of which the MESFET is most favourable for power amplification. The first power mesfet's appeared in 1973 and were of a planar construction, developed by Fukuta et al. It had 1.6W output power at 2GHz with 5dB power gain and 21% power added efficiency. By 1976, reported performance data ranged from 4W at 4GHz to 0.14W at 22GHz and power added efficiencies varied from 44% to 9% [16].

By 1979 powers had progressed to 18.5W at 4GHz [24]. (This was the most recent power FET development publication the author could find).

2.4 EVOLUTION OF MICROWAVE PRINTED CIRCUIT TRANSMISSION LINES.

The development of the printed circuit board enabled low-cost, mass-produced electronic systems. At microwave frequencies the equivalent development was that of the planar transmission line or microstrip as it is more commonly known. It does have some limitations however.

The earliest mention of the planar transmission line, according to H. Howe [25] was by H. Wheeler in 1936. He proposed two flat co-planar strips side-by-side to make a low-loss transmission line that could be rolled up to save space. It was not until 1952, that a group of engineers reported a form of the printed line known as the Microwave Printed Circuit (MPC) which was an adaptation of the planar geometry of the "two wire line" [26].

Throughout the 1950's, lack of materials were a key drawback to microstrip development.

One of the shortcomings of the MPC is that it is an unshielded system and it is thus more difficult to confine the energy in the vicinity of the strip, with the result that this line has an inherently low Q. These losses are particularly due to radiation and dielectric loss, however there are many circuit applications were a high Q-factor is unnecessary, and it is in these applications that MPC is as practical as, or more practical than, cylindrical or flat-strip co-axial structures. The planar

geometry was favoured since it offered certain advantages over the waveguide, co-axial line or two-wire line. These were: lower cost, ease of manufacture and reduced size.

In the 1960's a microfibre teflon fibreglass called DUROID was developed, as well as high purity alumina (Er=10), which could be polished and metallised for thin film circuit applications [26]. Duroid is nowadays widely used as the MPC substrate, because of its high quality and ease of use. Alumina, on the other hand, has the advantage of being far less lossy and therefore has a higher Q-factor, but it is fragile, difficult to machine, and has to be mounted on a matched temperature coefficient of expansion backing plate. A disadvantage of the microstrip and other transmission lines is that their characteristics are frequency dependant. Thus, any transmission line circuit utilising distributed element components will have a narrowband frequency response [27]. In the particular case of amplifiers, an important step forward occured in 1969 when J. Lange of Texas Instruments published a letter on a "New Interdigitated Stripline Quadrature Coupler" [28]. This development permitted octave bandwidth quadrature couplers to be used on microstrip and thus solved the bandwidth problem of microstrip distributed element amplifiers. Previous to this development, amplifiers were single-ended, for broadband amplification the input and output impedances of these amplifiers were generally near open/short circuit. This necessitated the use of isolators for broadband amplifiers. A short fall of the isolators is that their bandwidth is limited with a high insertion loss and are very costly. However, the Lange Coupler offered a good return loss over an octave bandwidth or more as

well as good isolation between amplifiers and 3-dB coupling over the same bandwidth. The Lange Coupler also allowed the use of balanced amplifiers with all the associated advantages such as increased interstage isolation, return loss and decreased gain ripple. One of the disadvantages is that the use of Lange couplers requires the operation of two amplifiers for each amplification stage and thus increases the overall current consumption.

By the 1970's stripline and microstrip assemblies were commonplace and a new transmission line emerged - The Finline; allowing operation into the millimeter wavelengths.

Today, computer-aided-design (CAD) techniques for microstrip circuit development are being used extensively, with the ability to design, optimise the circuits and then to cut the masks directly from the computer program. This all makes the use of microstrip, for low-cost development of microwave circuits and mass-production, very favourable when compared to waveguide, co-axial line, two-wire line or stripline.

With the development of high purity Gallium Arsenide (GaAs) in the early 1970's, Microwave Monolithic Integrated Circuits (MMIC's) were and still are being researched, using GaAs as the dielectric substrate.

Gallium Arsenide has a high dielectric constant of approximately twelve (Er=12), and thus coupled with its high resistivity could be used as the dielectric base of a microstrip transmission line, where the individual elements such as diodes and transistors could be implanted directly into the substrate, using the already

developed silicon digital integrated circuit photolithographic technology. The necessary distributed components and interconnections are then spluttered onto the substrate, thus reducing the size of the circuit. This type of circuit is known as a Microwave Monolithic Integrated Circuit (MMIC). This also enabled the use of lumped elements since the component parasitic reactances can be kept to a minimum due to the physical size of the components.

The MMIC technology had a very short 'adolescence', as it could use the already developed photolithographic techniques and layouts of the silicon integrated circuit technology.

The MMIC's, as did the silicon integrated circuits, offered the possibility of; higher reliability over conventional circuits, ruggedness, reduced group delays and wider bandwidth of operation (i.e. multi-octave bandwidth since lumped elements which are not frequency dependent were used). Thus, with this development microwave systems could be constructed out of mass-produced, low-cost, integrated circuit modules if there is a sufficiently large market to warrant the development costs. With the advent of direct satellite television reception these low-cost integrated circuit modules have become feasable.

The introduction of the GaAs MMIC, enabled broadband amplification in the 2 - 20GHz band [29].

As far as the author can determine there has been little work on low-noise, broadband microwave amplifiers using microstrip distributed elements, as the fundamental limitations of microstrip such as low Q-factor, narrowband characteristics and size have led researchers to persue the more dynamic field of

Microwave Monolithic Integrated Circuit technology. However, the MMIC technology has been limited, as the development costs of these circuits is extremely high. Thus, such costs can only be justified if there is a large enough market to warrant mass-production. For low-budget research and development, however, the microwave integrated circuit (MIC) does have the advantage. Power amplifiers have suffered the same fate to a certain extent, but power amplifiers rarely require wideband operation and are suited to use on MPC.

The first low-noise, broadband microwave amplifier on microstrip using distributed elements was reported by R. S. Engelbrecht et al [30]. This was a four-stage L-band FET amplifier with 20 ± 0.2 dB gain and a 6dB noise-figure. Since then, various low-noise amplifiers using distributed elements have been reported, but very few have been for broadband applications. In the 2 - 6 GHz range, work has been either been at 2-4 GHz or 4-8 GHz. R. S. Pengelly published a letter on a cryogenic 2-4 GHz FET amplifier, using double section matching transformers which have a limited bandwidth [31], and in 1981 he reported a 0.1 - 6 GHz monolithic amplifier [29]. Various attempts have been made to use lumped elements for matching broadband monolithic amplifiers, the first of which was R. Pengelly [32]. In 1975 he developed a 8-12 GHz amplifier using lumped elements. This technique was limited to a one-off basis since he had to characterise each element seperately and use this data to design the appropriate matching networks. The best results have been achieved with a combination of lumped and distributed components.

2.5 CONCLUSION

Power FET development has gone hand-in-hand with low-noise FET development, starting off with the first low microwave region power FET's in the early 1970's to high power internally matched 8W devices in X-band and broadband monolithic 1W amplifiers in the early 1980's.

Solid-state amplifiers were favoured since they had the advantages of lower voltage power supply, higher reliability, and a reduced size and weight when compared to the TWT amplifiers [7]. In the microwave frequencies however, 10W devices are the limit to the power handling capabilities of a single device. Radial cavity power combiner/divider techniques overcame this limitation to allow a number of 10W amplifying stages to be combined to form a higher power amplifier that challenged the Travelling Wave Tube amplifier.

Low-Noise solid-state amplifiers on the other hand developed at the same time, with the improvement of the GaAs manufacturing processes, and offer noise-figures as low as 0.8dB at 4-GHz uncooled. The advantages of the low-noise solid-state devices being lower cost, ease of production, lighter weight, improved efficiency, smaller size and higher reliability over the 0.1dB noise-figure range of the Maser or Paramp.

However, just as the TWT amplifier is still being used in certain power amplification applications, so are the Maser and Paramp being used in the most stringent of low-noise applications where the extra cost is warranted.

It would be a logical deduction to say that the microwave scenario is following that of silicon, but over a much shorter timespan since the microwave Gallium Arsenide technology has relied heavily on techniques of development developed for the silicon industry of micro-miniaturisation.

Thus, we could say that engineers are striving toward smaller, cheaper, more reliable and higher frequency electronic systems. This has determined the future of microwave systems to a large extent to be Microwave Monolithic Integrated circuits rather than the bulkier microstrip or Microwave Integrated circuits. This had a major impact on the microwave industry, since now the microwave integrated circuits could be sold direct to the public due to the low-cost. An important impetus for this technology was the development of direct satellite television in the 1980's and the ever increasing satellite industry. However, it must be remembered that microwave component research and development is a costly affair, especially for monolithic circuit development. This sets microwave integrated circuits as the favoured technology in low-budget, small market research and development.

000

CHAPTER 3. TOUCHSTONE

3.1 INTRODUCTION: A Review

The development of microwave systems is a very costly affair, as the technology involved requires the work of highly specialised design engineers. Thus, to keep the cost of development down, manufacturers have had to develop a means of reducing the time spent on development and also reduce the number of hardware iterations made in order to develop, for example, an amplifier.

The obvious solution was to have a computer to do the design and optimisation of the required microwave component or system. The engineer would then only have to input certain data such as: device characteristics, design specifications and the design limits, and then let the computer do the rest in a considerably shorter time span, with a significant reduction in the number of hardware iterations and hopefully, far more accurately and reliably than could have been achieved otherwise.

At first, engineers wrote their own programs in Fortran, which in itself took time, until a company called COMPACT ENGINEERING in the United States of America produced the first microwave circuit optimisation program in the mid 1970's. This program, called COMPACT, was available to users on a time-share basis but it was extremely expensive. At the time, personal computers were non-existent and thus it had to be run on a large computer.

Compact was purely an optimisation program and engineers still had to design the circuits manually (on a Smith Chart) and then use Compact to optimise the circuit performance. However, after

Compact, the same company produced three synthesis programs in succession. They were: (1) Ampsyn : which was an amplifier synthesis program using lumped elements, (2) Cadsyn : this was the same as Ampsyn but used distributed components in the synthesis, (3) Filsyn : a filter synthesis program.
These programs were also only available on a time-share basis but were far less costly than Compact.
With the synthesis programs, designers could synthesize circuits in far shorter time spans and they had the added advantage of synthesising circuits whose responses would be closer to that required than would be possible when designing with a Smith Chart. After synthesis the designer could then spend very little time on the expensive optimisation program - Compact. One of the problems with this program was that there were no graphics facilities to display the circuit responses whilst optimising. This was alleviated when a newer version of Compact called SUPER COMPACT, which had a few extra facilities and operated a graphics display, was brought onto the market.

Later, when personal computers became more flexible with more memory, Super Compact became available on floppy disk.

However, an American company EEsof Engineering and the University of California soon realised the potential of low cost computer-aided-engineering software, run on inexpensive personal computers. They produced computer aided design programs in competition to Compact and to each other. The University of

California developed two programs, one called SUGAR - to run on personal computers and SPICE - to run on large computers. Sugar has had limited success with TOUCHSTONE of EEsof being the present-day favourite due to its ease of use, low cost and versatility. Touchstone can be used on several small computers, including the IBM personal computers or compatibles, using floppy or hard disk drives. The program also requires the use of a graphics monitor to display the circuit responses.

Touchstone was used extensively to assist with amplifier designs reported in this dissertation and the following sections of this chapter will be limited to a discussion on how to operate the software package, Touchstone, in relation to microstrip amplifier design, as this is the application of the program in this dissertation.

3.2 TOUCHSTONE: applied to microstrip, broadband, amplifier design

3.2.1 Touchstone: General

Touchstone is a software package for computer-aided-engineering and is run on an IBM personal computer. This makes the software and computer, together, inexpensive and affordable by smaller industries and research centers.

The basic Touchstone program consists of a number of circuit element models which may be 'interconnected', to form a complete circuit, in a user file. These elements are 'connected' by nodal numbers as shown in Figure 3.2.1 below.

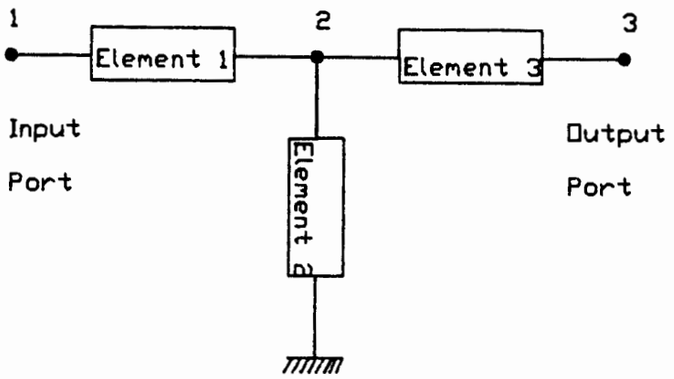

FIGURE 3.2.1: Nodal representation of a T-Network on Touchstone.

Touchstone performs a nodal analysis on the circuit, given the appropriate input parameters.

Thus, in the case of amplifier design, the transistor s-parameters are used to design the appropriate input/output matching networks and these are then written into a circuit file as individual circuit elements connected by means of node numbers as shown in Figure 3.2.2.

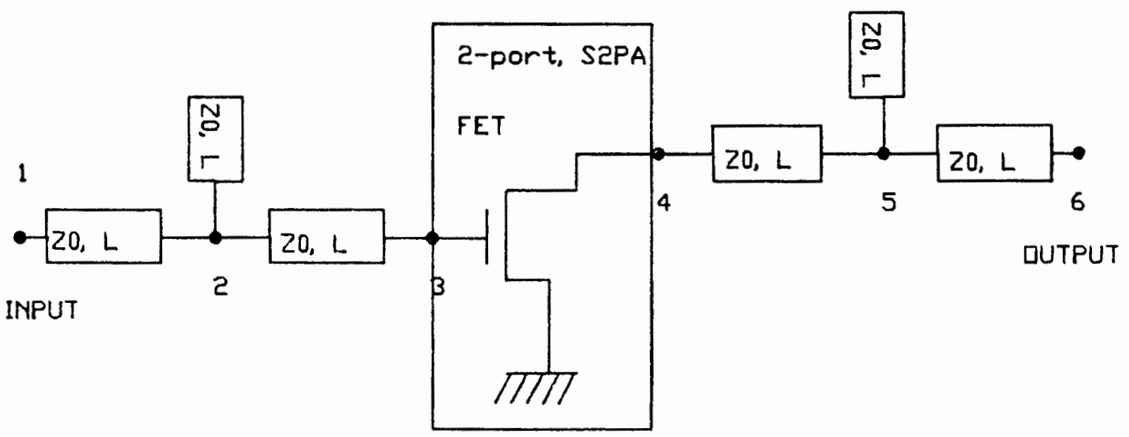

FIGURE 3.2.2: Touchstone microstrip amplifier nodal representation.

The transistor, itself is represented as a two-port network in the circuit file with its s-parameters stored in a special s-parameter file.

When Touchstone encounters such a two-port it immediately accesses the appropriate s-parameter file and then uses this information to continue and complete the circuit analysis.

3.2.2 Amplifier circuit elements

Since the amplifiers to be developed will be designed using microstrip distributed components, only the relevant microstrip elements will be considered as well as the two-port s-parameter element to model the transistor.

The microstrip models used, consist of:

1) Microstrip line including Open End effects. MLEF

FORM: MLEF n1 W=X1 L=X2

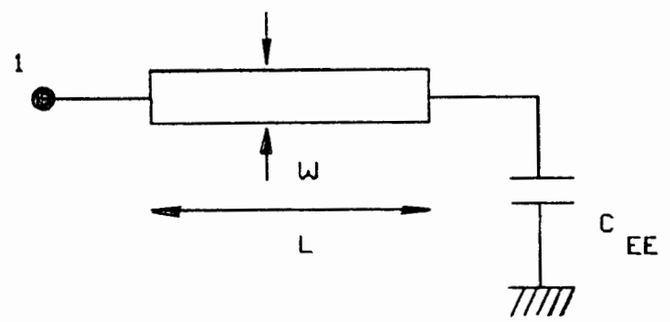

DATA: W= microstrip width

L= microstrip line length

Fringing at the open end of the line is calculated and included in the model.

2) Microstrip Line MLIN

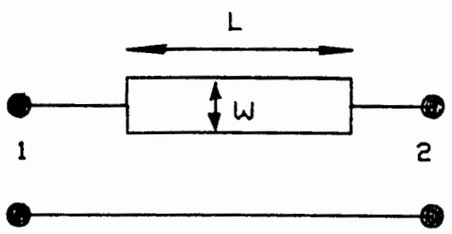

FORM: MLIN n1 n2 W=X1 L=X2

DATA: W= microstrip width

L= microstrip line length

3) Microstrip Tee-Junction MTEE

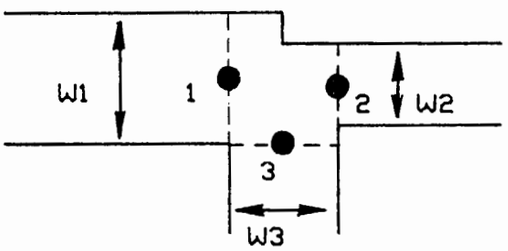

FORM: MTEE n1 n2 n3 W1=X1 W2=X2 W3=X3

DATA: W_i = line width at terminal i.

4) For all microstrip elements, substrate parameters are supplied by an MSUB statement preceeding them.

Microstrip Substrate MSUB

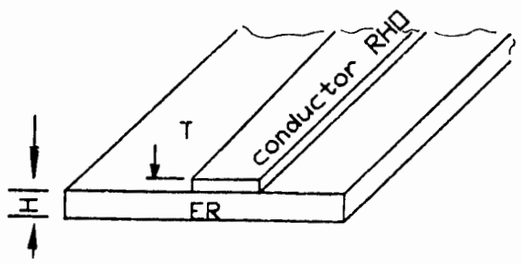

FORM: MSUB ER=X1 H=X2 T=X3 RHO=X4 RGH=X5

DATA: ER= substrate relative dielectric constant

H=substrate thickness

T=metal thickness

RHO=metal bulk resistivity normalised to that of gold

RGH=rms surface roughness

a) Touchstone uses 2.44 micro-ohm-centimeter for the bulk resistivity of gold. Losses are neglected if RHO=0.

b) RGH is in units of length.

Lastly, the transistors are represented as two-port networks as follows:

Two-Port S-Parameter S2PA

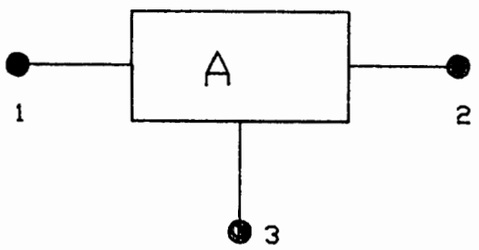

FORM: S2PA n1 n2 Filename

DATA: Filename

a) the file referenced by 'filename' must contain magnitude and angle of two-port s-parameters measured in the following configuration: Terminal 1 : Gate/Input.

Terminal 2 : Drain/Output.

Terminal 3 : Source/Common.

There are numerous other elements available on Touchstone but are not used extensively, if at all, in the design of the amplifiers and thus, the reader will be refered to the operating manual for further information.

3.2.3 Creating a Circuit File.

The first step in creating a circuit file is to split the designed circuit into elements as in Figure 2.
The choice of node numbers is arbitrary, and node numbers do not have to be sequential.

Each circuit in Touchstone is described by writing a file of "blocks" or sections.
The blocks used in the circuit files are:

DIM (Dimension) Sets Dimension to other than default.

VAR (Variable) Assigns values to symbols which are in turn used in one or more circuit element parameters.

CKT (Circuit) Describes the circuit elements and connections.

OUT (Output) Defines the measurements and directs the output to a polar or rectangular grid.

FREQ (Frequency) Names the frequencies over which the network will be simulated and measured.

GRID Describes the plotting characteristics of the rectangular grids.

OPT (Optimisation) Used to define error function to be minimised by the optimiser.

Thus a typical amplifier will be modelled on Touchstone as shown in Figure 3.2.3.

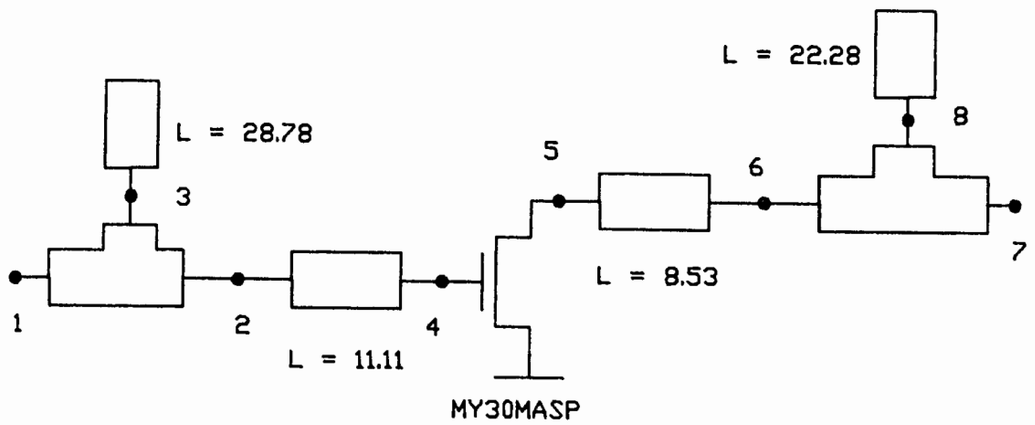

FIGURE 3.2.3: Touchstone microstrip amplifier model.

All lengths in millimeters and all widths set at 2.3965 mm which for a substrate dielectric constant, Er, of 2.2 gives a 50ohm characteristic impedance on all the transmission lines.

Example of the Touchstone file to model this circuit:

```
DIM
      LNG MM       ! Sets default length to mm.

CKT
      MSUB ER=2.2  H=0.7874  T=0.034  RHO=0.706  RGH=0
      MTEE   1 2 3   W1=2.3965 W2=2.3965 W3=2.3965
      MLIN   2 4     W=2.3965  L=11.11
      MLEF   3       W=2.3965  L=28.78
      S2PA   4 5 0   MY30MASP  !  Specifies transistor s-parameter
                               !  file to be accessed.
      MLIN   5 6     W=2.3965  L=8.53
      MTEE   6 7 8   W1=2.3965 W2=2.3965 W3=2.3965
      DEF2P  1 7     MICROA    ! Defines port 1 and 7 as the input
                                 and output of the network to be
                                 analysed and calls it MICROA.


OUT
      MICROA  DB[S11]  GR1     !  Instructs to plot the  magnitude
      MICROA  DB[S12]  GR1     !  of s-parameters on Grid 1.

cont: -
```

```
      MICROA   DB[S21]   GR1
      MICROA   DB[S22]   GR1

FREQ
      SWEEP  2   6   0.1    ! Frequency analysis from 2- to 6-GHz in
                              0.1 GHz steps.

GRID
      RANGE 2   6   0.2      ! Grid frequency range 2-to 6-GHz in
                              0.2 GHz steps.
      GR1 -40   15   5       ! Y-axis scale -40 to 15dB in 5dB steps.

OPT
      RANGE     3   5          ! Optimise for the condition below over
                                 3- to 5-GHz.
      MICROA    DB[S21] > 12.
```

The s-parameter file contains the transistor s- parameters and noise parameters if a noise analysis is required. The s-parameter file layout for the noise parameters is:

Frequency(GHz), Minimum noise-figure(dB), Magnitude of source reflection coefficient, Angle of source reflection coefficient, Normalised effective noise resistance.

The 'OUT' block specifies the type of measurements to be made. Two kinds of measurement are possible: 1). Individual measurements; s-parameters, simultaneous match, group delay and noise-figure and 2). Macro-measurements; s-parameters($S_{i,j}$), reflection coefficient(G_i), simultaneous match(GM_i), stability circles(SB_i), source mapping circles(MP_i). These are only available on the Smith charts however. An example of the described circuits' response is given in Figure 3.2.4.

The optimisation block - 'OPT' in the above example specifies that the optimiser must tailor specified circuit parameters such that the amplifier MICROA gain [S21] is greater than 12dB from 3- to 5-GHz.

This concludes the section on how the circuit file is created from an initial design using a Smith chart.

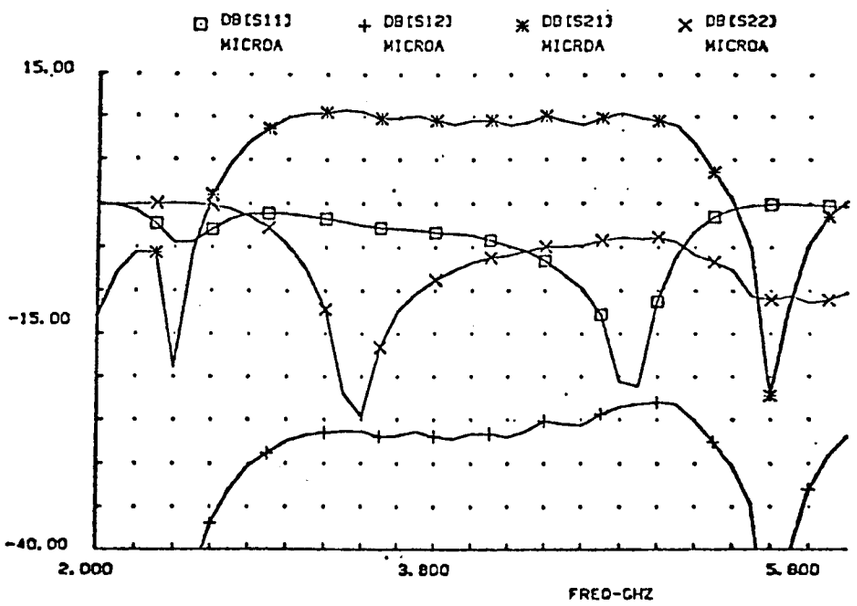

FIGURE 3.2.4: Touchstones' microstrip amplifier response.

3.2.4 The Optimiser

By far the greatest asset of Touchstone is its optimiser, which compares computed circuit responses with the desired response set out in the OPT block. It then changes circuit element parameters to minimise the difference between computed and desired responses. An "error" function is used to compare the two responses and is a measure of how close the two responses are. Thus, the action of the optimiser is to minimise the value of the error function.

The optimisation procedure is a "trial and error" process. Starting from an initial set of element values for which the error is known, a new set of values is obtained by perturbing each of the initial values by a random amount and the error function is re-evaluated. If the error is less, then the element values are replaced, otherwise Touchstone begins a new trial.

Another feature of Touchstone is that whilst it is optimising, the user may observe the continuously updated responses on a graphics monitor whilst the new element values are displayed on the monochrome monitor. When the desired circuit response is achieved, the user may then interrupt the optimiser and resume normal operation.

The element values to be optimised are identified by one of the following characters:

\ used when a starting value only is given.

used when lower bounds, starting value and an upper bound are given.

These characters are used as a replacement for "=" in the usual assignment. For example:

```
DIM
    LNG  MM

VAR
    L1 # 0.5  1  10

CKT
    - - - -  -  -
    MLIN  1  2  W \ 2.39  L^L1
    - - - -  -  -
    MLIN  6  7  W = 2.39  L^L1
```

Here L1 may be optimised starting with 1, between 0.5 and 10

millimeters and W is assigned a starting value of 2.39 but does not have any bounds placed on its value. (Touchstone assumes bounding values of zero and double the initial value).

This concludes the description of creating and optimising a typical Touchstone circuit file. However, all this information can be obtained in the manual supplied with the program. What the manual does not supply is how to manipulate the optimiser such that it converges as close as possible to the desired response over a wide frequency band.

3.3 USE OF THE OPTIMISER

To read through the operation manual is a tedious task, not to mention that by the time the reader has read the last chapter, the first chapter will have been forgotten. Thus to become fully acquainted with the program, such that the circuit designer uses it more efficiently, will take months of experimentation with the program.

This section is intended to short-cut this problem in the case of amplifier design by describing the best method of using the optimiser, found by the author.

In the case of broadband (2-6GHz) amplifier matching network design, the use of the Smith chart is limited and therefore requires a computer aided engineering software package, to optimise these network parameters to get the required response. In the absence of a suitable synthesis program, the simplest configuration should first be optimised, consisting of a single

matching stub at the input and a single stub at the output. However, over such a wide bandwidth, invariably two matching stubs are required (using distributed components) on both ports of the amplifier to achieve maximum and flat gain over the bandwidth. Thus the number of optimiser variables will increase to the limit on Touchstone, which is ten variables, if all of the variables possible are set to be optimised at once. This then increases the time between optimisation trials and consequently the time spent on the computer to reach a satisfactory response. The author also found that with a large number of variables (greater than four), the optimiser could not make significant improvements to the responses.

Thus, to solve this, since the transistors are practically unilateral, the input and output matching network parameters can be optimised independently.

First of all, all the input matching network parameters were optimised (for width and length of the microstrip transmission lines) over a narrow bandwidth (approximately a 50% bandwidth i.e. 3-5GHz) until there was relatively little change in the responses over a number of optimiser trials. Secondly, the same process was repeated for the output port matching network. Once both ports were so called 'pointed in the right direction', the optimisation was carried out over an increasingly wider bandwidth with only the line lengths as variables for both ports. When the optimiser could change this no further, the line lengths were fixed and the widths were set as variables and then optimised.

In general this procedure tended to 'point' the optimiser in the right direction and it thus converged on the required response far quicker than it would have otherwise. This technique also ensures that all the possible variables in the circuit are optimised sufficiently to give the maximum gain-bandwidth possible.

This program is not infallible, however, and requires a certain amount of intuition on the part of the designer/operator to ensure that the optimised variables are practical and realisable. Often, the optimiser wishes to change line lengths and widths to values which may just not be practical and in the real world may never function as Touchstone analyses it. Such an example is shown in the diagram below, where no limits were placed on the line widths, or the limits placed on the variables were not practical.

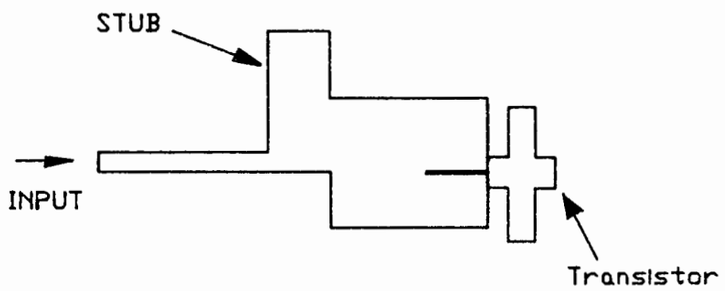

It is obvious that the T-junction effects, such as radiation at the corners and reflections at the stub, will be so severe that the response of the matching network will be completely distorted. Also the transition between the device and the input matching circuit is so great that there will be considerable signal reflection at this terminal as well as fringing effects

from the open circuit stub.

Thus caution must be applied when specifying the variables and their limits in order to ensure a realistic optimised circuit.

3.4 CONCLUSION

Essentially, Touchstone is an optimisation program and does not offer the facility of circuit synthesis.
However, once the program has been paid for, the time spent running the program is not an additional cost as in the time-share programs. Thus the optimiser could be used to synthesise the required circuit parameters without ever manually designing an amplifier. All that is required is the same circuit file as before with arbitrary circuit parameters, set as variables. The desired response is set in the OPT block and the optimiser will do the necessary 'designing' to achieve the required response. This technique would of course not be considered on a time-share computer program since the cost of running the optimiser for such a length of time would be far too excessive.
This would be extremely useful when designing low-noise amplifiers as this involves a tedious task of plotting noise-figure and gain circles on a Smith chart and then finding the required matching impedance for minimum noise-figure operation.

The advantage of Touchstone, as an engineers design tool, are extensive. The main advantage being that it reduces time spent on

circuit development, as the optimisation process is done on software, automatically, rather than manually by a very expensive and time consuming 'cut-and-try' method. This cut-and-try method gives results per-chance, as well, and thus cannot be relied upon to give the best performance possible. Also, the program Touchstone and the personal computer, together, are inexpensive and can thus be afforded and used by smaller industries and research centers such as universities.

Although it is a useful design aid, it does not predict the real world accurately. This is due to the element models not being able to accurately model the real world and thereby accurately predict the behaviour of the circuits. One of the biggest sources of error is the inefficient T-junction and open-end effect models. However EEsof is continuously updating their programs, adding extra features and improving their circuit models.
However, Touchstone is still used even though it cannot model the real world accurately, as it does reduce the time spent in developing microwave circuits by being able to produce circuits which are closer to that required than would have normally been possible by using the Smith Chart on its own.

Finally it must be noted that although this chapter deals with microwave amplifier design using distributed components, Touchstone could also be used, equally well, for the design of I.F. amplifiers using lumped element components as well as for the design of oscillators and filters.

CHAPTER 4. DEVICE CHARACTERISATION.

4.1. INTRODUCTION

Generally, the transistor manufacturers supply the device characteristics in the specification sheets (see Appendix C). However these characteristics, including the s-parameters, are often inaccurate and difficult to read off the Smith Charts, and are sometimes not quoted for the range of frequencies with which the designer may be dealing.

Thus it is often necessary for the designer to carry out the measurement of these parameters in the laboratory. This proves extremely useful when the transistors are to be used for the design of ultra-broadband amplifiers, requiring extremely accurate designs in order to achieve the required bandwidths.

There are two fundamental types of transistor characterisation, based on the input signal level. These are: firstly, small-signal characterisation, where the transistor is operating in the linear region of its transfer characteristics (i.e. Class-A) and secondly, large-signal characterisation, where the transistor is driven into saturation and is thus operating in the non-linear region (i.e. Class-B or -C).

The design of transistor amplifiers requires the appropriate device characterisation, according to the type of amplifier to be designed. Small-signal characterisations are used in the design of low-noise and maximum gain amplifiers, whereas, large-signal characterisation is necessary for power amplifier design.

4.2. SMALL-SIGNAL TRANSISTOR CHARACTERISATION. (MGF-1403 & 2116)

4.2.1. Introduction

Small-signal device characterisation, at microwave frequencies, consists of the determination of the transistor s-parameters (Descriptions of two-port network parameters are readily available in the literature [38]).

The accuracy of these measurements will determine the accuracy to which the amplifier can be designed, for a specific response.

The manufacturers data sheets, however, do supply the necessary s-parameters, in the case of the MGF-1403 and 2116 transistors, with limited accuracy, since the manufacturer publishes the average s-parameters for a batch of transistors rather than for each individual device. Thus, device-to-device variations in the s-parameters will inherently occur and the amplifiers will therefore have some error in their designs and thus their responses. (Refer to Appendix C for the data sheets).

4.2.2. S-parameter measurement test set.

The transistor s-parameters will be measured on the HP8410C Network Analyser controlled by an HP85 Desktop computer with the HP11873A Accuracy Enhancement Pack. A block diagram of the equipment set-up is shown in Figure 4.2.1.

The transistors are mounted in the HP11608A Transistor Fixture as shown in Figure 4.2.2.

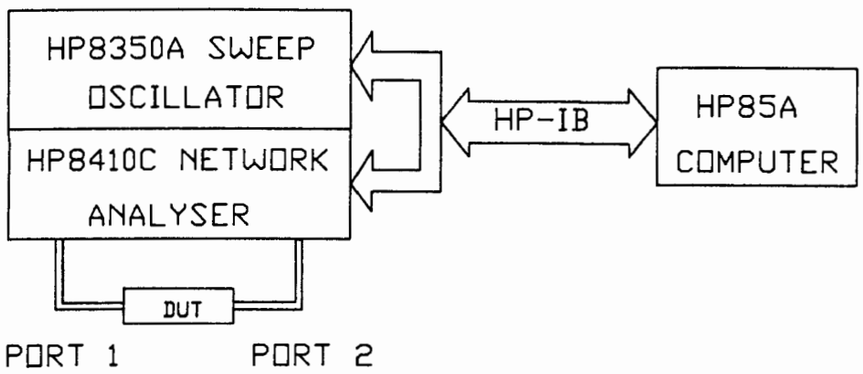

FIGURE 4.2.1: HP8410C Network Analyser.

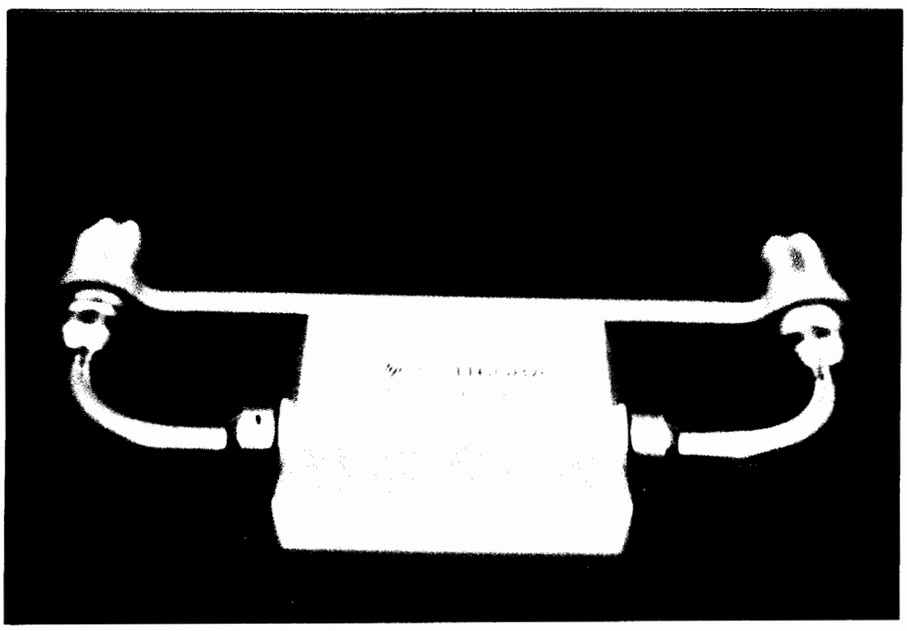

FIGURE 4.2.2: Transistor Test Fixture.

4.2.3. S-parameter test-set calibration and measurements.

The HP8410C network analyser performs all the necessary power measurements to determine each of the s-parameters [38], depending on which measurement is selected on the front panel controls.

When run by the accuracy enhancement pack, the system is calibrated by connecting the appropriate terminations to Port 1 of the test-set, when required to do so by the software package. Thus, the accuracy enhancement pack requires the frequency range of the measurements (1-7GHz) and the frequency steps at which the measurements are to be taken and then performs a series of measurements on firstly, a 50ohm termination, a short circuit, a shielded open circuit and lastly a through line from Port 1 to Port 2. This is known as the calibration procedure. When performing the measurements of S11 and S21 on the device, it then automatically displays the calibrated and error corrected results on the computer screen.
It must be noted, however, that the accuracy enhancement pack only performs measurements at Port 1 and therefore only measures S11 and S21 (the device is reversed to measure S22 and S12).

To measure the device s-parameters, the measurements and calibrations should be performed at the point where the device is seated, so as not to include lengths of transmission lines in the s-parameters (this appears as a change in phase). Since the device is mounted in a test fixture where calibration is impossible , the calibration is carried out at Port 1 and then the s-parameter, S21, is measured with the device replaced by an exact brass replica, which then achieves a short circuit at the exact point where the device will be mounted. The error corrected results of the phase of S21 are then displayed on the computer whilst the reference plane of the measurements are adjusted in software, until the phase reads 0° over the entire bandwidth.

(This is the characteristic of a perfect short circuit)
Now the device is inserted, biased to the correct drain current, and the measurement of S11 and S21 is performed. On displaying the results, the reference plane is adjusted in software by entering the same value as that that was entered for a zero degree phase shift for the brass short circuit. The results are then error corrected and measured at the transistor terminals.
To obtain the s-parameters, S22 and S12, the transistor is reinserted with the gate on Port 2 of the transistor test fixture and thus of the network analyser. The measurements are performed in the same manner as for S11 and S21.

4.2.4. MGF-1403 and 2116 S-parameters.

Two sets of s-parameters are required of the MGF1403 GaAs FET, covering the frequency range of 1-7GHz, since it is to be used firstly in a 2-6GHz maximum gain amplifier, where the drain current should be high in order to maximise the gain and where noise-figure is of no concern and secondly, in a 2-6GHz low-noise amplifier where the drain current must be low, in order to minimise the transistor noise-figure.
The s-parameters were measured as described in Section 4.2.3 and are listed in Table 4.2.1 and Table 4.2.2 below.

The MGF2116 Power transistor s-parameters are measured at 200mA drain current and 7V drain to source voltage for maximum output power, and are listed in Table 4.2.3.

MGF1403 S-PARAMETERS, Id=10mA				
FREQ	S11	S21	S12	S22
1.0	0.966/-19	2.85/158	0.025/74	0.733/-14
1.5	0.955/-26	2.57/152	0.036/69	0.741/-19
2.0	0.902/-34	2.54/142	0.040/72	0.692/-25
2.5	0.840/-30	2.27/134	0.042/69	0.653/-28
3.0	0.820/-43	2.24/132	0.045/72	0.646/-30
3.5	0.770/-47	2.07/127	0.043/76	0.617/-31
4.0	0.750/-50	2.16/124	0.043/86	0.603/-33
4.5	0.670/-54	1.99/115	0.040/102	0.556/-34
5.0	0.670/-58	2.14/112	0.051/123	0.550/-37
5.5	0.620/-64	2.24/104	0.077/139	0.519/-41
6.0	0.600/-72	2.09/100	0.096/141	0.507/-47
6.5	0.700/-83	2.66/114	0.085/71	0.582/-46
7.0	0.700/-89	2.72/111	0.093/76	0.603/-48

TABLE 4.2.1: MGF1403: 10mA drain current S-parameters.

MGF1403 S-PARAMETERS, Id=30mA				
FREQ	S11	S21	S12	S22
1.0	0.955/-22	3.39/155	0.023/75	0.700/-14
1.5	0.923/-29	3.35/147	0.032/70	0.708/-18
2.0	0.871/-38	3.27/139	0.034/75	0.631/-24
2.5	0.813/-44	2.99/133	0.036/75	0.596/-25
3.0	0.776/-47	2.851/128	0.039/81	0.596/-27
3.5	0.716/-51	2.60/124	0.038/89	0.569/-28
4.0	0.692/-54	2.69/120	0.042/102	0.556/-28
4.5	0.617/-57	2.63/111	0.046/112	0.519/-30
5.0	0.603/-61	2.51/109	0.057/129	0.513/-30
5.5	0.556/-67	2.69/102	0.090/141	0.496/-34
6.0	0.543/-74	2.48/98	0.108/140	0.490/-39
6.5	0.661/-90	3.06/112	0.086/89	0.556/-43
7.0	0.676/-96	3.20/109	0.099/94	0.569/-45

TABLE 4.2.2: MGF1403: 30mA drain current S-parameters.

MGF2116 S-PARAMETERS, Id=200mA				
FREQ (GHz)	S11	S21	S12	S22
1.0	0.861/-87	3.802/122	0.044/44	0.282/-74
1.5	0.794/-115	3.981/102	0.054/33	0.285/-97
2.0	0.759/-129	3.802/92	0.055/28	0.275/-103
2.5	0.750/-144	3.430/82	0.056/26	0.285/-117
3.0	0.716/-151	3.090/72	0.056/23	0.279/-122
3.5	0.724/-164	2.661/63	0.056/26	0.309/-137
4.0	0.724/-171	2.455/57	0.056/25	0.320/-143
4.5	0.741/-179	2.089/52	0.055/33	0.363/-153
5.0	0.733/177	1.995/45	0.060/31	0.394/-158
5.5	0.750/169	1.622/36	0.058/33	0.437/-169
6.0	0.759/166	1.641/31	0.067/32	0.484/-172
6.5	0.776/163	1.462/23	0.067/29	0.513/-175
7.0	0.759/158	1.479/19	0.074/28	0.531/-179

TABLE 4.2.3: MGF2116: 200mA drain current S-parameters.

4.2.5 The Manufacturers Data or S-Parameters.

The measurement of transistor s-parameters is a tedious process requiring extremely accurate measurements on the part of the designer.

It has long been argued that the s-parameters supplied by the manufacturer are adequate even though they are the average values for a batch of transistors and deviate somewhat from the true device s-parameters.

Considering the numerous sources of uncertainty in the design accuracy, these s-parameters are usually accurate enough. For the purpose of comparison, the MGF1403 s-parameters will be compared. The easiest and quickest comparison of the measured and quoted s-parameters is a visual one, where the s-parameters are plotted on a Smith Chart. Thus, the corresponding s-parameters are shown in Figure 4.2.3.

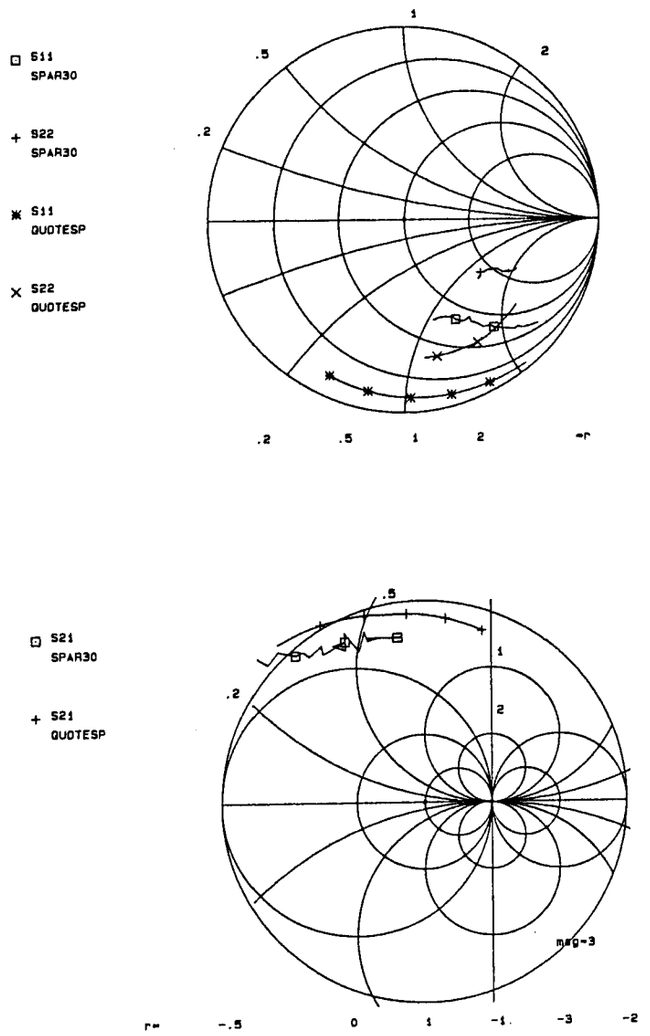

FIGURE 4.2.3: MGF1403 S-Parameters, measured and quoted.

Here in the figure, the measured s-parameters are labelled as SPAR30 and the corresponding manufacturers data is given as QUOTES2P (S12 is negligible in both cases and is therefore ignored). From the figures it can be seen that there are considerable differences in S11 and S22 as well as those for S21, where the measured transistor gain is less than that quoted. S12 has a slight difference but nevertheless is still negligible in value.

With such a considerable difference in the s-parameters, it would

be expected that amplifier performances using the same transistor, for circuits designed using either sets of data, would differ considerably.

Thus, in Chapter 5 under maximum gain amplifier design, the design of an amplifier using the manufacturers data will be presented without any details of the design procedure and then the results will be compared in Chapter 7.

4.3 TRANSISTOR NOISE PARAMETER CHARACTERISATION (MGF1403).

4.3.1. Introduction.

Where the s-parameters completely describe the small-signal behaviour of the transistor, the noise-parameters (refer to Appendix A for fundamental Noise-Figure definitions and a derivation of the condition of amplifier minimum Noise-Figure operation), describe the noise behaviour of the transistor. Noise parameters are necessary for the design of amplifiers where the amplifier noise-figure is an important consideration. The noise parameters consist of: Minimum Noise-Figure NF_{min}, the associated source reflection coefficient Γ_s and the equivalent noise resistance r_n at each frequency of interest.

These parameters however are rarely supplied by the manufacturer, as in the case of the MGF1403 GaAs FET and thus have to be measured accurately by the designer.

4.3.2. Noise-Figure measurement equipment.

For the noise-figure measurements, the HP8970A Noise-Figure meter was used as the main instrument. This instrument is significantly different to other noise meters since it employs an on-board microprocessor to calculate the selected noise parameter (noise-figure or effective input noise temperature) from the raw Y-factor data ([38], for Y-factor theory). The microprocessor is also used to correct the results for second-stage noise and cold temperature deviations. The HP8970A also provides a simultaneous readout of the device under test (DUT) gain.

However, the HP8970A can only operate with frequencies in the range 10 to 1500MHz and thus for amplifier or transistor characterisation between 1- and 7-GHz it requires an external local oscillator and broadband mixer in order to perform the noise measurements at a suitable Intermediate Frequency (I.F.).

The external local oscillator used is the HP8350B sweep oscillator and is controlled by the HP8970A Noise meter over a HP-IB (interface bus). A broadband 2- to 10-GHz balanced mixer was used to mix the signal down to a suitable I.F., chosen as 40MHz.

The noise generator used is the HP346B 0.01-18GHz solid-state noise source.

The variable source and load impedances are provided by co-axial double sliding-stub tuners and the device is mounted in a 50 ohm microstrip softboard test-jig (RT Duroid 5880).

A block diagram of the complete test set-up is shown in Figure 4.3.1.

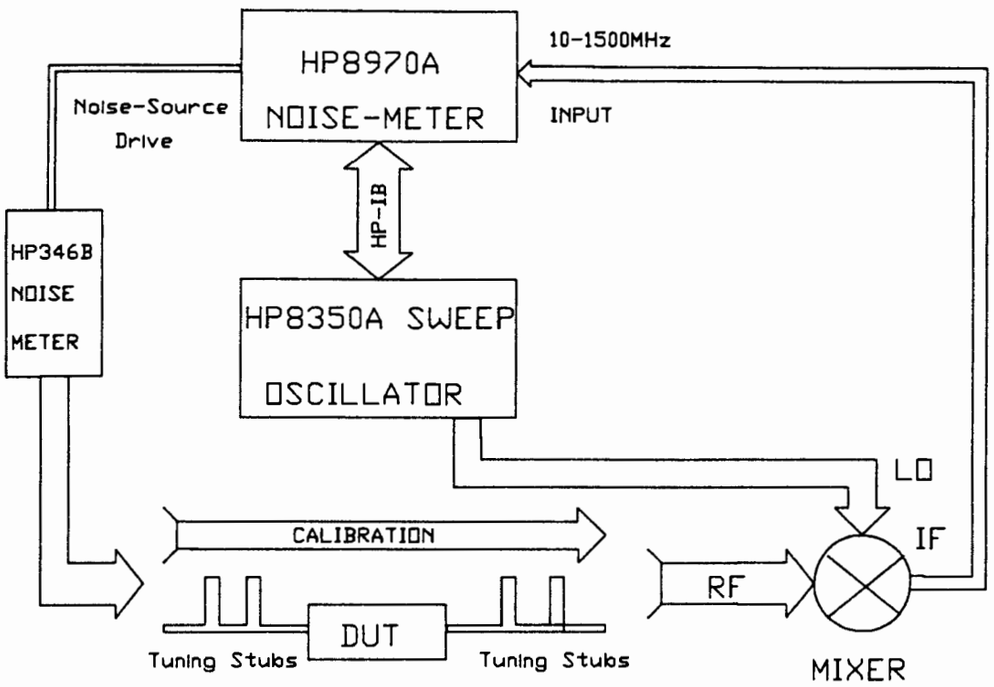

FIGURE 4.3.1: Noise measurement equipment set-up.

4.3.3. Noise-Parameter calibration and measurements.

With the equipment connected as shown in Figure 4.3.1, with a calibration through line in place of the DUT (i.e. a 50ohm microstrip softboard through line) and the tuning stubs tuned out completely, the noise meter is set up for calibration over a bandwidth of 2-GHz from 1- to 3-GHz at first. The measurements are set to be taken at 500MHz steps. The noise meter then automatically calibrates itself over this frequency range, the DUT is inserted, the local oscillator frequency set at 2-GHz, the transistor bias turned on to 10mA drain current and the HP8970A

noise meter now automatically displays the DUT noise figure and gain in decibels (dB), corrected for second stage noise and insertion loss over the calibration bandwidth.

Setting the frequency of the noise measurement at 2-GHz, the source admittance is now varied, by means of the tuners, to obtain a minimum in the noise-figure. (refer to Appendix A for a detailed analysis of the dependance of amplifier noise-figure on the source impedance). The source impedance, for minimum noise-figure, is known as Z_{opt} and the device is then said to be operating at its minimum noise-figure.

The load admittance is varied to maximise the amplifier gain.

These impedances are then set, the test jig is seperated, so that SMA launchers can be mounted at the site where the device gate and drain leads were soldered onto the microstrip and the HP8410C network analyser is then used to measure the source- and load-reflection coefficients, at 2-GHz, that were presented/connected to the device for minimum noise-figure operation.

This process from calibration to source reflection coefficient measurement is then repeated for 2, 3, 5 and 7 GHz to form a complete set of noise-parameters over the bandwidth of interest.

4.3.4. MGF 1403 Noise Parameters.

Only one set of noise-parameters is required at a 10mA drain current in order to completely describe the low-noise characteristics of the transistor, the s-parameters having been measured in Section 4.2.4.

First of all the noise-figure for a 50 ohm source line impedance was read (F_{T,Z_0}) and then the minimum noise-figure was read off

the noise meter (F_{min}).

The associated source reflection coefficients were then measured for each frequency, on the HP8410C Network Analyser thus completing the measurement of the noise-parameters.

MGF1403 NOISE-PARAMETERS, Id=10mA				
FREQ	$F_{Ts=0}$	F_{MIN}	Γ_0	r_n
2.0	6.3	2.24	0.881/31	4.285
3.0	5.15	4.26	0.343/-16	3.4141
4.0	5.5	5.3	0.140/-52	3.3278
5.0	5.92	5.9	0.02/-78	13.005

TABLE 4.3.1: MGF 1403 Noise Parameters.

The only parameter then left to determine was the equivalent noise resistance, r_n which can be found after measuring F_{min}, T_0 and $F_{Ts=0}$ and substituting into Equation 4.3.1.

For $T_s=0$,

$$r_n = [F_{Ts=0} - F_{min}] \frac{|1 + \Gamma_0|^2}{4|\Gamma_0|^2} \qquad - - - - (4.3.1)$$

T_s = source reflection coefficient.

T_0 = source reflection coefficient for minimum noise-figure.

Refer to [38] for the derivation of Equation 4.3.1.

This completes the set of noise parameters which are listed in Table 4.3.1. above.

4.4 LARGE-SIGNAL CHARACTERISATION

4.4.1. Introduction

In contrast to the optimisation of the source impedance for minimum noise-figure amplifier operation (Z_{opt}, which gives an input impedance other than 50 ohms), power amplifiers must be designed for optimum output-power and efficiency under large-signal conditions. The problem is that, under these conditions, the device output impedance is a function of the output-power and thus requires the optimisation of the load impedance. The load impedance required to match the device to 50 ohms is also a function of the output-power and the manner in which the optimum load impedance shifts as a function of output power is unpredictable. The review of the techniques of measuring the required load impedances is covered in Appendix B.

The question may now be asked: 'If the load impedance determines the output power, what effect does the source impedance have on the amplifier characteristics?'

In practice, the input network is usually designed on the basis of small-signal s-parameters and then experimentally adjusted after defining the output network. Such an approach does not give any information on the effect of the source impedance change, so that a simultaneous optimisation of input and output networks under large-signal conditions is not possible [33].

Thus, the source impedance is normally designed, using the small-signal s-parameters, for optimal gain and input VSWR. This results in a less than optimal power amplifier design, needing

extensive tuning in most cases.

Therefore, for the purposes of the characterisation of power transistors, both the source-pull and load-pull techniques will be used in this dissertation.

4.4.2. Load-Pull Measurement Test Set.

The requirements of the power amplifier, outlined in Chapter 1, specify that the amplifier must operate over the 3.7- to 4.2-GHz frequency band, with a minimum output power of 400mW. The amplifier must also operate at 1dB gain compression in Class-AB for increased efficiency and minimum distortion.

The HP8350A sweep oscillator can only deliver 15dBm (32mW) and thus, in order to drive the Device Under Test (DUT) into saturation, a driver amplifier stage was designed using the MGF2116 small-signal s-parameters.

This driver amplifier was then calibrated by plotting its power output (Pout) versus power input (Pin) curves at 0.1GHz intervals from 3.6- to 4.4-GHz, in order that the power output of the driver amplifier is accurately known for given input power levels.

The measurement test set block diagram is given in Figure 4.4.1 below:

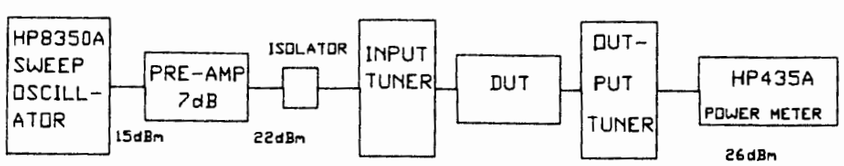

FIGURE 4.4.1: MGF2116 Source-Pull and Load-Pull Measurement Test Set.

The HP8350A sweep oscillator is used as the microwave-source signal and is pre-calibrated to frequency and power output.
Since the DUT requires 20dBm input power in order to saturate, a driver amplifier is used to raise the sweeper power by 7dB to a power of 22dBm.
An isolator is included between the input tuner and the pre-amplifier in order to buffer the driver amplifier from the effects of tuning the input tuner.
The tuners are two-stub co-axial tuners and the device (MGF2116) is mounted in a RT-Duroid 5880, E_r = 2.2, 50ohm line-impedance, microstrip test jig and is biased through 0.15mm diameter copper wire turned once through a ferrite bead [34].
It must be noted that due to the excessive gain of the power transistor at low RF frequencies, bias circuit oscillations are bound to occur. It is thus common practise to decouple the bias circuits to ground, by means of chip capacitors in order to create a low-pass filter. This was achieved by using 2.2nF capacitors on both bias circuits.
From the output tuner the power output of the DUT is measured on an HP435A Power Meter.
Thus, with the pre-amplifier calibrated, the DUT power gain and thus power output can be determined accurately and therefore can be tuned for optimal power operation.

4.4.3 Load-Pull Measurements.

In order to obtain the correct load and source impedances, the sweeper power is sequentially increased whilst the DUT tuners are

adjusted for maximum output power at each input power level until the DUT is well into gain compression i.e. Pout vs Pin decreases by 3dB.

The input power level is then adjusted such that the device is operating at 1dB gain compression, this is then the required input power level for the amplifier. Finally the stub tuners are finely adjusted to give the required minimum of 400mW of power output.

These stub impedances are then measured on the HP8410C Network Analyser in the same manner as for the low-noise source impedance measurements in Section 4.3.3.

This procedure is then repeated for 3.6, 3.8, 4.0, 4.2, and 4.4GHz to complete the set of Load-Pull Data recorded in Table 4.4.1 below:

MGF2116 LOAD-PULL DATA				
FREQ (GHz)	Pout (dBm)	Pin (dBm)	$S11^*$	$S22^*$
3.6	26.2	21.7	0.339/-169	0.193/-170
3.8	26.3	21.8	0.199/-132	0.138/-142
4.0	26.2	21.5	0.146/-140	0.133/-138
4.2	26.4	21.6	0.186/-145	0.170/176
4.4	26.3	21.5	0.175/-150	0.178/160

TABLE 4.4.1: MGF2116 Load-Pull and Source-Pull Data.

It must be noted that these s-parameters are considerably different to the small-signal s-parameters measured previously in Section 4.2.

Also it must be added that the efficiency of the amplifier is not considered in this design since maximum power capability is required and therefore power cannot be traded for efficiency and thus eliminates the necessity of plotting Load-Contours at each frequency on the Smith Chart [35]. This greatly simplifies the design and measurements by only requiring one set of load-pull measurements at each frequency.

J.L. Hutchings describes the equipment required and the necessary measurements needed for the complete load-pull characterisation of power transistors in his Thesis [35].

CHAPTER 5. AMPLIFIER DESIGN AND OPTIMISATION.

5.1. INTRODUCTION

High frequency amplifier design, in general, is performed using a Smith Chart by calculating the necessary amplifier source and load impedances required to achieve a desired response. These calculated impedances are then realised with either distributed transmission line elements or with lumped element components.

However, designs using Smith Charts become increasingly limited in application as the required bandwidth of the amplifier increases. The result is that the Smith Chart is rarely used as the only design tool in broadband amplifier design and is normally used in conjunction with circuit optimisation programs, which are able to adjust designed circuit parameters, in order to improve the amplifier theoretical responses. This is normally done by searching, in software, for a global minimum in the error between the theoretical and desired responses. Such an optimisation program is Touchstone, described in Chapter 3. Touchstone will be used for the circuit optimisation process in this dissertation.

Since the amplifiers are to be designed on microstrip softboard, the Smith Chart will be used to design the required distributed component impedance networks for the device, using the appropriate device characterisation parameters listed in Chapter 4 Table 4.2.1-3.

These designs will then be used as a basis from which Touchstone can optimize the appropriate networks for the required amplifier

responses.

Once the desired response has been obtained, the microstrip circuit mask will be drawn at an enlarged scale and photographically reduced in order for it to be etched onto the microstrip softboard, using conventional etching techniques.

An important consideration in amplifier design is the amplifier stability which is often very critical, especially in the case of power amplifiers which have extremely high gains at lower frequencies.

To determine the regions on a Smith Chart, or impedances, that will produce oscillations, stability circles are plotted for each frequency of interest. The facility of plotting stability circles is offered by Touchstone and it is therefore unnecessary to discuss the relevant equations [38].

In order to determine the regions of stability with the stability circles, the source and load reflection coefficients are checked within and without the circles.

If the source/load reflection coefficient is less than unity in the circle, then this region is the stable region, if it is greater than unity, then this is the unstable region and the rest of the Smith Chart is the stable region.

At this point it must be noted, however, that since Touchstones optimiser is to be used to optimize the amplifier responses, at no cost of using the program a limit has to be set on the accuracy required in the initial Smith Chart design, in order to save time.

A suitable limit, is to design the appropriate matching networks at the arithmetic center frequency of the bandwidth, for the maximum unilateral gain, noise-figure or output power.
Thus, the design is essentially narrowband with Touchstone being used to 'design' for a wider bandwidth of operation.
Now, since the amplifiers are required to achieve a 2- to 6-GHz bandwidth, suitably efficient matching networks should be chosen. It is well known that for microstrip, the broadest bandwidth can be achieved with open or short circuit stubs. (It is difficult to obtain good short circuits without expensive through-hole plating facilities). However the less stubs used, the less losses are incurred by the networks and thus, both single- and double-stub matching networks will be investigated for each amplifier.

5.2. MAXIMUM GAIN AMPLIFIERS

5.2.1. Introduction

In the design of the maximum gain amplifier, the most important consideration is the transistor power gain.
Since, for FET's, S12 is negligible, the transistors may be considered unilateral.
It is well covered in the literature, that the maximum unilateral gain occurs for conjugate matching of the input and output ports of the transistor, as shown in Figure 5.2.1, [36].
For $T_s = S_{11}^*$, G_s is equal to a maximum and for $|T_s| = 1$, G_s has a value of zero. Thus for any value of G_s between these extremes, solutions of T_s lie on a circle [Equation

5.2.11.

For $G_s = 0 < g < G_{s\,max}$

$$g = \frac{1-|\Gamma_s|^2}{|1-\Gamma_s S_{11}|^2} \qquad \ldots\ldots (5.2.1)$$

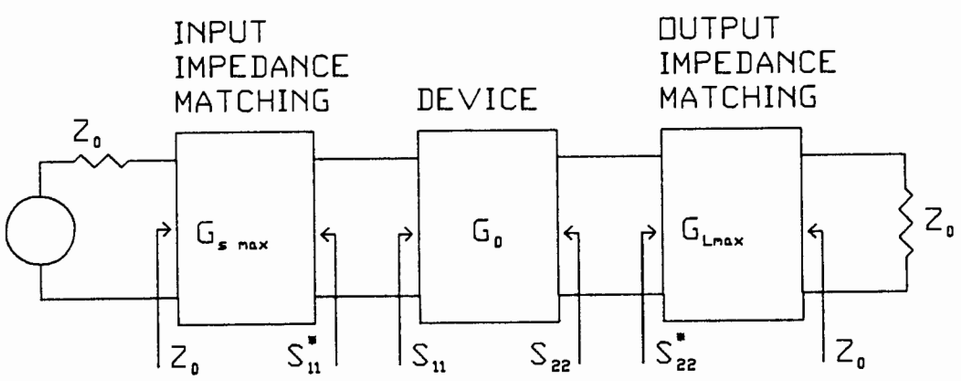

$$G_{umax} = \frac{1}{1-|S_{11}|^2} \cdot |S_{21}|^2 \cdot \frac{1}{1-|S_{22}|^2}$$

$$= G_{smax}\,[dB] + G_0\,[dB] + G_{lmax}\,[dB]$$

FIGURE 5.2.1: Amplifier Maximum Unilateral Gain. Where G_0 is the transistor gain S21, G_{SMAX} - the input network gain and G_{LMAX} - the output network gain.

In the design of amplifiers it is convenient, although time consuming, to plot these circles on a Smith Chart so that a suitable matching impedance (Γ_s) may be chosen to satisfy certain gain-bandwidth requirements. However, Touchstone can plot these circles automatically and therefore the equations will not be discussed in this dissertation [38].

Thus using the results of Section 4.2.4, Table 4.2.1-3, the device s-parameters and the the gain circles, the amplifiers can be designed for any gain and theoretically for any bandwidth.
For broadband designs however, the gain circles are plotted for two frequencies, at the band-edges, and then a corresponding matching network derived that satisfies the gain requirements at the band edges, thereby ensuring a flat gain response. However this technique is limited to small bandwidths of an octave or less, above which, circuit optimisation programs, such as Touchstone, are necessary.

In order to maximise the transistor gain, the input and output ports must be conjugately matched. Before this can be done, the stability of the amplifier must be investigated to determine whether it will oscillate with certain values of impedance used for the matching networks.

The stability circles of the devices were plotted with the regions of instability within the circles. This implies that a source or load impedance lying within these circles will produce oscillations. Thus for the design, the realised network impedances must be well clear of the circles.

5.2.2. Maximum Gain Amplifier Design (MGF1403, 2-6GHz)

a) **MGF1403 Single-stub Matching:** Choosing the arithmetic center frequency of 4-GHz, from Table 4.2.2 the device s-parameters at 30mA drain current are:

$$S11 = 0.692 \angle -54^\circ \qquad S21 = 2.692 \angle 120^\circ$$

$$S12 = 0.042 \angle 102^\circ \qquad S22 = 0.556 \angle -29^\circ$$

Using this data, a single stub amplifier was designed at 4-GHz and then optimised for gain and bandwidth on TOUCHSTONE in order to investigate the maximum bandwidth achievable with single-stub matching circuits. The optimised circuits response is shown in Figure 5.2.2 below:

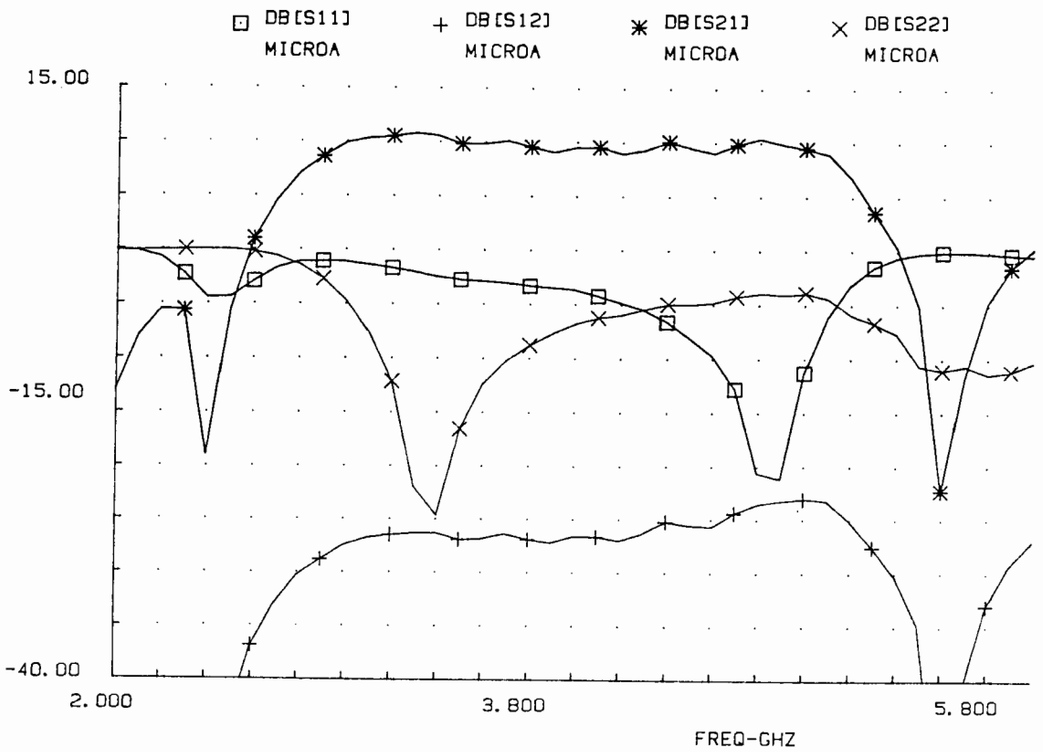

FIGURE 5.2.2: MGF1403 Single-Stub matching: - optimised for gain-bandwidth, on Touchstone.

With single-stub matching Touchstone predicted a maximum bandwidth of 3- to 5-GHz at a gain of 9.8 ± 0.9dB as shown in Figure 5.2.2.

Since the bandwidth requirements of the amplifier, set out in the dissertation objective, is a bandwidth of operation from 2- to 6-GHz, single-stub matching is inadequate. Thus, to increase the bandwidth, two-stub matching networks will now be designed.

b) **MGF1403 Double-Stub Matching:** As in the case of single-stub matching in (a) above, double-stub matching will be performed for best match at the arithmetic center frequency, 4-GHz. Thus, using the same s-parameters in Table 4.2.1, a double-stub matching circuit is designed on a Smith Chart. The techniques of which are well covered in the literature [36].

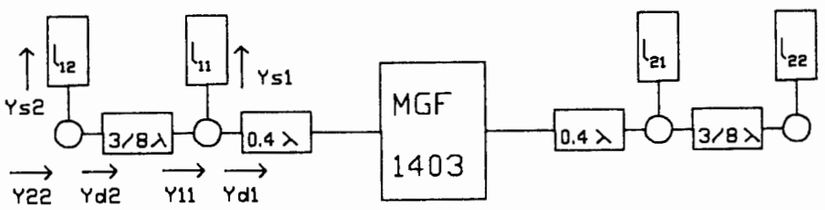

FIGURE 5.2.3: MGF1403 Schematic diagram of amplifier using double-stub matching, showing line lengths found on the Smith Chart.

NOTE: The following steps to convert the Smith Chart designed data into microstrip circuits on Touchstone are repeated for all the following amplifier designs and therefore for the sake of repetitiveness will not be repeated in the future sections.

From the Smith Chart the appropriate microstrip line lengths in Figure 5.2.3 are found:

$l_{12} = 0.289\ \lambda_m$ $\quad$ $l_{21} = 0.353\ \lambda_m$

$l_{11} = 0.467\ \lambda_m$ $\quad$ $l_{22} = 0.300\ \lambda_m$

Taking the wavelength in microstrip, λ_m, as 57.69mm the corresponding microstrip line lengths are: [APPENDIX D Wheelers' graphs]:

$l_{11} = 26.94$mm $\quad$ $l_{21} = 20.36$mm

$l_{12} = 16.67$mm $\quad$ $l_{22} = 17.31$mm

The distance between stubs is 3/8 λ_m = 21.63mm and the distance of the first stub from the device is 0.4 λ_m = 23.08mm.

Using RT Duroid 5880 microstrip softboard and a 50 ohm characteristic impedance as in (a), the line widths are: W=2.3965mm (from Formula 9 in Reference [37]).

This circuit was then modelled and optimised on Touchstone, as described in Chapter 3, to obtain a flat gain response from 2- to 6-GHz.

The final result was an amplifier with 9.54 ± 1.8dB gain from 2- to 6-GHz. The response is shown in Figure 5.2.4 with a schematic of the amplifier showing the line dimensions.

Now that the amplifier has been designed and optimised for a 2- to 6-GHz bandwidth it can now be fabricated. However, the stability of the amplifier must be investigated to ensure that the amplifier will not oscillate.

Touchstones facility to plot the stability circles of the amplifier was used, with the amplifier stability circles given

in Figure 5.2.5 below. The regions of instability are within the circles.

It can be seen that the amplifiers' output is open or short circuit unstable, with the regions of instability limited to extremes of the Smith Chart. Thus, since the amplifier will be connected to a 50 ohm load, the amplifier will be stable under the normal range of operating conditions.

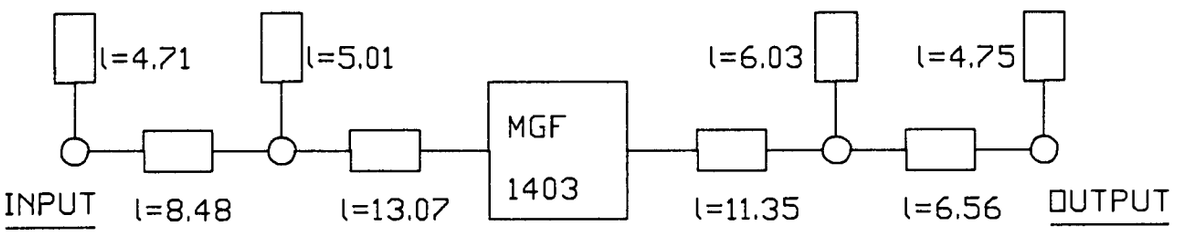

(all line lengths are in millimeters and line characteristic impedance is 50 ohms)

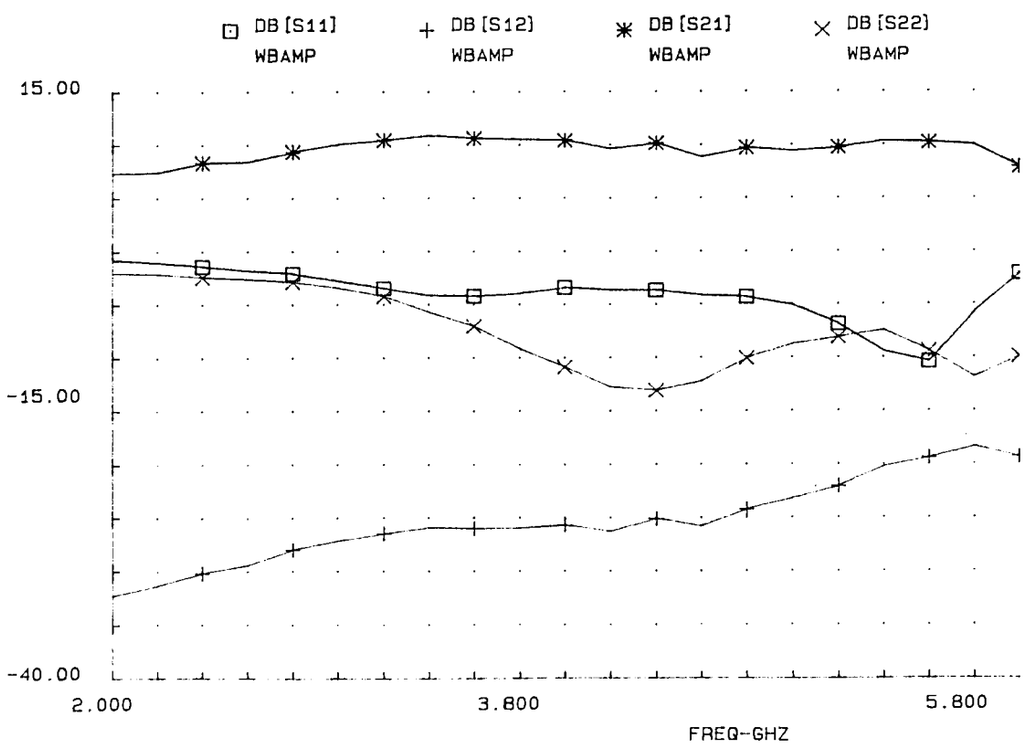

FIGURE 5.2.4: MGF1403 Touchstones optimised double-stub amplifier circuit and its response.

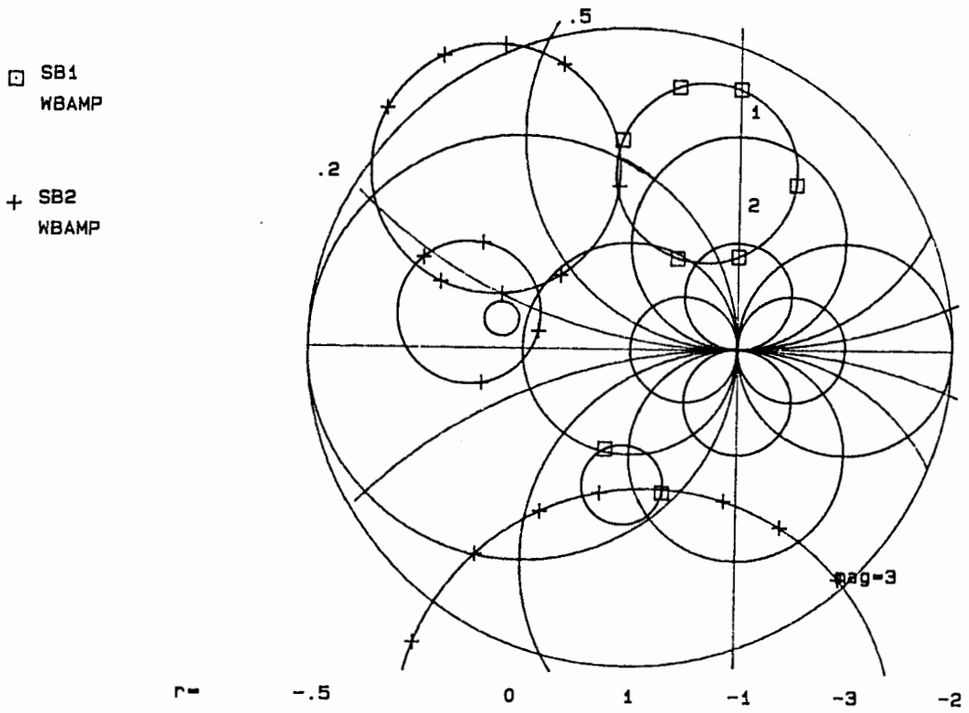

FIGURE 5.2.5: MGF1403 Maximum Gain Amplifier Stability Circles.

This amplifier layout is now drawn to 4-times full scale and then photographically reduced to the correct size. The photomask used for etching the circuit is shown below:

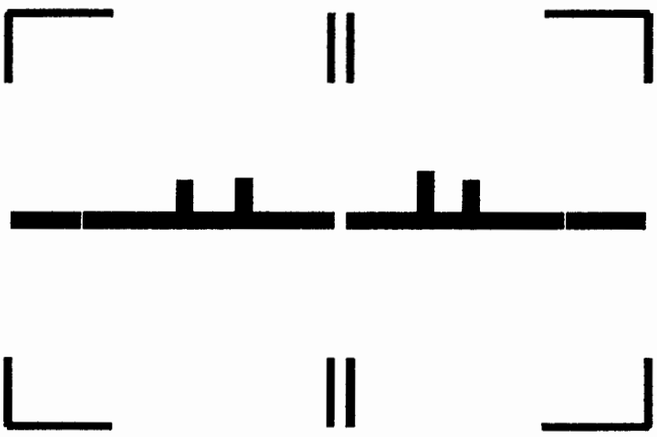

FIGURE 5.2.6: MGF1403 Maximum Gain Amplifier Mask.

5.2.3 Maximum Gain Amplifier Design using the Manufacturers Data (MGF1403)

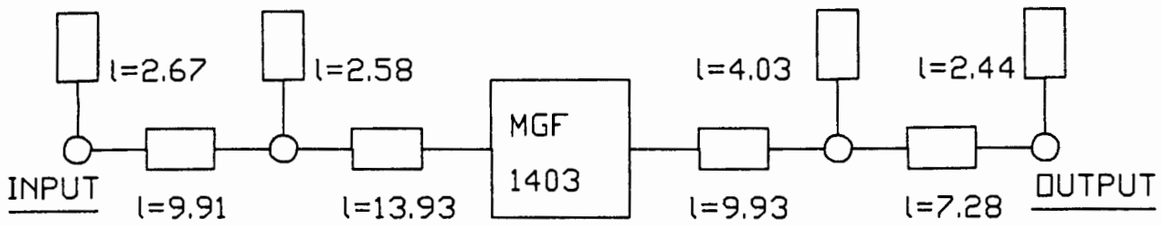

(all line lengths are in millimeters and line characteristic impedance is 50 ohms)

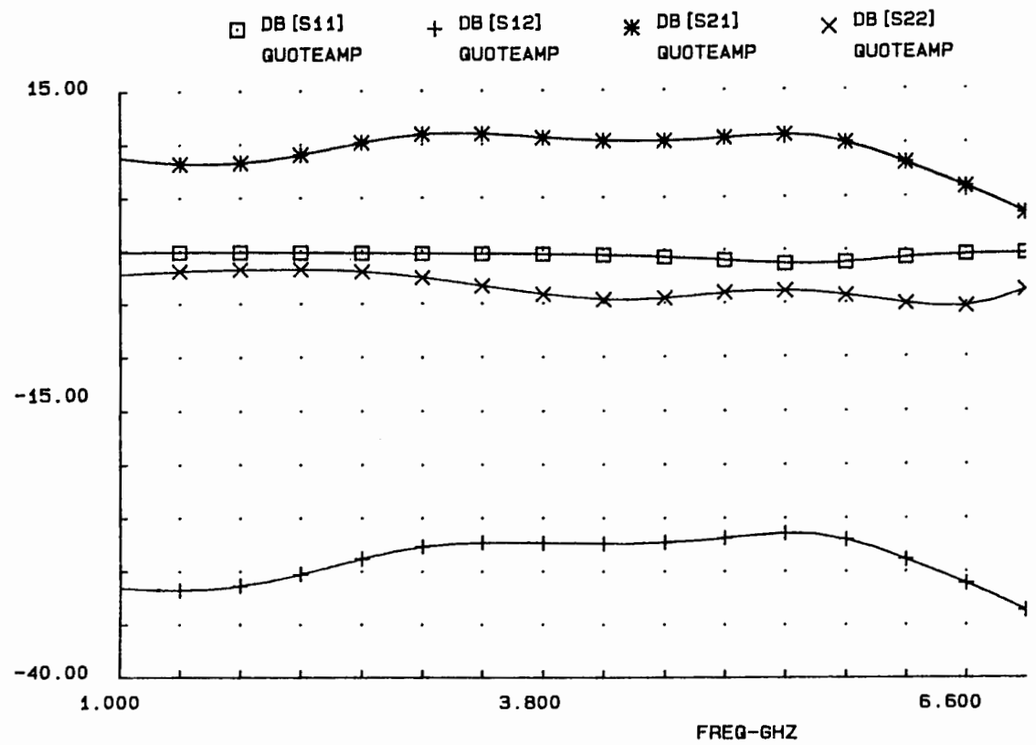

FIGURE 5.2.7: a) Schematic diagram of the optimised maximum gain amplifier using the manufacturers data.
b) Predicted amplifier response.

From Appendix C, Section A, the manufacturers s-parameters at 4-GHz and 30mA drain current for the MGF1403 GaAs FET are:

S11 = 0.933 / -81.3° S21 = 2.851 / 101.3°

S12 = 0.037 / 36.5° S22 = 0.741 / -56.9°

Using this data, double-stub impedance matching networks were

designed and then optimised on Touchstone.

The schematic diagram of the optimised circuit and its predicted response is given in Figure 5.2.7 above.

This predicted response gives an amplifier with:

10.3 ± 1.2dB gain from 2- to 6-GHz,

as opposed to the design using the measured s-parameters, which gave an amplifier with:

9.54 ± 1.8dB gain from 2- to 6-GHz.

Thus it seems that Touchstone is able to optimize the manufacturers data circuit far easier than the measured data circuit. However, a real comparison can only be made by constructing the amplifiers and testing them.

5.2.4. Maximum Gain Power Pre-Amplifier (MGF2116, 3.7 - 4.2GHz).

In order that a power amplifier operate efficiently, it must be driven into saturation. The input power level required to do so is achieved by cascading the required number of small-signal power pre-amplifiers.

The small-signal power amplifiers are designed in the same manner as for the Maximum Gain Amplifier using the MGF1403 transistor in Section 5.2. The resulting amplifiers are thus designed for linear operation.

However, when the transistor saturates, its s-parameters vary as a function of the input power level and thus forces the designer to carry out load-pull measurements and to use this data for the design of the power amplifier stage.

It must be recalled that for the purposes of a more exact design,

both the source and load impedance were measured under large-signal conditions.

The value in carrying out the 'Source-Pull' measurements can be found by comparison of the s-parameters of the source-pull data and the small-signal s-parameter-S11.

Using the small-signal s-parameters of the MGF2116 in Table 4.2.3, the procedure of designing the pre-amplifier for maximum gain was carried out in the same manner as for the maximum gain amplifier designed in Section 5.2.2. The s-parameters at a frequency of 4GHz are:

S11 = 0.724 / -171° S21 = 2.455 / 57°

S12 = 0.056 / 25° S22 = 0.320 / -143°

Firstly single-stub matching was attempted, but the bandwidth was too narrow, and finally double-stub matching proved to be the solution for an amplifier with 11 $\pm$ 0.5dB gain from 3.7- to 4.2-GHz.

Note that the bandwidth obtainable for this transistor is less than that for the low-noise transistor. This is due to the power transistor package having more parasitic reactances and the fact that the physical layout of the transistor necessary for power operation degrades the input impedance to a near open circuit characteristic.

Touchstones' optimiser was used extensively in order to obtain the required gain and frequency response of the amplifier as described in Chapter 3.

The resulting amplifier schematic diagram is shown below in Figure 5.2.8.

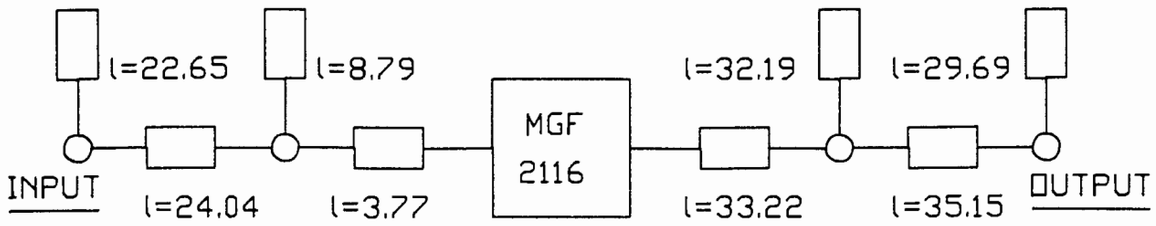

(all line lengths are in millimeters and line characteristic impedance is 50 ohms)

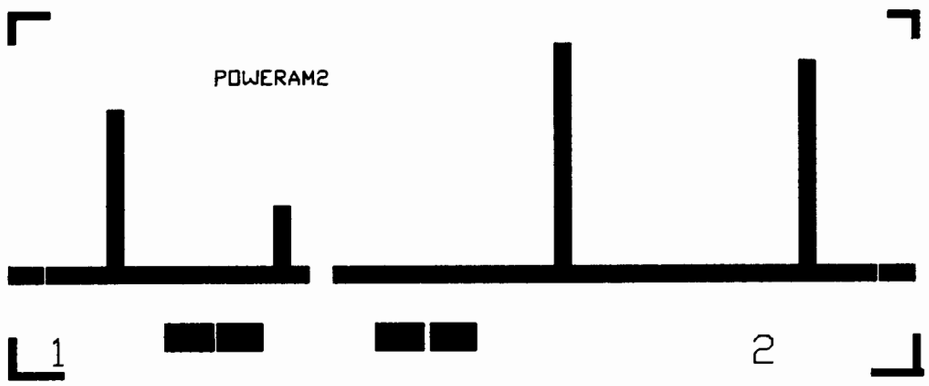

FIGURE 5.2.8: MGF2116 Power Pre-Amplifier Schematic diagram and Circuit Mask.

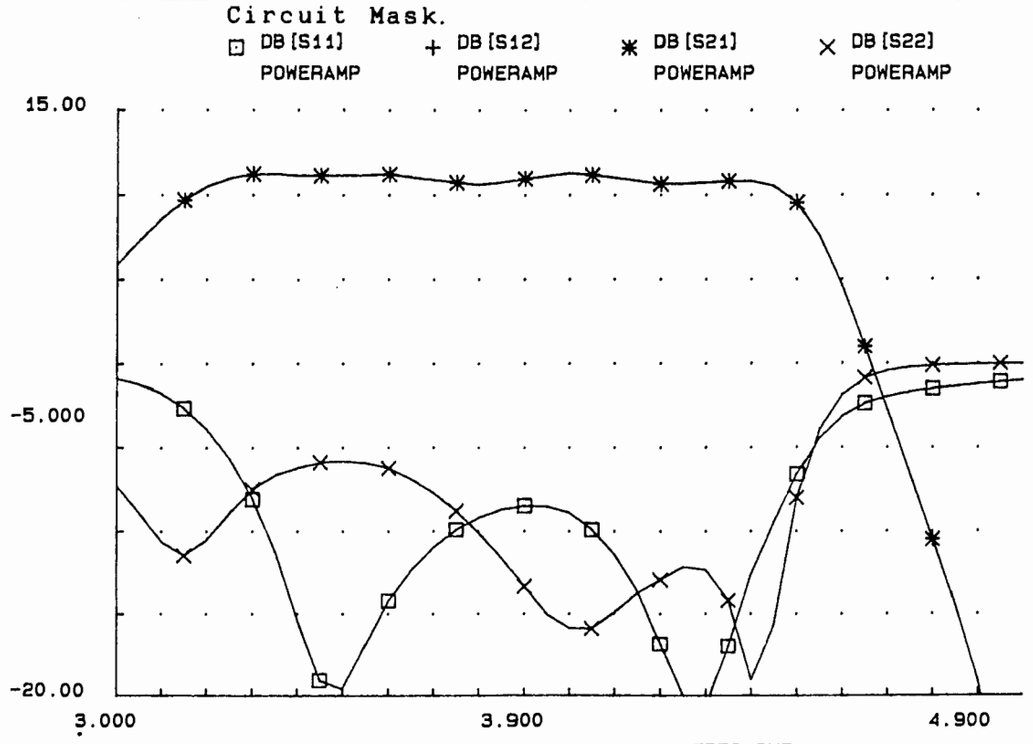

FIGURE 5.2.9: MGF2116 Power Pre-Amplifier Theoretical Response.

Touchstones' optimised predicted response for the amplifier is shown in Figure 5.2.9 above.

Finally, the stability of the amplifier was checked by plotting the stability circles on Touchstone. The relevant stability circles are shown in Figure 5.2.10 below.

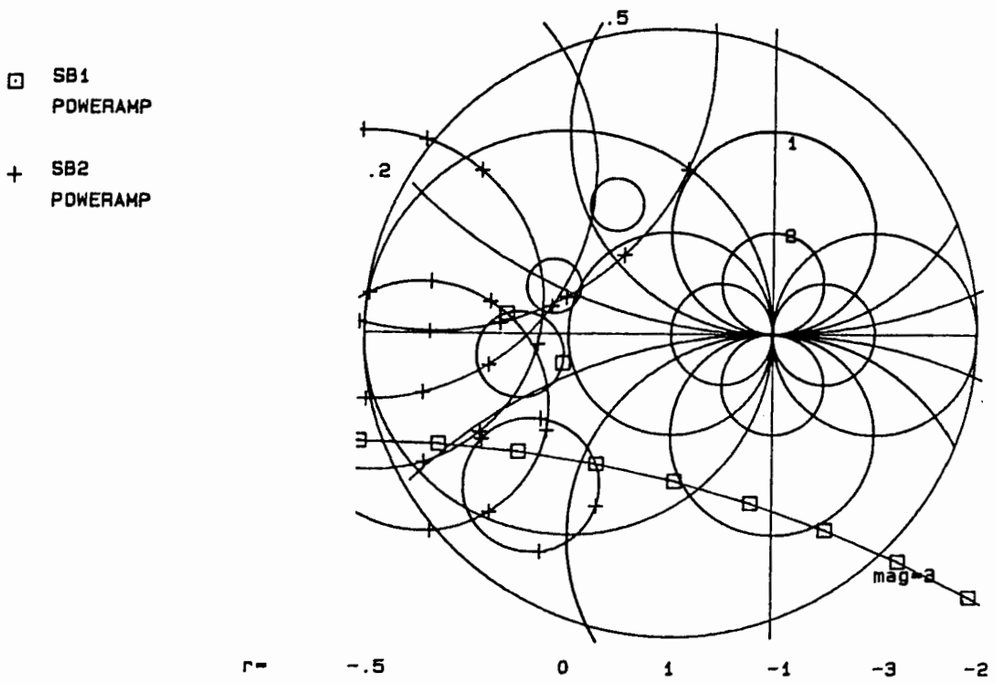

FIGURE 5.2.10: MGF2116 Pre-Amplifier Stability Circles.

The regions of instability are inside the circles and are all well away from the 50 ohm impedance point. Thus, since the amplifier is to be tested and used in a 50 ohm characteristic impedance environment, the amplifier will be stable.

5.3 LOW-NOISE AMPLIFIER DESIGN(MGF1403, 2-6GHz).

5.3.1 Introduction

For the design of low-noise amplifiers, the most important consideration is the amplifier noise-figure. However, this is not the only consideration. The amplifier gain must also be at a maximum, without deteriorating the noise-figure and in the case of wide-band amplifiers, the gain response must be as flat as possible.

Another important consideration in the design is amplifier stability, as in the case of the previous maximum gain amplifiers.

5.3.2 Low-Noise Amplifier Design.

Using the noise-parameters in Table 4.3.1, a family of noise-figure circles can be plotted on a Smith Chart, [38], either manually using the appropriate equations or by Touchstone.

The plotting of these circles then gives the noise-figure for the transistor (MGF1403) for any arbitrary source impedance at a particular frequency.

Since the gain of the amplifier must also be taken into account, a family of gain circles will also be plotted, on the same Smith Chart as the noise-figure circles, using the device s-parameters measured at 10mA drain current for low-noise operation, (see Appendix A) and listed in Table 4.2.1.

These families of noise-figure and gain circles are plotted for

both 3- and 5-GHz, to enable the design to be broad-banded and are shown in Figure 5.3.1, for the input circuit.

From the input gain and noise-figure circles in Figure 5.3.1 (a), one can observe the necessary design trade-offs between best noise-figure or best gain. Since the requirement of the amplifier is to have as low a noise-figure as possible, the shaded region of the Smith Chart indicates the range of source impedances required to realise a broadband, low-noise amplifier.

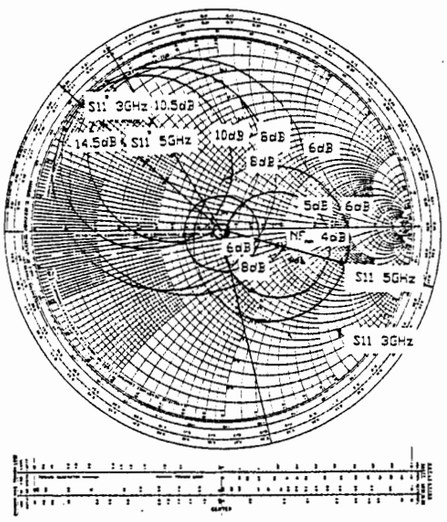

FIGURE 5.3.1: MGF1403 Input Noise-Figure and Gain circles at 10mA drain current for 3- and 5-GHz.

Thus, from the Smith Chart, choosing an impedance in this region will give an amplifier with less than 5dB noise-figure at 3GHz. The gain will vary from greater than 6dB at 5GHz to greater than 8dB at 3GHz. However it must be noted that the source impedance required is practically that of 50 ohms - the characteristic line impedance and thus, theoretically, no matching networks are

required on the amplifier input.

So far, the amplifier minimum noise-figure has been taken into account with the source impedance.

In order to maximise the amplifier gain, the load impedance is now designed on a Smith Chart, for best conjugate match at 4-GHz. Thus, taking the device s-parameters at 4-GHz and 10mA drain current, listed in Table 4.2.1:

$$S11 = 0.750 \angle -50^{\circ} \qquad S21 = 2.16 \angle 124^{\circ}$$

$$S12 = 0.043 \angle 86^{\circ} \qquad S22 = 0.603 \angle -33^{\circ}$$

and plotting S22 and S22* on a Smith Chart, the appropriate double-stub matching network is found and shown in Figure 5.3.2.

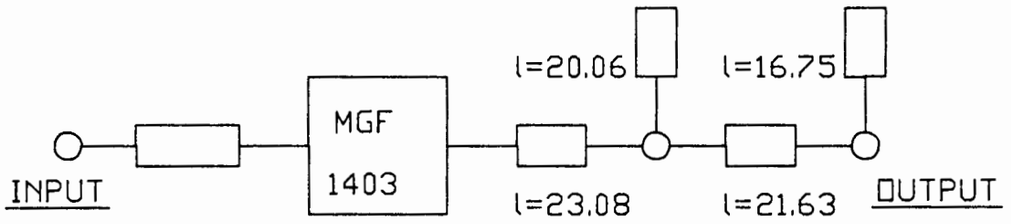

(all line lengths are in millimeters and line characteristic impedance is 50 ohms)

FIGURE 5.3.2: The Low-Noise Amplifier design schematic diagram.

5.3.3 Optimising the Low-Noise Amplifier.

It must be noted that the plotting of the gain and noise-figure circles has a limited accuracy and may thus introduce a certain amount of error in the subsequent design.

Thus, in order to acheive the best noise-figure, an arbitrary value input impedance matching network was entered onto Touchstone along with the associated designed output matching network.

The circuit entered onto Touchstone for optimisation consisted of a single stub matching network at the input, with arbitrary length and a double-stub matching network on the output, using previously designed lengths given in Figure 5.3.2.

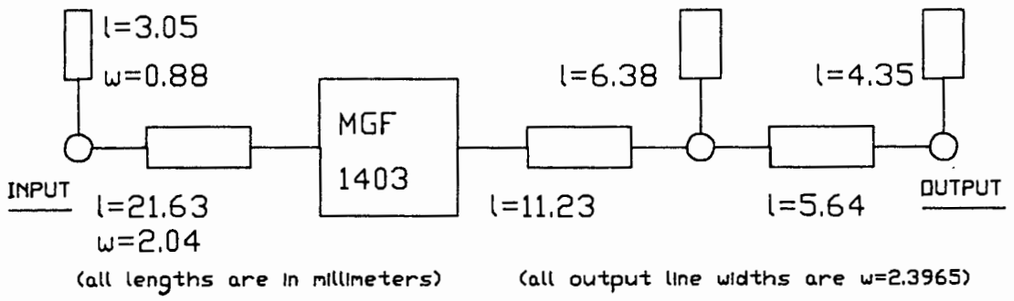

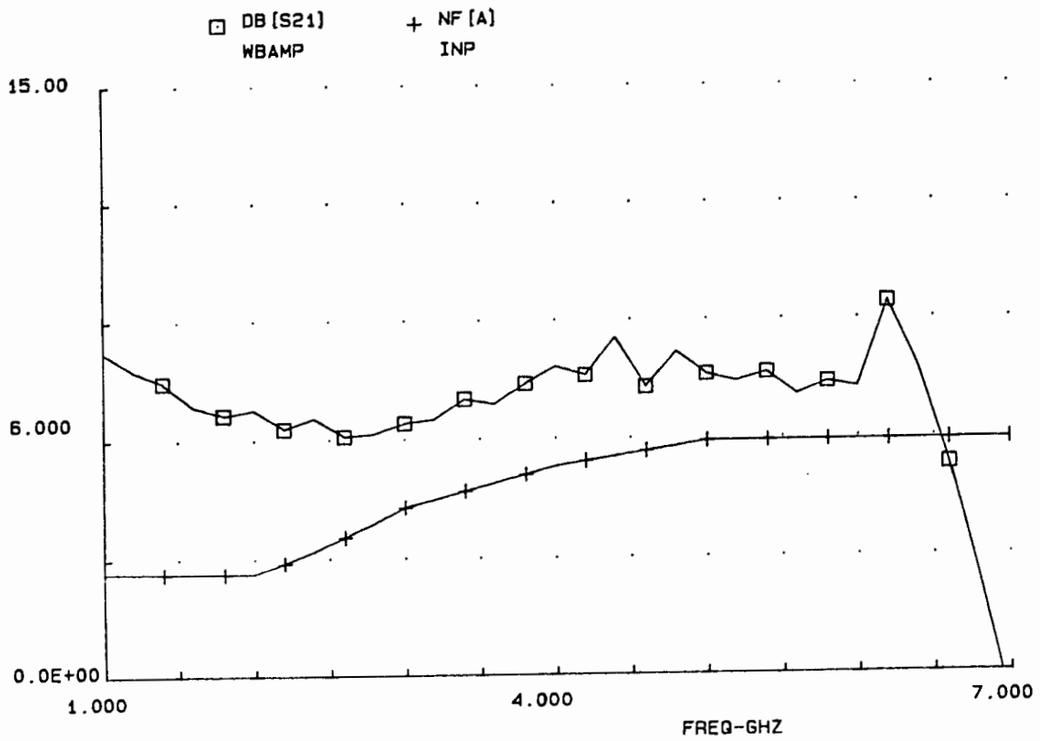

FIGURE 5.3.3: (a) Optimised LNA schematic diagram.
(b) Noise-Figure and Gain response.

The optimiser was then used in the same manner as described in Chapter 3, to firstly optimize the input circuit for best noise-figure and then the output for a flat gain from 2- to 6-GHz. The result was an amplifier (schematic shown in Figure 5.3.3(a)) with a noise-figure less than 6dB and a gain of 7 ± 1.2dB from 2- to 6-GHz. The response is shown in Figure 5.3.3 (b).

Finally, the amplifier stability was checked by plotting the stability circles on Touchstone. The stability circles are shown in Figure 5.3.4. As can be seen, the amplifier is stable over the frequency band and is thus satisfactory.

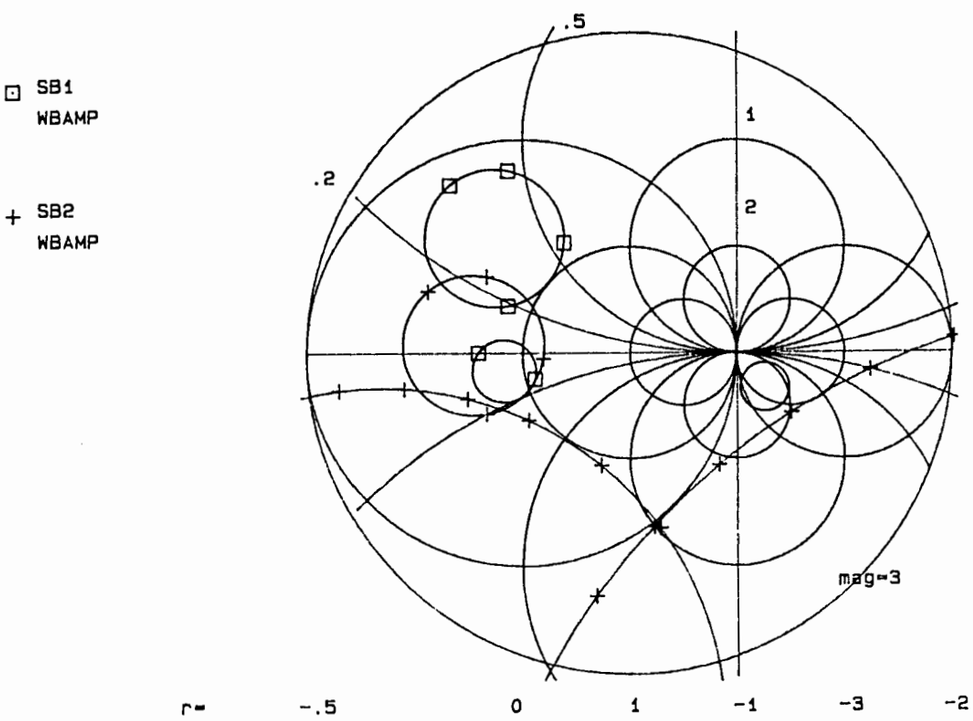

FIGURE 5.3.4: MGF1403 Low-Noise Amplifier Stability Circles.

The corresponding microstrip circuit layout was drawn and photographically reduced to produce a mask which is shown in

Figure 5.3.5.

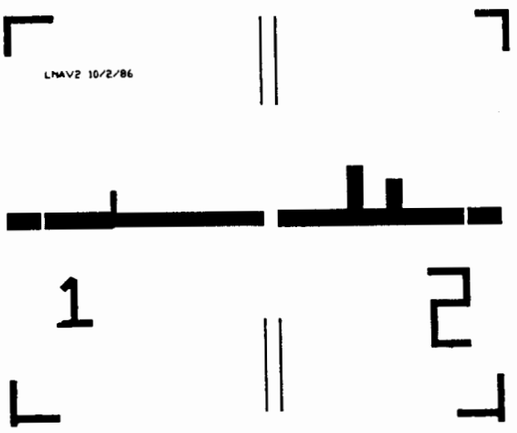

FIGURE 5.3.5: Low-Noise Amplifier circuit mask.

5.4. POWER AMPLIFIER DESIGN (MGF2116, 3.7 - 4.2GHz).

5.4.1. Introduction.

Power amplifier design involves the realisation of the required source and load impedances for the desired operation of the transistor.

These impedances are realised in order to achieve the maximum power output and efficiency of the device over the required bandwidth.

However, in this design the efficiency is of secondary importance to the output power and thus is not considered as a design factor.

Another important consideration in the design is the amplifier stability although this can only be ensured by taking care that

the device does not oscillate whilst doing the load- and source-pull measurements.

5.4.2. Power Amplifier Design and Optimisation.

As in the design of the Maximum Gain Amplifier in Section 5.2, designed for maximum (unilateral) gain, the power amplifier design uses the load- and source-pull data instead of the small-signal s-parameters to design input and output port matching networks that simultaneously conjugately match the transistor under large-signal conditions to 50 ohms.

This achieves maximum power transfer through the transistor amplifier.

However, such information as the device gain -S21 and reverse gain -S12 cannot be determined and are therefore not used in the designs.

Thus, using the Load-pull data in Table 4.4.1 and selecting 4-GHz as the initial Smith Chart design frequency, the required input and output port matching networks were designed by conjugate matching (as in Section 5.2).

Both single- and double-stub matching was attempted and optimised on Touchstone for best conjugate match over the frequency band of interest. As was expected, the double-stub networks yielded the best results. Touchstone predicted that the input and output return loss of the power amplifier to be less than 20dB, as shown in Figure 5.4.1.

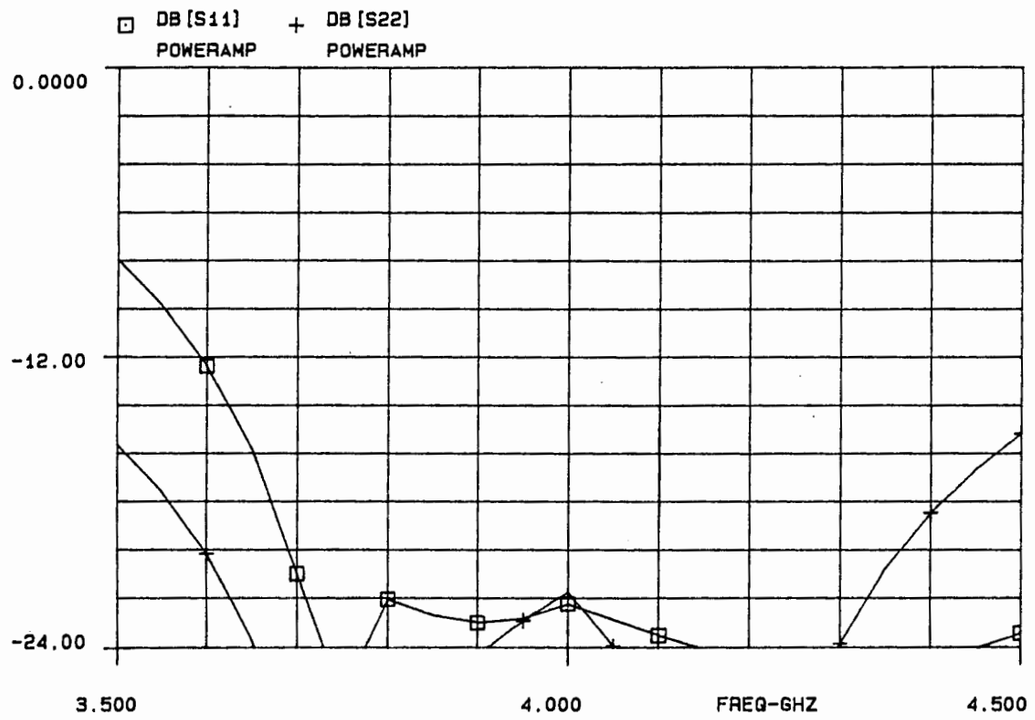

FIGURE 5.4.1: MGF2116 TOUCHSTONE Power Amplifier Input and Output Return Loss (S11 & S22) using Double-stub matching.

A schematic diagram of the optimised power amplifier is given in Figure 5.4.2 below as well as the circuit mask in Figure 5.4.3.

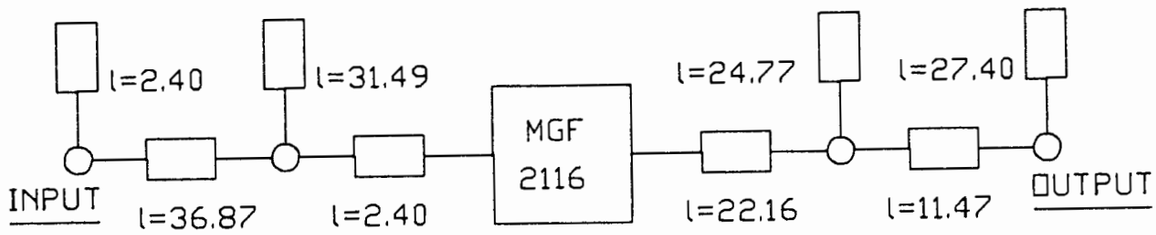

(all line lengths are in millimeters and line characteristic impedance is 50 ohms)

FIGURE 5.4.2: MGF2116 Touchstone optimised double-stub power amplifier schematic diagram.

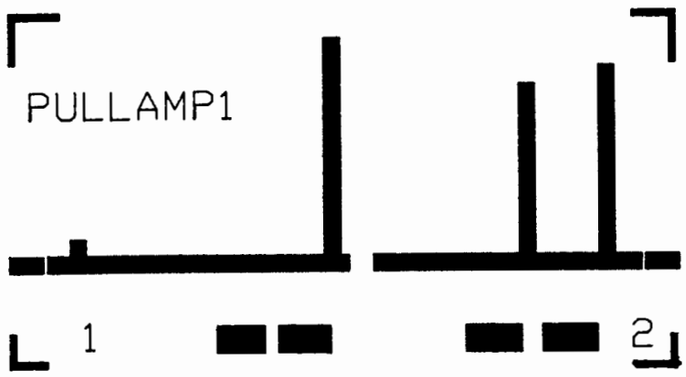

FIGURE 5.4.3: MGF2116 Power Amplifier Mask.

5.5 A NOTE ON BIAS NETWORKS AND DC BLOCKING CAPACITORS

In order to supply power to the active devices in the amplifiers, some means of applying a d.c. bias voltage to the gate and drain leads of the transistor is necessary, the easiest of which is simply to solder the bias leads directly onto the microstrip. However, these leads will significantly effect the amplifier performance by absorbing microwave power or by reflecting it back down the transmission line.

A technique of overcoming this is to use a quarter wavelength high/low-impedance line to supply the dc power. However this technique is frequency dependant and thus is not good for broadband designs.

A suitable technique for broadband biasing, which was used by the author for all the designs, is to supply the dc bias through a

0.15mm diameter wire, threaded twice through a ferrite bead, where the bead is placed as close as possible to the microstrip line. The thin wire acts as a high impedance line, thereby limiting the amount of microwave power entering the bias circuit and the ferrite bead acts to absorb any microwave power that does enter the line, [34].

This power supply, must now be isolated from preceding and following stages of signal processing and is acheived by interrupting the microstrip line at both ports with a 0.5mm gap and then bridging the gap with a thick film 22pF chip capacitor. The use of chip capacitors will introduce significant loss in the circuits since at microwave frequencies, these capacitors are lossy.

CHAPTER 6. AMPLIFIER RESULTS.

6.1 INTRODUCTION

In the design of broadband microwave amplifiers, the use of circuit optimisation programs is essential.
However, these programs use models which are less than perfect. One can therefore not expect them to model the real world accurately. Also, the mere changes in s-parameters from device-to-device play an important role in altering the expected results.

The designer or producer is thus compelled to make certain final adjustments to each and every amplifier or microwave circuit produced, if optimum performance is required.
In lower frequency amplifiers, (I.F. Amplifiers) using discrete components, the use of trimming capacitors is perfectly acceptable for final tuning adjustments. However, at microwave frequencies there is no such thing as trimming capacitors!

There are various techniques of side-stepping this problem on microstrip softboard, all of which consist of sliding pieces of thin conductive material (copper) along the matching networks until the desired response is attained and then glueing them onto the microstrip.
For the following amplifiers, 8BA washers were used for the final tuning of the amplifiers and were glued down with Cyanocrylate adhesive.

It must be noted however that the initial design response must be relatively close to the desired response as the tuning ability is limited to fine tuning.

The amplifiers were etched, using conventional etching techniques, onto RT-Duroid 5880 microstrip softboard. The boards were then machined so as to enable the transistors to be mounted appropriately.

The testing of the amplifiers was carried out with the HP8410C Automatic Network Analyser (ANA), the HP8970A Noise-Meter and the HP435A Power Meter depending on the type of measurements that were performed.

6.2 THE MAXIMUM GAIN AMPLIFIERS.

6.2.1. MGF1403 Maximum Gain Amplifier.

This amplifier, designed in Chapter 5 Section 5.2.2, was tested using the HP8410C ANA.

The ANA was calibrated over the 1- to 7-GHz frequency band, since the amplifier bandwidth is to be 2- to 6-GHz.

A plot of the error corrected gain-S21, of the amplifier was obtained and is shown in Figure 6.2.1.

Clearly this gain response is unsatisfactory, since the gain at 6-GHz is a mere 3dB and 7dB at 2-GHz, rising to 10.2dB at 2.8-GHz and will thus require some tuning in order to achieve the desired gain and bandwidth predicted by Touchstone in Figure 5.2.5.

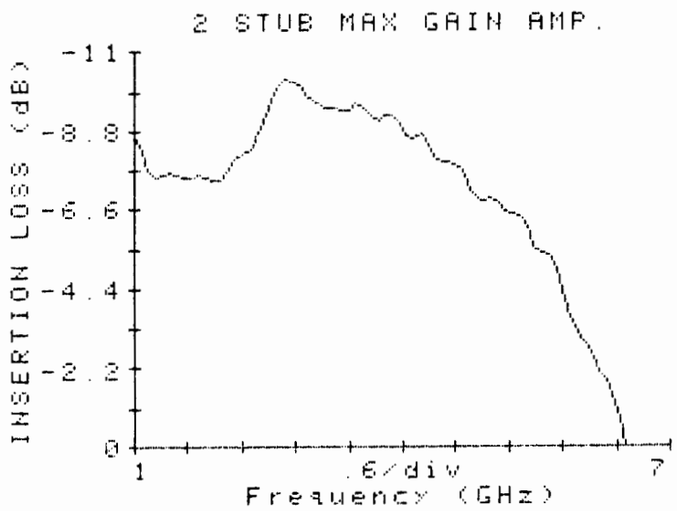

FIGURE 6.2.1: MGF1403 Maximum Gain Amplifier Gain Response.

Note that the input and output impedances are not given as in a balanced amplifier the port impedances of the two individual amplifiers are improved by the quadrature couplers.

Using washers to tune the amplifier, the response improved to 10 ± 1.5dB gain from 2- to 6-GHz. A plot of the tuned gain response is given in Figure 6.2.2.

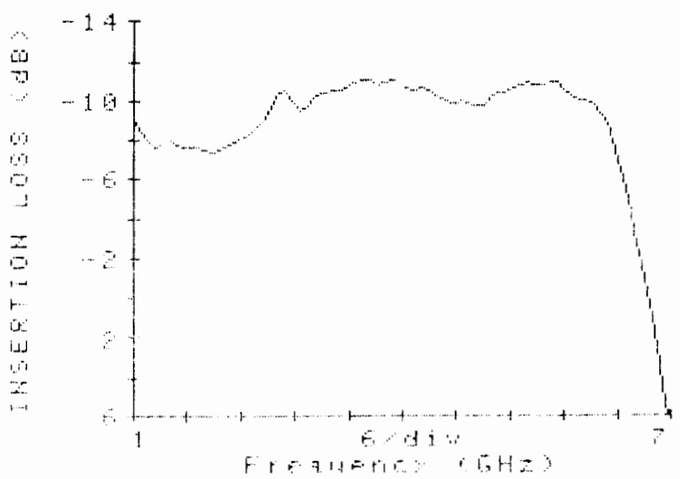

FIGURE 6.2.2: MGF1403 Tuned Maximum Gain Amplifier Gain Response(2-6GHz).

Although the response is quoted from 2-GHz, the amplifier gain remains at 10dB down to 200MHz where the DC blocking capacitors attenuate the signal.
This response now compares favourably with Touchstone in Figure 5.2.4, with approximately 1dB more gain than predicted.

Finally, the noise-figure of the amplifier was measured to be less than 10dB over the bandwidth.

6.2.2. MGF1403 Maximum Gain Amplifier using the Manufacturers Data.

As in Section 6.2.1, the amplifier designed using the manufacturers s-parameters was tested on the ANA, with the plot of the gain response shown in Figure 6.2.3.

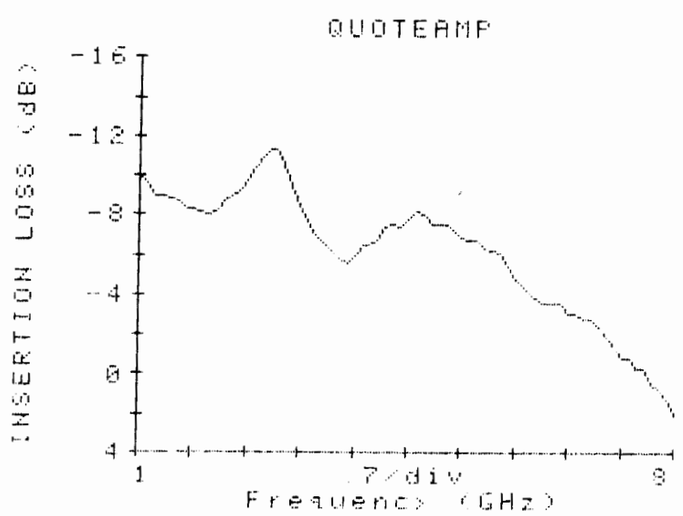

FIGURE 6.2.3: MGF1403 Maximum Gain Amplifier using the Manufacturers data -Gain response.

It can be seen that this response is just as unacceptable as that in Figure 6.2.1. However, for comparison, a table of the gain at specific frequencies is given for the two amplifiers.

MGF1403 Maximum Gain Amplifiers			
FREQ (GHz)	Gain for Figure 6.2.1.	Gain for Figure 6.2.3	Gain difference
1.0	8.7	9.9	1.2
2.0	7.7	8.2	0.5
3.0	9.6	9.5	0.1
4.0	8.6	6.4	2.2
5.0	6.9	7.6	0.7
6.0	3.0	4.3	1.3
7.0	-8.0	2.4	10.4

TABLE 6.2.1: Maximum Gain Amplifier comparisons.

From the table, referring to the differences in the gain, the two amplifiers are very much the same.

The slight deviations can be accounted for by the transistor s-parameter tolerances and in the errors incurred in the photographic reduction process of the amplifier masks as well as in the machining process.

6.2.3. MGF2116 Maximum Gain Power Pre-Amplifier.

The Power Pre-Amplifier is also tested on the ANA. However, since the amplifier was designed to operate over the 3.7- to 4.2-GHz frequency band, the calibration and measurements were performed from 3.0- to 5.0-GHz.

The corresponding plot of the amplifier gain and input return loss is given in Figure 6.2.4.

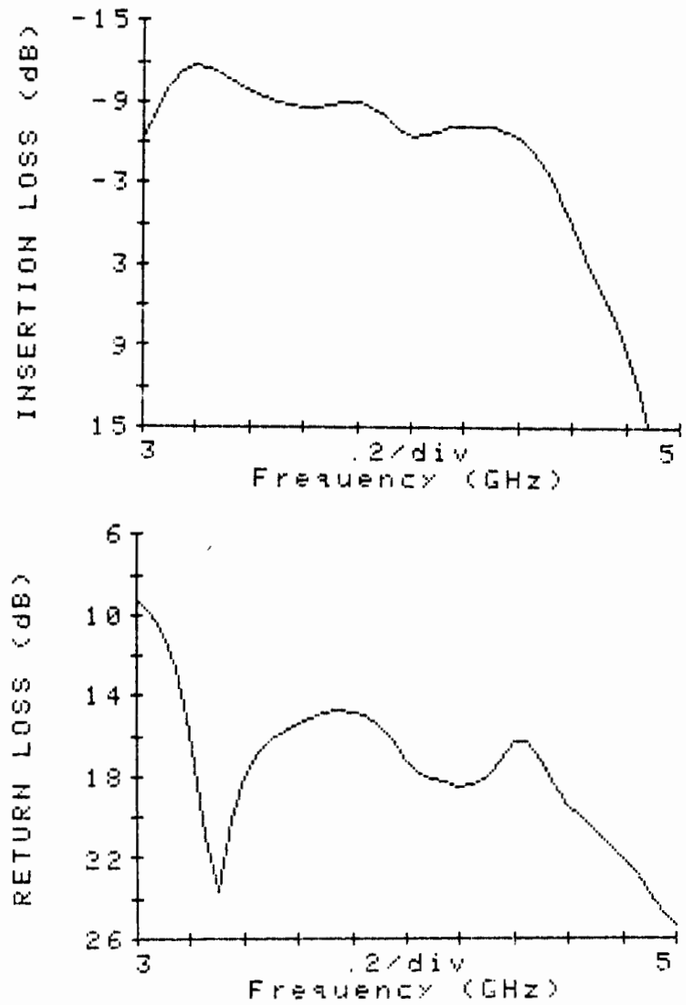

FIGURE 6.2.4: MGF2116 Maximum Gain Power Pre-Amplifier Gain and Input Return Loss.

Since this amplifier is to be used single-ended, the input and output return losses must be less than 20dB for a satisfactory VSWR.

From Figure 6.2.4 it can be seen that some tuning is required in order to obtain a satisfactory response.

The amplifier was tuned with its response given in Figure 6.2.5.

The return loss of both ports was better than 15dB (only the input graph given) with a gain of 8 $\pm$ 0.35dB from 3.7- to 4.2-GHz.

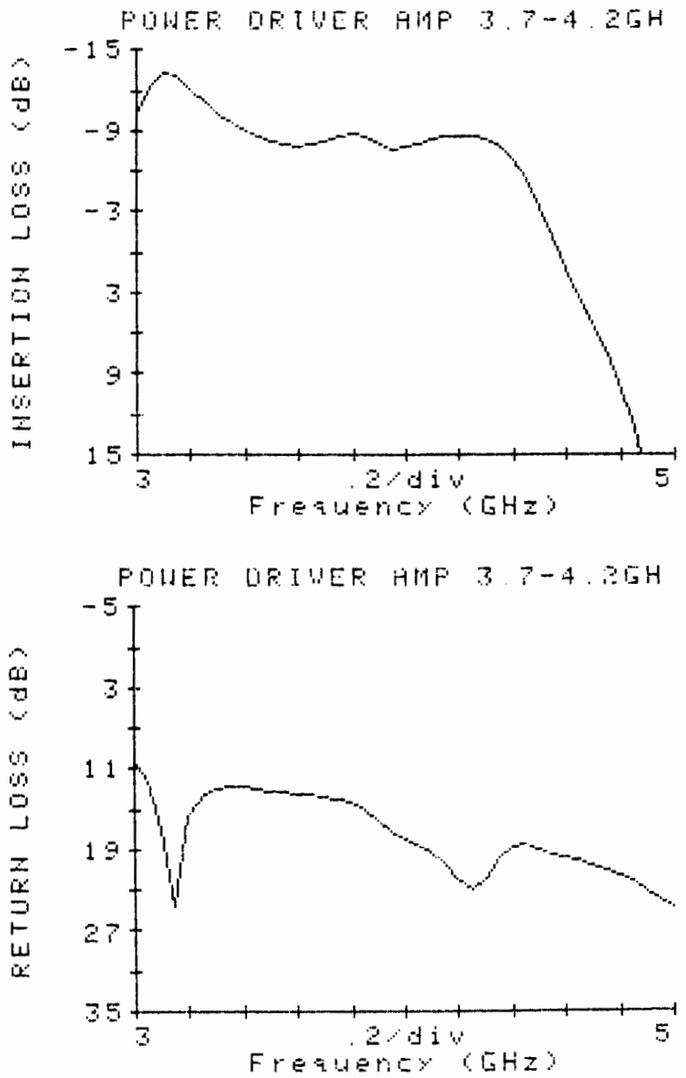

FIGURE 6.2.5: MGF2116 Tuned Maximum Gain Power Pre-Amplifier Gain and Input Return Loss.

Touchstones gain response for this amplifier was 11 ± 0.5dB (Figure 5.2.9.).

There is thus a discrepancy of 2.8dB, which can mainly be attributed to the use of thick film capacitors for DC blocking. Thick-film capacitors are extremely lossy at microwave frequencies (no microwave capacitors were available).

Touchstones circuit models played a role in further deteriorating

the gain of the amplifier, as well as the variations in device s-parameters.

However, the gain response of the amplifier in Figure 6.2.5 is satisfactory for the purposes of driving the power amplifier, where a flat gain response over the bandwidth is essential.

6.3 THE LOW-NOISE AMPLIFIER.

The low-noise amplifier was tested in a Faraday cage to reduce interference, using the HP8970A Noise Meter and its associated peripheral equipment, discussed in Chapter 5 for the noise parameter characterisation.

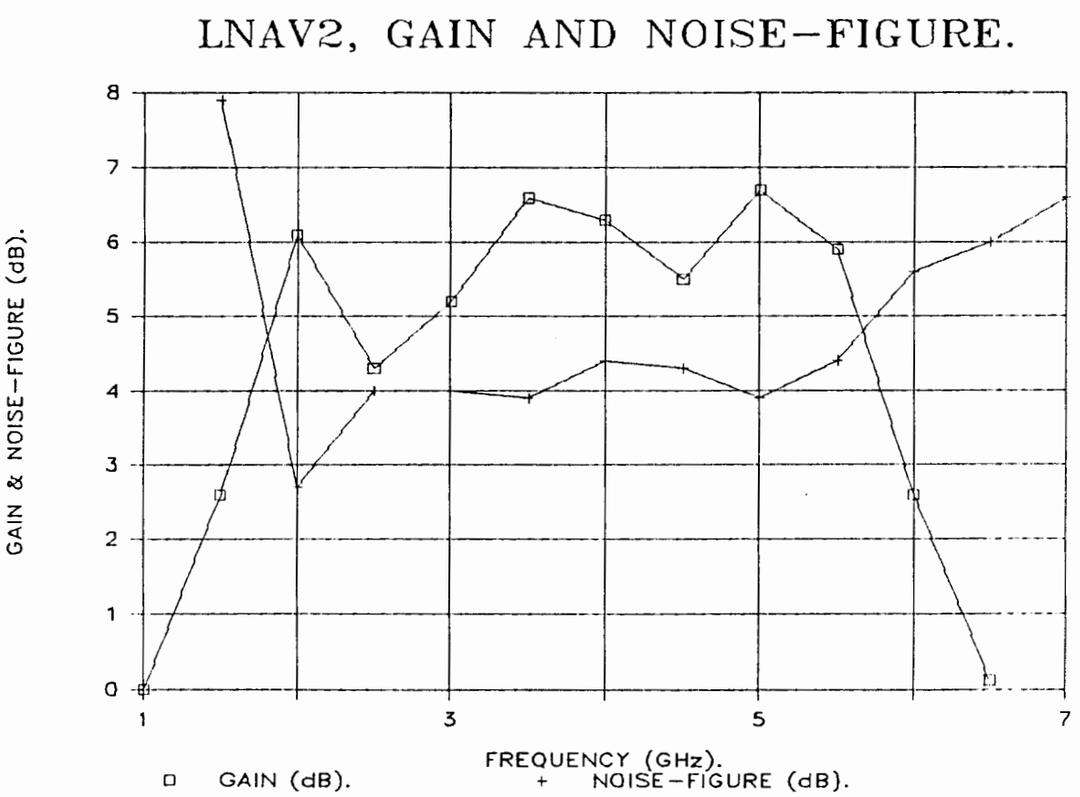

FIGURE 6.3.1: MGF1403 Low-Noise Amplifier Gain and Noise-Figure.

As discussed in Section 6.1, the initial amplifier measurements indicated that it required some tuning, in order to acheive a flatter gain response and a noise-figure of better than 6-dB over the 2- to 6-GHz bandwidth.

A graph of the untuned low-noise amplifier noise-figure and gain is given in Figure 6.3.1.

Using washers for tuning the amplifier, the amplifier gave a noise-figure of less than 5dB from 2- to 6-GHz with the lowest noise-figure of 2.7dB at 2-GHz.

The associated gain was 5.4 ± 1.4dB over the bandwidth as shown in Figure 6.3.2.

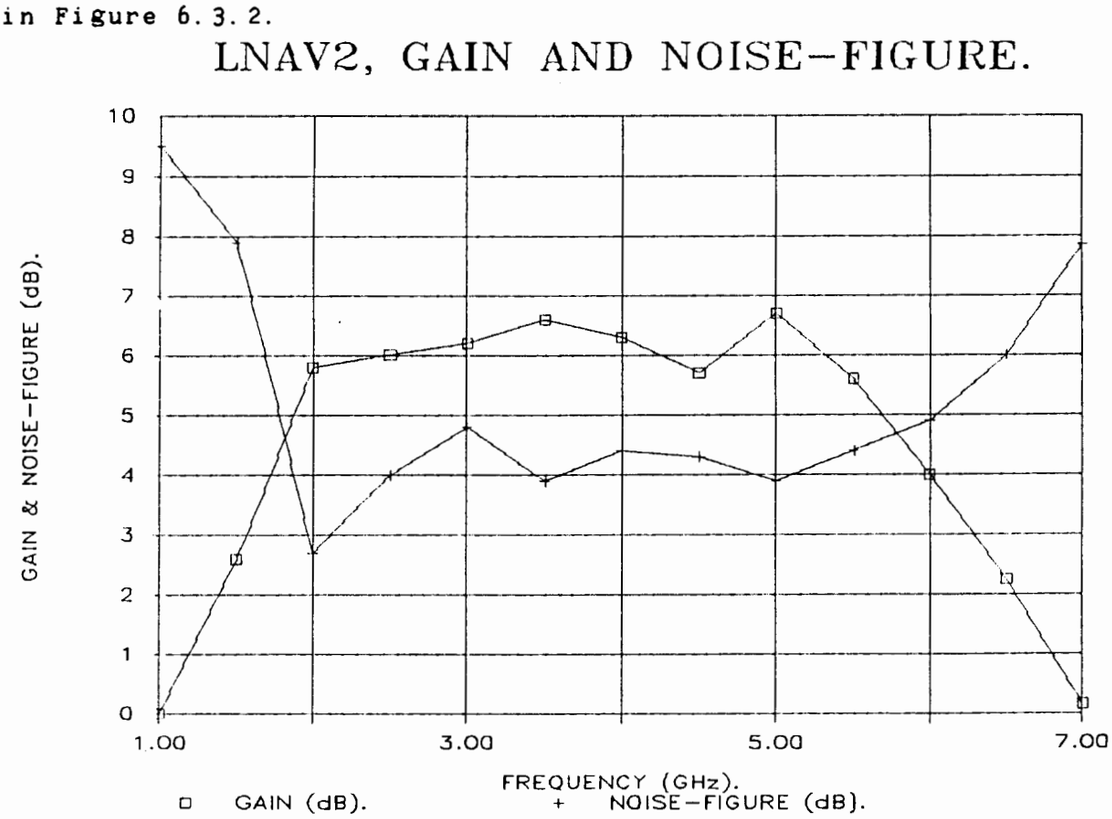

FIGURE 6.3.2: MGF1403 Tuned Low-Noise Amplifier Gain and Noise-Figure.

It can be seen from the above graphs that the initial amplifier response was close to the desired response, thus requiring little tuning.

Comparing the tuned response in Figure 6.3.2 and that predicted by Touchstone in Figure 5.3.3(b), one can observe that the actual noise-figure is 1dB lower, but the gain is less than the predicted 7 ± 1.2dB at 5.4 ± 1.4dB.

The difference in the noise-figure is small, but nevertheless must be attributed to errors in the noise-parameter measurements which are critical. The equipment used was not ideal for calibrating all the second stage noise contributions out of the system.

A smaller source of error in this case is Touchstones noise analysis.

Also, any losses incurred in the amplifier circuit would be exhibited as a reduction in the noise-figure and gain of the amplifier.

There is also a 2dB discrepancy in the gain. This can be attributed to the fact that a better noise-figure requires a source impedance of Z_{opt}, which gives a poor Voltage Standing Wave Ratio (VSWR) in the general case. Also the effect of the load impedance on the noise-figure cannot be ignored and was tuned to obtain a minimum noise-figure, rather than a maximum gain. This resulted in a degradation of the amplifier gain.

Finally, the Low-Noise Amplifier input and output return losses were measured on the HP8410C ANA. The return loss on the input

was better than 5dB and the output return loss was better than 10dB over the 2- to 6-GHz bandwidth.
Since Low-Noise amplifiers are used in a balanced configuration, the poor return losses are not of any concern (refer to Chapter 1).

6.4 THE POWER AMPLIFIER.

The Power Amplifier was tested using the HP8672 Sweep Oscillator with the Power Pre-Amplifier in Section 6.2.3 as the microwave power source and the HP435A Power Meter to measure the output power of the amplifier.

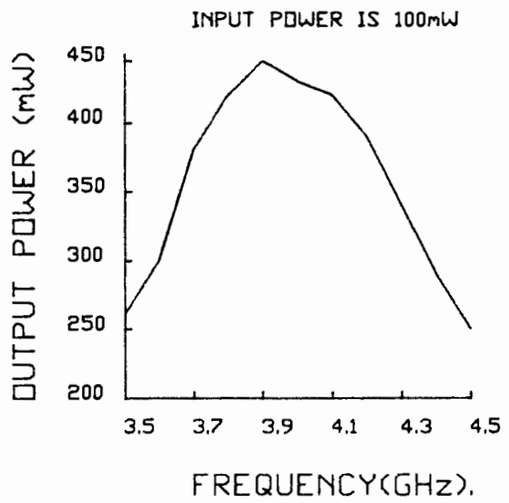

FIGURE 6.4.1: MGF2116 Tuned Power Amplifier Output Power versus Frequency.

Setting the input power at 100mW (20dBm-the 1dB gain compression level), the output power was measured at 0.1GHz intervals from 3.5- to 4.5-GHz. The power amplifier output power was better than

340mW and less than 390mW over the 3.7- to 4.2-GHz bandwidth. Since the transistor was rated at 400mW, and in the load-pull experiments in Chapter 5, the output power was better than 400mW at each frequency in the bandwidth, the amplifier will require some tuning in order to be within the specifications.

With a small amount of tuning the amplifier output power was increased to be better than 390mW and to have a maximum of 450mW at the band center frequency of 3.9GHz as shown in Figure 6.4.1.

From the graph in Figure 6.4.1, it can be seen that the output power at 3.7GHz is 10mW under the minimum specified in Chapter 1.

In a broadband design, the required load and source impedances for maximum power cannot be realised exactly, over the entire bandwidth and thus requires a trade-off of power versus bandwidth.
However, with the use of a swept gain system, the load-pull measurements and the tuning of the amplifier can be carried out far more accurately, for broadband designs. One can therefore expect an improvement in the results by using a more sophisticated measurement system.
Since the amplifier is operating under large-signal conditions and the HP8410C ANA cannot be used to measure the associated s-parameters, no comparison can be made with Touchstones predicted return losses for the amplifier ports.

Lastly, the efficiency of the amplifier is calculated for each frequency, using the efficiency definitions below, and is plotted in Figure 6.4.2.

Drain Efficiency:

= (A.C. POWER OUTPUT) / (D.C. INPUT POWER)

Power Added Efficiency:

= (A.C. POWER OUTPUT) - (A.C. POWER INPUT) / (D.C. INPUT POWER)

The amplifier power added efficiency is better than 20%, reaching 25% at 3.9GHz. This efficiency is comparible with commercially available power amplifiers which have efficiencies of 20-30%.

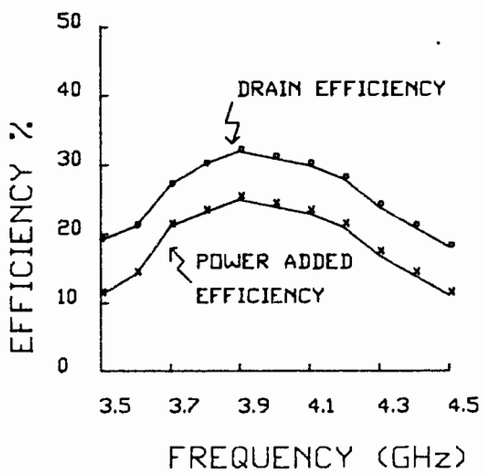

FIGURE 6.4.2: MGF2116 Power Amplifier, Drain and Power Added Efficiency versus Frequency.

Another important feature of power amplifiers is their output power versus input power curves, shown in Figure 6.4.3 for 3.7-, 4.9- and 4.2-GHz.

For comparison, the same curves are plotted for the Power Pre-Amplifier of Section 6.2.3 and are shown in Figure 6.4.4.

The distinguishing feature of the two amplifiers is that the power amplifier enters saturation quickly, i.e. the saturation knee in the above curves are sharper than those for the pre-amplifier, although this feature is not clearly defined in the following Graphs.

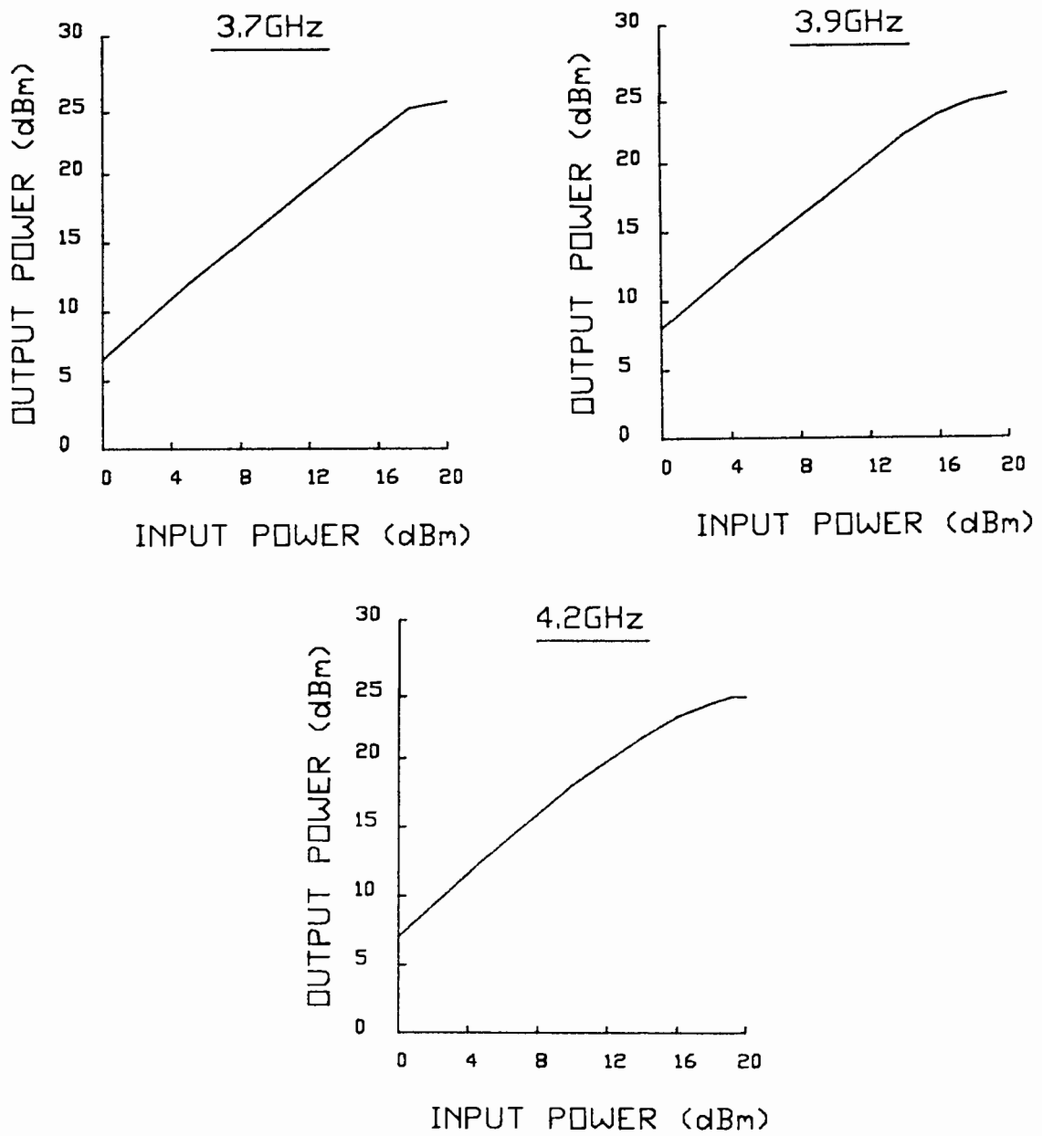

FIGURE 6.4.3: MGF2116 Power Output versus Power Input for the Power Amplifier.

This is due to the power amplifier being correctly matched for saturated operation rather than being matched for linear power operation as in the case of the pre-amplifier.

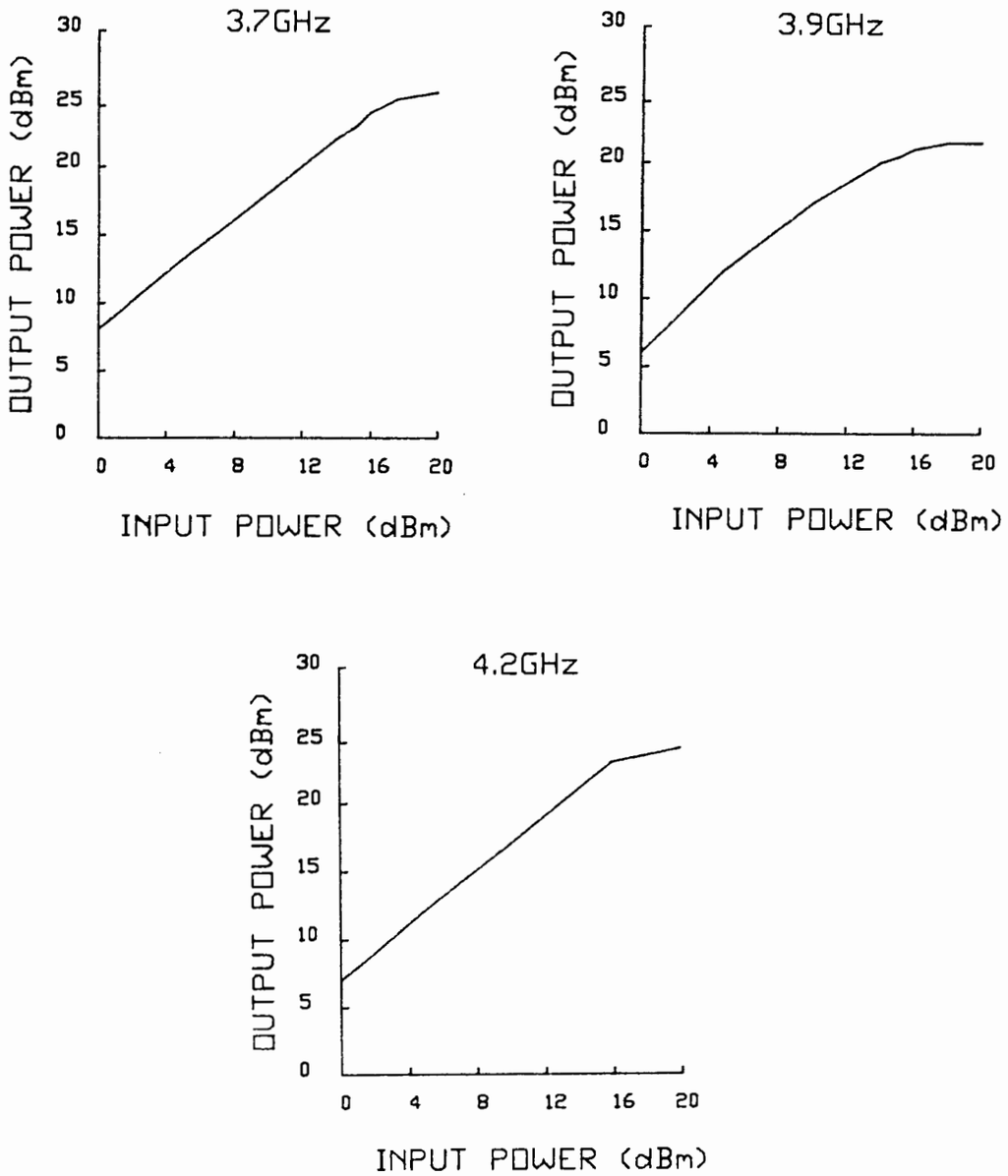

FIGURE 6.4.4: MGF2116 Power Output versus Power Input for the Power Pre-Amplifier.

The sharp knee characteristic of the power amplifier is desireable since it minimises the power output fluctuations with input power, gain, frequency, temperature and time changes over the designed bandwidth. This applies as long as the input power is above the minimum level of 100mW (i.e. the 1dB gain compression level).

From the curves of Figure 6.4.3 it can also be seen that, at 3.7-GHz the amplifier goes into saturation at a higher input power level than at 4.2GHz, i.e. at 3.7GHz and 100mW input power the amplifier is in 1dB gain compression and at 4.2GHz and 100mW input power the amplifier is in 3dB gain compression.

Ideally, the power amplifier would be required to remain in 1dB gain compression throughout the bandwidth. However, since the transistor itself would go further into saturation at lower frequencies as the gain increases, the power amplifier matching networks have over compensated in this case.
This phenomenon may be overlooked, so long as the harmonic distortion from further gain compression can be tolerated.

CHAPTER 7. CONCLUSION.

The design of Broadband Low-Noise and Power Microwave Amplifiers involved the appropriate and accurate characterisation of the Gallium Arsenide Field Effect Transistors.

In order to design a Low Noise Amplifier both the small signal s-parameters and noise parameters of the MGF1403 GaAs FET were measured over the 1- to 7- GHz frequency band. For the Power Amplifier, the MGF2116 GaAs FET's required the measurement of Source-Pull and Load-Pull data over the 3.5- to 4.5-GHz, these being the more precise of device large-signal characterisations. However, these measurements required the design and use of a small-signal pre-amplifier, in order to increase the available signal-source power. Thus, the device small-signal s-parameters were also measured.

These parameters were used to design, firstly, a maximum gain amplifier (MGF1403), a Low-Noise amplifier, a Power Amplifier and a Maximum Gain Power Pre-Amplifier using RT-Duroid 5880 microstrip softboard.

In the design process, techniques of broadband matching were investigated, with Double-Stub matching yielding the broadest bandwidth for these transistors.

The computer package - TOUCHSTONE, by EESof run on an IBM PC, was used to optimise the amplifier input and output impedance networks for the required gain, Noise-Figure, Power Output and

bandwidth, according to the type of amplifier that was being designed.

The computer optimised circuits were etched onto microstrip and tested.

Each amplifier required some fine trimming in order to peak the responses over the bandwidths.

The results of the tuned amplifiers are:

1) 10.1 ± 1.5dB Gain from 2- to 6- GHz for the Maximum Gain Amplifier.
2) Less than 5- dB Noise-Figure and 5.4 ± 1.4 dB Gain over the 2- to 6- GHz frequency band.
3) 8 ± 0.35dB Gain from 3.7- to 4.2- GHz for the Maximum Gain Power Pre-Amplifier.
4) A maximum of 390 mW Output Power from 3.7- to 4.2-GHz for the Power Amplifier.

The results compared favourably with the responses predicted by Touchstone. However, the amplifiers did require some trimming.

Thus, Touchstone is not ideal in analysing the microwave amplifier performances, but does significantly increase the design bandwidth capabilities, of Engineers, without the extra cost of numerous hardware iterations, in order to achieve these bandwidths, with manual Smith Chart designs.

The necessity of s-parameter measurements was investigated, as opposed to using the manufacturers data, for the MGF1403 Maximum Gain Amplifier.

The results of a design using the manufacturers data were recorded and compared with the design using the measured s-parameters. There were no significant shortcomings of either method, with the latter being the more precise an thus yielding slightly better results.

It was thus concluded that for the more stringent of designs the measurement of the s-parameters is a necessity, in order to maximise the design capabilities with more accurate device characterisation.

Finally, there exists a similarity in the design of the Low-Noise and Power amplifiers in that for low-noise amplifier operation, the source impedance is tuned and measured for minimum noise-figure operation of the transistor. The required source impedance is then realised in the design process.
For power amplifier design (using load pull measurements) the load impedance is tuned and measured for maximum gain, power output and efficiency and this is then realised in the design process in the same way as for the Low-Noise Amplifier.

APPENDIX A.

TRANSISTOR MINIMUM NOISE-FIGURE (NFmin) AND ITS RELATION TO THE AMPLIFIER SOURCE IMPEDANCE

The Noise Figure of an amplifying four-pole is the ratio of input to output signal-to-noise ratios:

$$F = \frac{(Signal/Noise)_{input}}{(Signal/Noise)_{output}} \qquad \ldots\ldots(A1)$$

according to the IEEE Standards on measuring noise [39].

As the input-signal and the noise are amplified by the same amount when passing through an amplifier, the significance of this formula is the noise added to the signal by the amplifier. Thus a noise-figure of unity would imply a noise free device, which is impossible to realise.

According to H. Friis [3], the overall noise-figure of a multi-stage amplifier is influenced by each stage by an extent which is inversely proportional to the gain of the first stage. This formula is given below:

$$F_T = F_1 + \frac{F_2 - 1}{G_1} + \frac{F_3 - 1}{G_1 G_2} + \ldots\ldots(A2)$$

where, F_T is the overall noise-factor, and F_i, G_i are the noise-factors and gains of the ith stages respectively.

It is commonly known that the noise-figure of a Gallium-Arsenide

Field Effect Transistor (GaAs FET) has a very distinct minimum for a source (signal source) impedance that is substantially different from the normal 50 ohm characteristic impedance, used in transmission lines. This impedance is commonly known as Z_{opt} and its implementation will give the resulting amplifier a poor input voltage standing wave ratio (VSWR), or return loss, in the general case. Thus, the curious may ask why should the minimum noise-figure occur for a source impedance that offers a poor VSWR? To understand this it is necessary to consider the noise sources of the FET and the equivalent circuit for noise analysis. It will then be possible to observe how the gate loading effects the noise power at the amplifier output.

The GaAs MESFET is a low-noise device since only majority carriers participate in its operation. However, in practical devices, extrinsic resistances are unavoidable, and the parasitic resistances are mainly responsible for the noise behaviour of the transistors.

The equivalent circuit for noise analysis is shown in Figure A1 below [40].

Noise sources i_{ng}, i_{nd}, e_{ng} and e_{ns} represent the induced gate noise, drain circuit noise, thermal noise of the gate metallisation resistance R_G, and thermal noise of the source series resistance R_S, respectively. The e_s and Z_s are the signal source voltage and source impedance. The circuit within the dashed lines corresponds to the intrinsic MESFET.

The optimum noise-figure for the GaAs FET has been obtained from

the equivalent circuit [41]:

$$F_0 = 1 + \frac{fL\sqrt{g_M (R_S + R_G)}}{4} \quad \ldots\ldots (A3)$$

where f is the operating frequency, L is gate length in mirometers, g_m is the transconductance, R_G is the gate resistance and R_S is the source resistance.

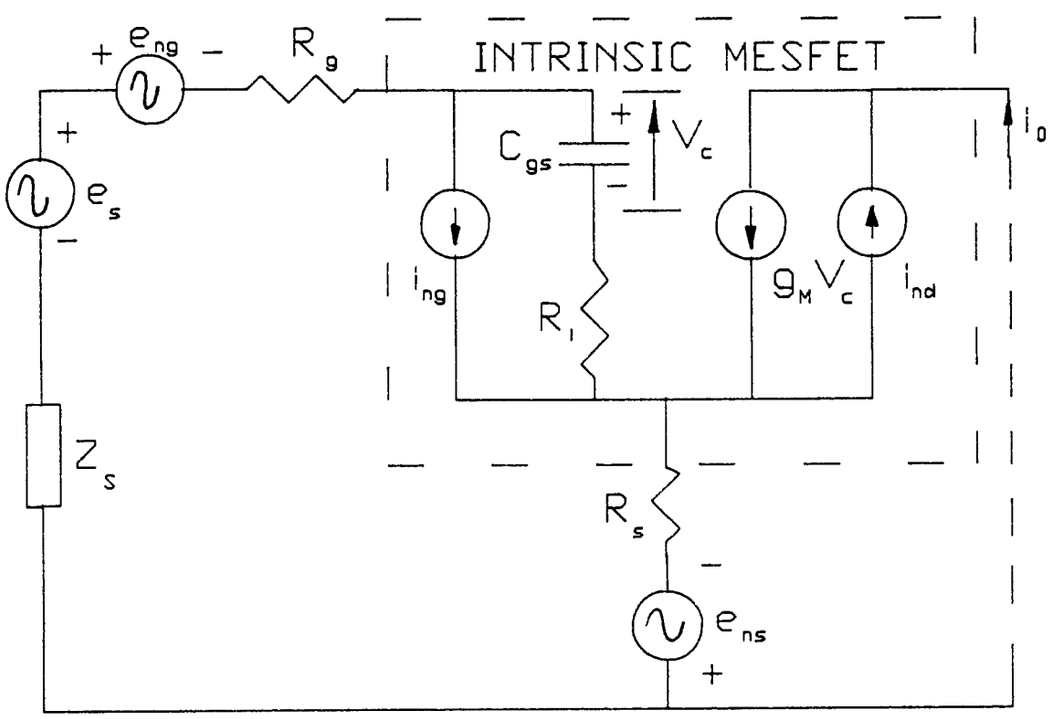

FIGURE A1: Equivalent circuit for noise analysis. (After Pucel, Haus and Statz).

Clearly, for low-noise operation, one should reduce the gate length and minimise the parasitic source and gate resistances. Note, however, that R_G and R_S are parasitics and remain unchanged in the normal operating range of conditions and that the transistor noise-figure is strongly dependant on the drain

current. However it is unnecessary to deal with the theory of this for the purposes of this dissertation as long as it is understood that this is the case [41].

This concludes the discussion on the dependance of the device noise figure on the device parasitic impedances. It now remains to investigate the dependance of the amplifier noise-figure on the source impedance. For this purpose, a more general noise analysis will be dealt with, being applicable to any noisy four-pole. This has been dealt with by a number of authors [42].
According to H. Rothe and W. Dahlke [43], noisy four-poles may be represented as a noise-free four-pole plus external noise sources.

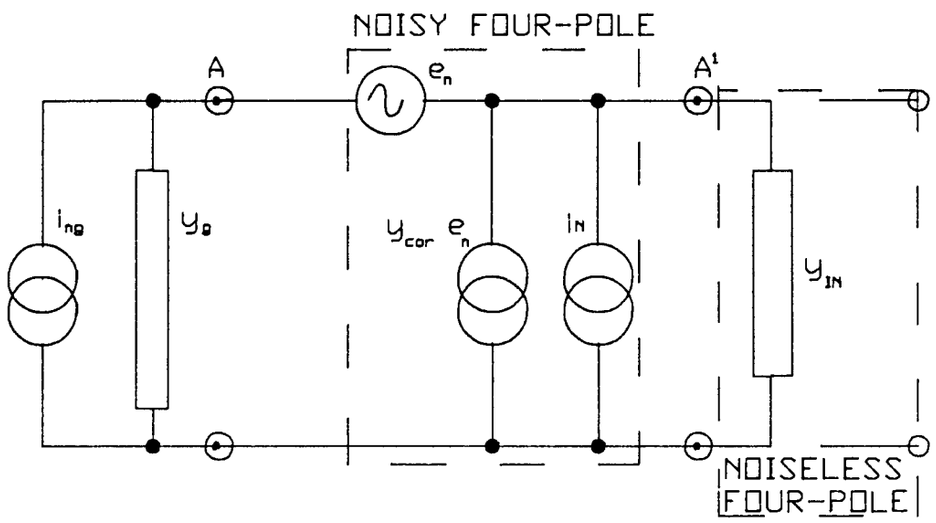

FIGURE A2: Noisy Four-pole equivalent circuit.

In this equivalent circuit, the noise generators are seperated from the remaining four-pole elements. The circuit thus consists

of two parts: the noise generators and a noiseless four-pole. The four-pole input is terminated by the generator admittance y_g which itself generates noise, taken into account by the noise generator of source current i_{ng}.

The noisy four-pole may be characterised by three noise sources, of which those having a source voltage e_n and a source current i_n are independant, while the source current of the third current generator is correlated to the voltage e_n; this is taken into account with the correlation admittance y_{cor}. This equivalent circuit can be adopted to all noisy four-poles which can be considered linear. According to the equivalent circuit, the noise-figure of the noisy four-pole is determined by adding the noise powers at the internal point A', and relating the sum of the noise power available from the generator at the input point A. Since the part following A is noise free, it has no effect on the noise-figure: furthermore, the effect of the gain is also removed by reducing the noise generator to the input. Expressing the noise power ratio between A and A' we get an expression of the noise-figure:

$$F = 1 + \frac{|\overline{i_n}|^2 + |\overline{e_n}|^2 |y_g + y_{cor}|^2}{|\overline{i_{ng}}|^2} \qquad \ldots\ldots (A4)$$

The noise power of the noise generator with source current i_{ng} is given by:

$$|\overline{i_{ng}}|^2 = 4 g_g k T \Delta F \qquad \ldots\ldots (A5)$$

[H. Friis, Noise-Figure of Radio Receivers, IRE, July 1944.]

where g_s is the real part of the generator admittance, k is the Boltzmann constant, T is the absolute temperature and delta f is the bandwidth.

Instead of noise powers the concepts of noise and noise conductance will now be used.

$$|\overline{e_n}|^2 = 4kT\Delta f R_n \qquad \ldots\ldots (A6)$$

$$|\overline{i_n}|^2 = 4kT\Delta f g_n \qquad \ldots\ldots (A7)$$

Expressing the noise figure formula given in equation A4 by quantities R_n and g_n:

$$F = 1 + \frac{g_n + R_n|y_s + y_{cor}|^2}{g_s} \qquad \ldots\ldots (A8)$$

Here the generator admittance and correlation admittance are complex quantities characterised by their real and imaginary parts, i.e. $y_s = g_s + jb_s$ and $y_{cor} = g_{cor} + jb_{cor}$.
It can be seen from equation A8 that a minimum occurs when the following condition is satisfied:

$$b_s + b_{cor} = 0 \qquad \ldots\ldots (A9)$$

This condition is called "tuned-out" noise because of the cancelling of imaginary parts. This condition does not necessarily coincide with the condition providing optimum conjugate matching for power gain, in fact, generally, there is a considerable difference between the two.

By substitution of equation A9, the noise-figure in the tuned out

condition is:

$$F_{min} = 1 + \frac{g_n + R_n (g_g + g_{cor})^2}{g_g} \qquad \ldots\ldots (A10)$$

This function may be considered to be a function of generator conductance g_g, and reaches a minimum value, F_{min}, at the conductance value $g_g = g_g^*$.

The generator conductance resulting in the lowest noise figure is determined from the equation:

$$\frac{dF}{dg_g} = 0$$

and from this:

$$g_g^* = \sqrt{\frac{g_n}{R_n} + g_{cor}^2} \qquad \ldots\ldots (A11)$$

with this value of matched generator conductance, the minimum noise figure will be:

$$F_{min}^* = 1 + 2R_n \left(\sqrt{\frac{g_n}{R_n} + g_{cor}^2} + g_{cor}\right) \qquad \ldots\ldots (A12)$$

This noise figure is an absolute minimum value when the condition of tuned out noise and noise matching are simultaneously met. The second term in equation A11 is what is expected:- the best performance calls for a matched input. However, that result is only true when the input conductance is much greater than the ratio of the source conductance g_g and the noise resistance, R_n. For FET's, with their negligible input conductances, the first term completely dominates and is determined by the

amplifier noise mechanisms. Thus the generator conductance resulting in minimum noise figure does not necessarily coincide with that for optimum power gain [44].

This source impedance required for minimum noise figure operation is commonly referred to as Z_{opt}. As mentioned before, Z_{opt} does not give an optimum impedance match and thus causes low-noise amplifiers to have a poor input VSWR.

However, there are two techniques used in overcoming this problem: the first is to precede the amplifier with an isolator and the second is to use 3-dB quadrature couplers.

The advantage, of isolators, is that only one isolator is needed per stage. However the isolators are very expensive, have limited bandwidth and the insertion loss is at best 1dB over a wide bandwidth. Lange couplers, on the other hand, have a 0.3dB insertion loss, 3dB coupling over octave bandwidths, low VSWR and as technology is advancing are becoming relatively inexpensive.

The only disadvantage, of Lange couplers, being the fact that two amplifiers per stage are required and thus extra cost per stage and current drain on the supply.

APPENDIX B.

LARGE-SIGNAL TRANSISTOR CHARACTERISATION: A Review.

In the case of power transistors operating in the saturated region of the transfer characteristics, the associated s-parameters differ greatly from the small-signal s-parameters and they are strongly dependant on the input power level. Thus there has been considerable discussion concerning appropriate characterisation methods for microwave power transistors.

Several authors have considered large-signal s-parameter characterisation of power transistors and other workers in the field have used "load-pull" techniques.

Chaffin and Leighton [45] described an experimental method for measuring large-signal s-parameters similar to that used for small-signal devices. Their experimental results showed the dependence of s-parameters on input power level and bias conditions.

Chaffin, Leighton and Webb later consolidated their work to demonstrate the applicability of large-signal s-parameters and small-signal design techniques to the design of power amplifiers. Results showed: firstly that, over a wide range of input power, with the exception of S21, the s-parameters are not a strong-function of input power. This is apparently in conflict with what Chaffin and Leighton found. Secondly, that measured s-

parameters are a function of measurement conditions and thus must be measured under conditions approximating those of the intended amplifier. Thirdly, best agreement between theoretical and experimental amplifier performance occurs when s-parameter measurements are made with the same average d.c. current flow through the device as that expected in the intended amplifier. Finally, that the least accurately known s-parameters are S12 and S22 [46].

Mazumder and van der Puije [47] realised the problems encountered and developed a new and simple method, called the "two-signal" method of measuring the s-parameters of transistors. Their results showed that their method predicted the performance of the power amplifier with greater accuracy than that used by Leighton et al. The apparent advantage lay in the fact that the parameters S12 and S22 are measured with the transistor drawing appreciable current, resulting in a more realistic measurement.

In spite of the apparent success of measuring large-signal s-parameters and their subsequent use in the design of power amplifiers using small-signal design methods, some workers in the field [48] are of the opinion that the use of s-parameter characterisation to describe large-signal characteristics of power transistors is generally inadequate. It is argued that while s-parameter characterisation is excellent for assuring stability and level power gain in broadband designs, there are no meaningful means for s-parameter consideration of the two vital large-signal design factors: saturated output power capability and collector efficiency. These two factors are a function of the

load line impedance. It has also been argued that the use of s-parameters is generally invalidated by the constraint of a fixed normalisation constant, usually equal to 50 ohms. Large-signal measurements performed using equipment designed with fixed terminations lead to data which can be accurately interpreted only with respect to those terminations, because the large-signal characteristics of the device under test are functions of the load impedance.

Another approach of characterisation at large-signal levels involves the use of "load-pull" measurements. The load-pull measurement method consists of operating a transistor at some specific drive power, collector supply voltage and frequency while monitoring the output power, d.c. collector current and stability as a function of collector load-line impedance. These measurements produce a closed constant-output-power contour on a Smith Chart from which all possible load impedances pertaining to that contour can be read.

A drawback of this method however, is that measurements are usually manually made using stub-tuners for presenting the range of load impedances desired. This procedure is time consuming for thorough characterisation which may require some 10-30 collector impedances for each contour and this only at one frequency! This technique continues to find favour in the large-signal characterisation of microwave transistors. Since 1972, when a 1-2GHz 10W linear amplifier was reported [49], a number of papers have been published on "load-pull" measurement techniques for the large-signal characterisation of microwave power transistors [50].

APPENDIX C

TRANSISTOR DATA SHEETS.

A). MGF1403 GaAs Low-Noise Field Effect Transistor.

B). MGF2116 GaAs Power Field Effect Transistor.

MITSUBISHI SEMICONDUCTOR <GaAs FET>

MGF1403 (2SK276)

FOR MICROWAVE LOW-NOISE AMPLIFIERS
N-CHANNEL SCHOTTKY BARRIER GATE TYPE

DESCRIPTION

The MGF1403 (2SK276) low-noise GaAs FET with an N-channel Schottky gate is designed for use in S- to Ku-band amplifiers. The hermetically sealed metal-ceramic package assures minimum parasitic losses, and has a configuration suitable for microstrip circuits.

FEATURES

- High maximum frequency of oscillation f_{max} = 90 GHz (TYP.)
- Low noise figure NF = 1.8 dB (TYP.) @f = 12 GHz
- High associated gain Gs = 10.5 dB (TYP.) @f = 12 GHz
- High reliability and stability

APPLICATION

S- to Ku-band low-noise amplifiers.

OUTLINE DRAWING

Unit: millimeters (inches)

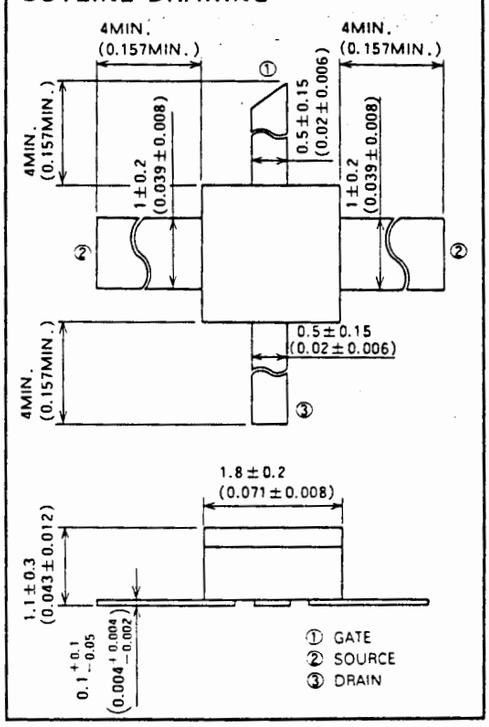

ABSOLUTE MAXIMUM RATINGS (Ta = 25°C)

Symbol	Parameter	Limits	Unit
V_{GDO}	Gate to drain voltage	−6	V
V_{GSO}	Gate to source voltage	−6	V
I_D	Drain current	80	mA
P_T	Total power dissipation	200	mW
Tch	Channel temperature	150	°C
Tstg	Storage temperature	−55 ~ +150	°C

ELECTRICAL CHARACTERISTICS (Ta = 25°C)

Symbol	Parameter	Conditions		Limits Min	Limits Typ	Limits Max	Unit
$V_{(BR)GDO}$	Gate to drain breakdown voltage	I_G = −100μA		−6			V
$V_{(BR)GSO}$	Gate to source breakdown voltage	I_G = −100μA		−6			V
I_{GSS}	Gate to source leakage current	V_{GS} = −3V, V_{DS} = 0V				10	μA
I_{DSS}	Saturated drain current	V_{GS} = 0V, V_{DS} = 3V		15	40	80	mA
$V_{GS(off)}$	Gate to source cut-off voltage	V_{DS} = 3V, I_D = 100μA		−0.3		−3.5	V
g_m	Transconductance	V_{DS} = 3V, I_D = 10mA		20	40		ms
Gs	Associated gain	V_{DS} = 3V, I_D = 10mA	f = 4 GHz		14		dB
			f = 8 GHz		12		
			f = 12GHz	8	10.5		
NFmin	Minimum noise figure	V_{DS} = 3V, I_D = 10mA	f = 4 GHz		0.8		dB
			f = 8 GHz		1.3		
			f = 12GHz		1.8	2.3	
MAG	Maximum available gain	V_{DS} = 3V, I_D = 30mA	f = 4 GHz		19		dB
			f = 8 GHz		16		
			f = 12GHz		14		
fmax	Maximum frequency of oscillation	V_{DS} = 3V, I_D = 30mA			90		GHz

MGF1403 (2SK276)

FOR MICROWAVE LOW-NOISE AMPLIFIERS
N-CHANNEL SCHOTTKY BARRIER GATE TYPE

TYPICAL CHARACTERISTICS

I_D vs. V_{DS}

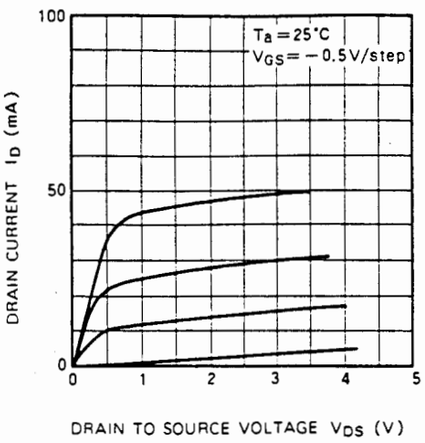

MSG, MAG, U & K vs. f

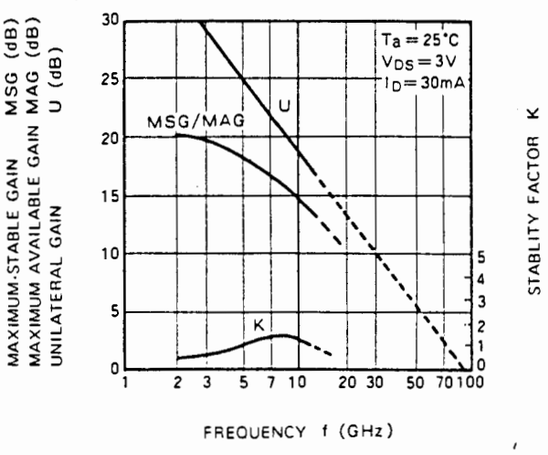

NF_{min} & Gs vs. f

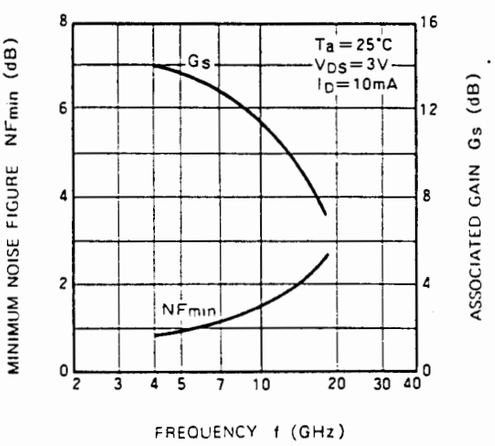

NF & Gs vs. I_D (f = 4 GHz)

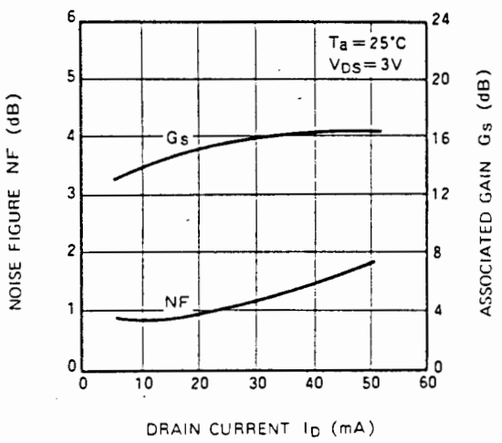

NF & Gs vs. I_D (f = 8 GHz)

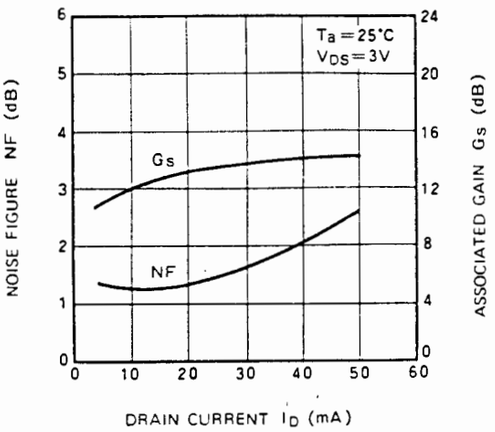

NF & Gs vs. I_D (f = 12 GHz)

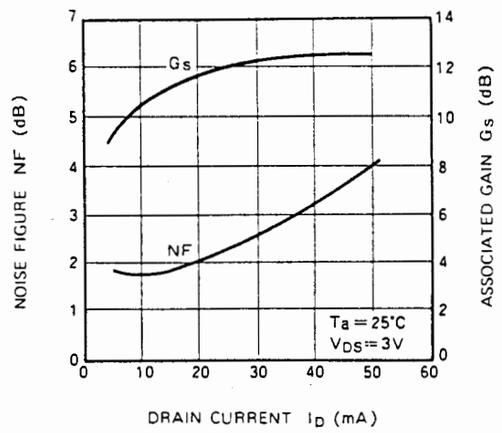

MGF1403 (2SK276)

FOR MICROWAVE LOW-NOISE AMPLIFIERS
N-CHANNEL SCHOTTKY BARRIER GATE TYPE

NF & Gs vs. I_D (f = 18 GHz)

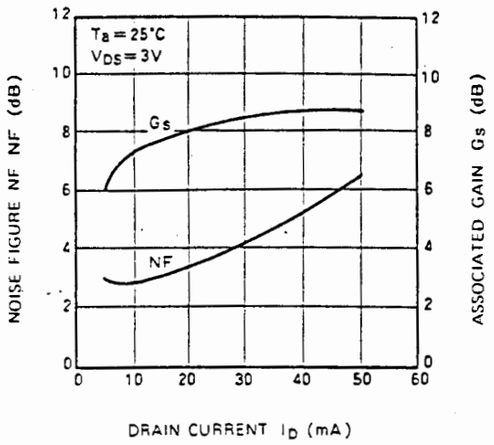

S_{11}, S_{22} vs. f

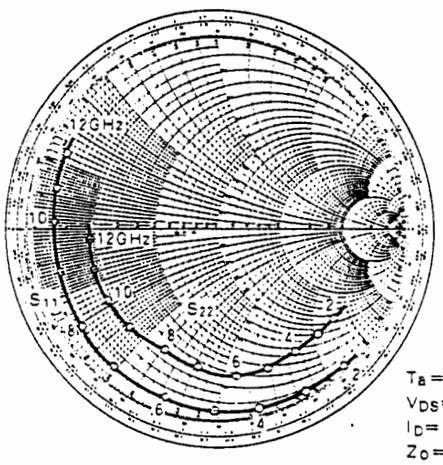

S_{12}, S_{21} vs. f

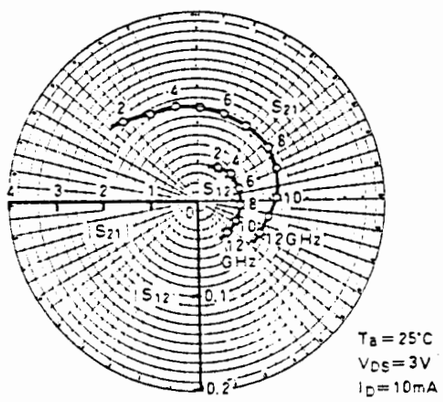

S_{11}, S_{22} vs. f

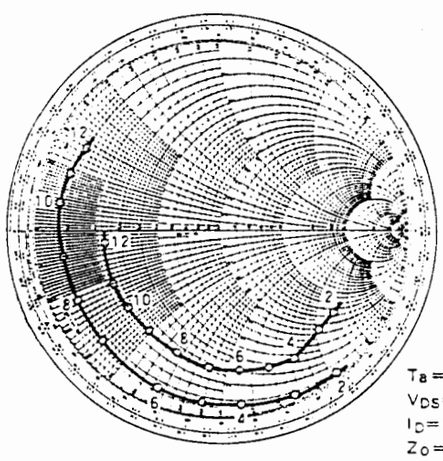

S_{12}, S_{21} vs. f

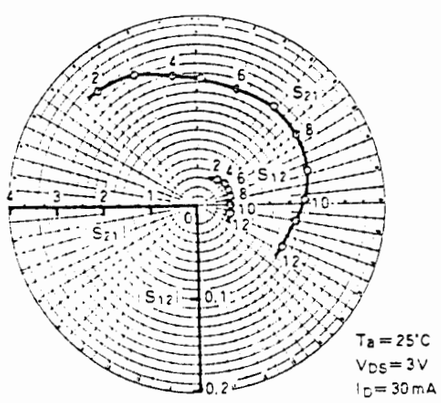

MITSUBISHI ELECTRIC

S PARAMETERS (T_a=25°C, V_{DS}=3V)

I_D (mA)	f (GHz)	S Parameters (TYP.)							
		S_{11}		S_{12}		S_{21}		S_{22}	
		Magn.	Angle (deg.)	Magn.	Angle (deg.)	Magn.	Angle (deg.)	Magn.	Angle (deg.)
10	2	0.977	− 47.3	0.040	50.1	2.239	133.3	0.767	− 38.2
	4	0.966	− 77.5	0.044	32.9	2.018	102.9	0.772	− 58.9
	6	0.933	−108.3	0.046	15.5	1.928	72.3	0.767	− 84.5
	8	0.912	−145.2	0.047	− 6.8	1.862	39.2	0.700	−115.3
	10	0.891	178.8	0.046	−25.2	1.641	1.6	0.692	−148.6
	12	0.881	155.3	0.045	−45.1	1.462	−28.3	0.700	−177.5

I_D (mA)	f (GHz)	S Parameters (TYP.)							
		S_{11}		S_{12}		S_{21}		S_{22}	
		Magn.	Angle (deg.)	Magn.	Angle (deg.)	Magn.	Angle (deg.)	Magn.	Angle (deg.)
30	2	0.972	− 50.1	0.034	50.1	3.199	132.7	0.724	− 37.7
	4	0.933	− 81.3	0.037	36.5	2.851	101.3	0.741	− 56.9
	6	0.891	−115.3	0.038	23.2	2.692	71.2	0.724	− 81.6
	8	0.861	−154.2	0.036	10.9	2.570	39.9	0.676	−111.3
	10	0.841	173.5	0.035	− 3.6	2.291	2.3	0.653	−141.8
	12	0.841	148.3	0.035	−15.1	1.820	−26.5	0.653	−173.4

I_D (mA)	f (GHz)	S Parameters (TYP.)							
		S_{11}		S_{12}		S_{21}		S_{22}	
		Magn.	Angle (deg.)	Magn.	Angle (deg.)	Magn.	Angle (deg.)	Magn.	Angle (deg.)
50	2	0.972	− 52.5	0.030	50.6	3.548	131.0	0.716	− 36.8
	4	0.923	− 83.1	0.032	42.4	3.090	101.3	0.724	− 55.2
	6	0.881	−120.2	0.032	34.0	2.884	71.5	0.708	− 79.0
	8	0.841	−157.4	0.033	25.3	2.692	39.2	0.668	−108.2
	10	0.822	170.4	0.034	16.3	2.317	2.2	0.646	−138.0
	12	0.832	144.8	0.033	10.4	1.905	−25.7	0.638	−168.6

QUALITY GRADE: INDUSTRIAL GRADE (I.G)

TYPICAL CHARACTERISTICS

MSG, MAG, U & K vs. f

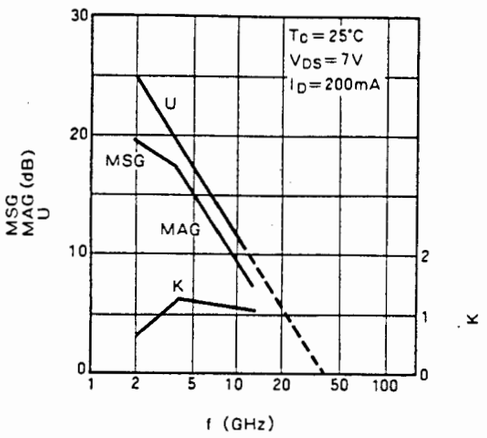

P_o η_{add} vs. P_{in}

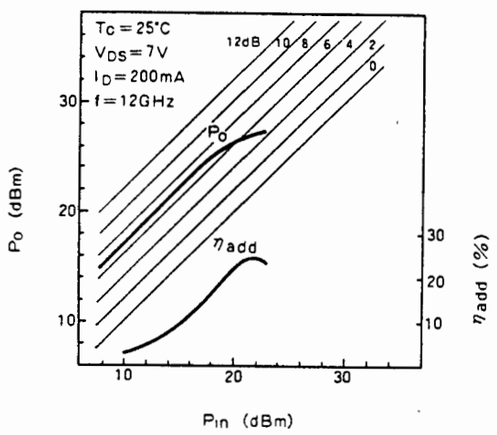

S_{11}, S_{22} vs. f

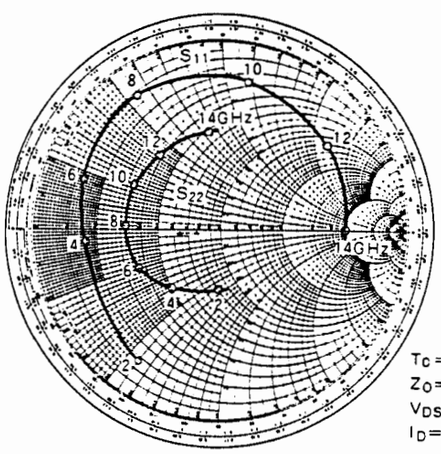

S_{12}, S_{21} vs. f

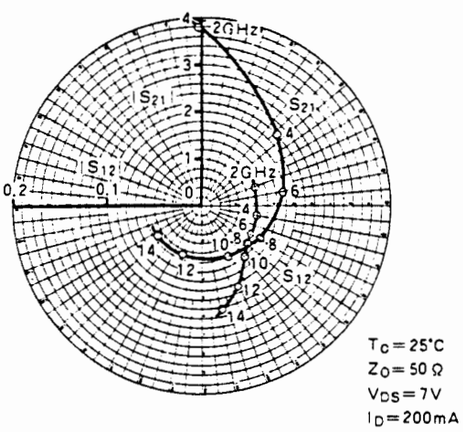

S PARAMETERS (T_C = 25°C, V_{DS} = 7V, I_D = 200mA)

f (GHz)	S Parameters (typ.)							
	S_{11}		S_{12}		S_{21}		S_{22}	
	Magn.	Angle (deg.)	Magn.	Angle (deg.)	Magn.	Angle (deg.)	Magn.	Angle (deg.)
2	0.812	−121.4	0.059	19.1	3.78	91.3	0.340	−93.0
4	0.739	−172.8	0.055	−12.5	2.12	43.0	0.414	−130.3
6	0.776	160.7	0.061	−30.9	1.73	10.1	0.498	−153.6
8	0.823	122.2	0.068	−42.5	1.48	−29.8	0.523	179.1
10	0.798	80.0	0.078	−52.1	1.26	−63.4	0.520	154.1
12	0.731	37.2	0.096	−66.9	1.15	−109.3	0.519	129.7
14	0.667	−0.4	0.113	−79.2	1.13	−146.8	0.532	98.9

APPENDIX D

GRAPHS BY WHEELER FOR MICROSTRIP APPROXIMATIONS.

MICROSTRIP CHARACTERISTIC IMPEDANCE CALCULATED FROM WORK OF WHEELER

WIDE STRIP APPROXIMATION (W/H > .1)

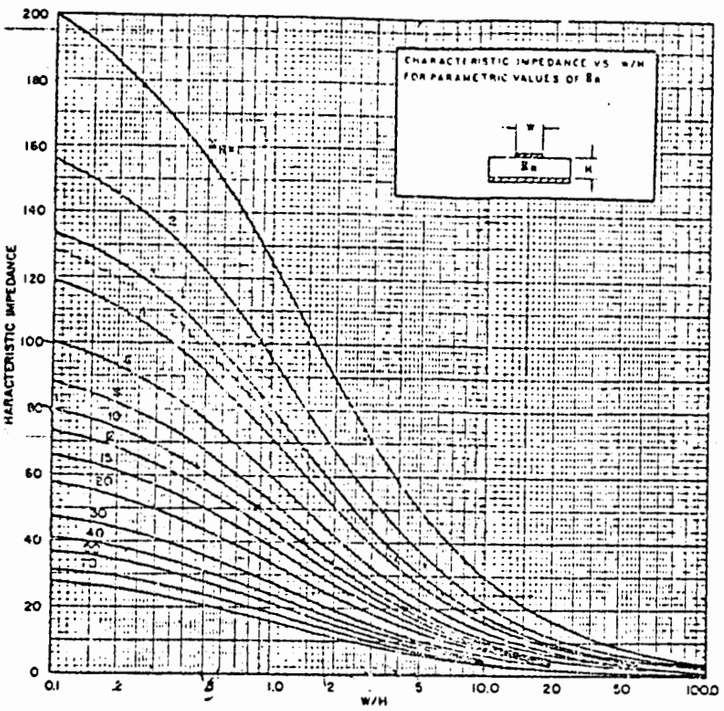

NARROW STRIP APPROXIMATION (W/H < 1.0)

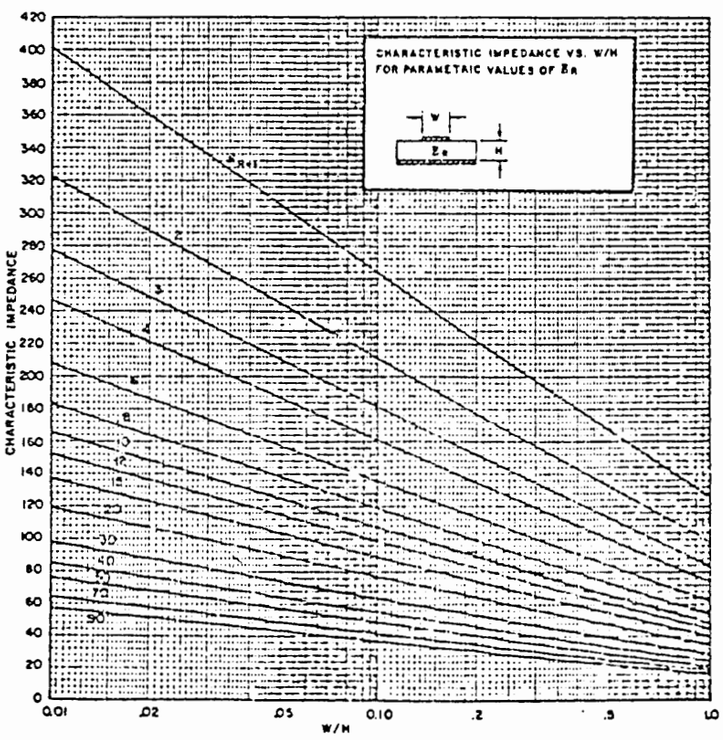

Courtesy of Burke, Gelnovatch and Chase after Wheeler

RATIO OF FREE SPACE WAVELENGTH (λ_o) TO MICROSTRIP WAVELENGTH (λ_m) CALCULATED FROM WORK OF WHEELER

WIDE STRIP APPROXIMATION ($W/H > .1$)

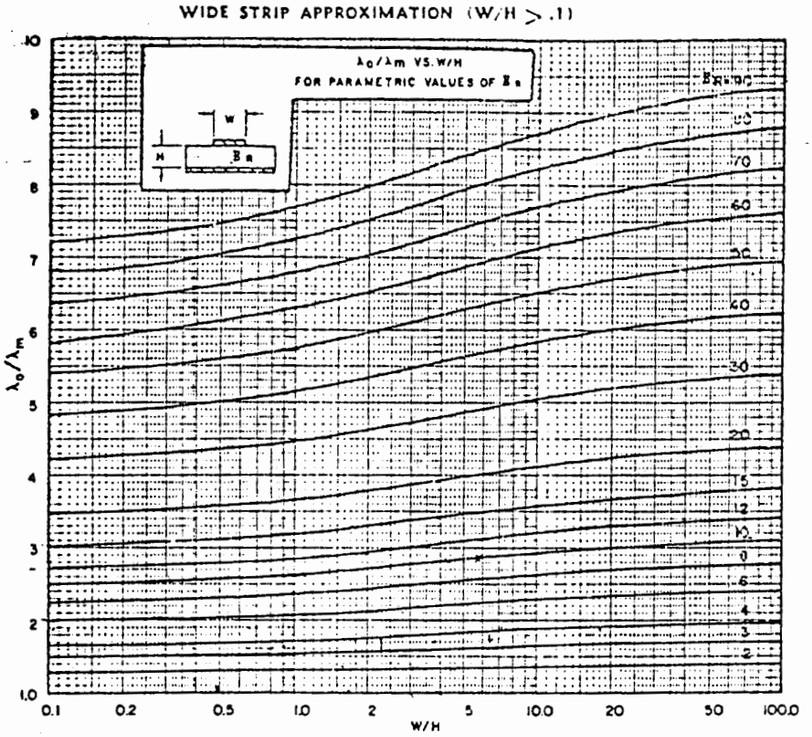

NARROW STRIP APPROXIMATION ($W/H < 1.0$)

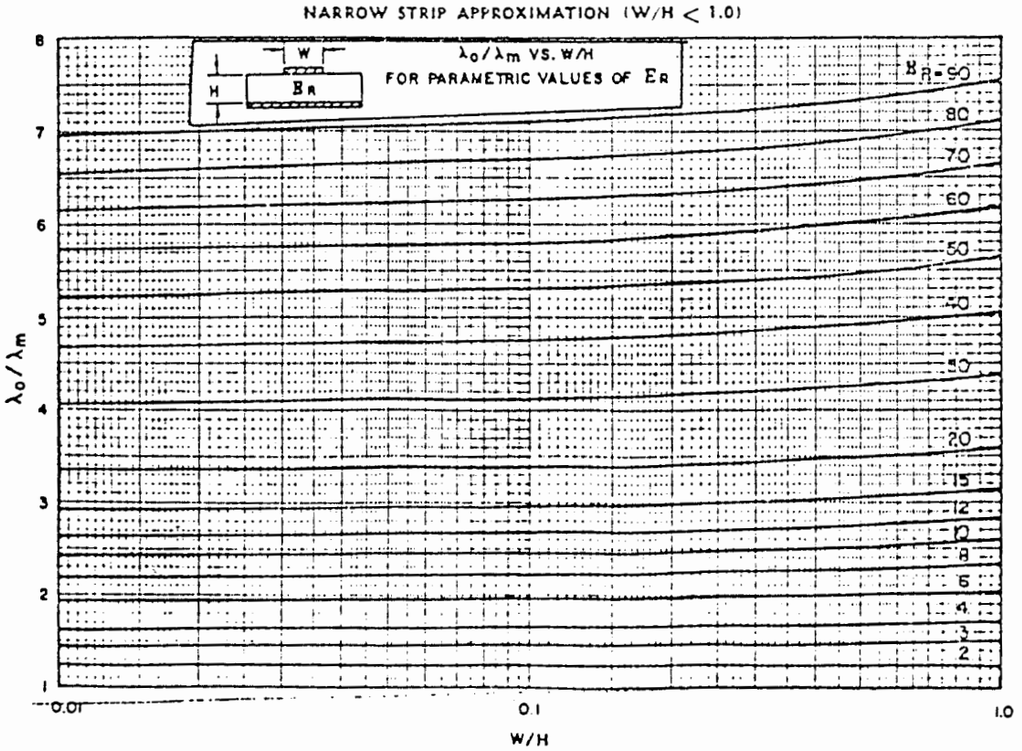

Courtesy of Burke, Gelnovatch and Chase after Wheeler

REFERENCES

[1]. Electronic Fundamentals and Applications, 3rd edition, J.D. Ryder, Sir Isaac Pitman and Sons Ltd., London, 1964.

[2]. B.J. Downing, Private Communication, The University of Cape Town.

[3]. H.T. Friis, "Noise Figure of Radio Recievers", Proc. of IRE, July 1944, pp. 419-422.

[4]. Daglish, Armstrong, Walling and Foxell, "Low-Noise Microwave Amplifiers", Cambridge University Press, 1968.

[5]. S. Okwit, "An Historical view of the evolution of Low-Noise Concepts and Techniques", IEEE Trans. MTT, Vol. MTT-32, No. 9, Sept. 1984, pp. 1068-1082.

[6]. P.D. Strum, "A note on Noise Temperature", IRE Trans. on MTT, Vol. MTT-4, No. 3, pp. 145-151, July 1956.

[7]. "Microwave Tubes and Semi-conductor Devices", G.D. Sims and I.M. Stephenson, Blackie and Son Limited, Glasgow, 1963.

[8]. J. Goel, " A K-band GaAs FET Amplifier with 8.2W output Power", IEEE Trans. on MTT, Vol. MTT-32, No. 3, March 1984.

[9]. T.C. Cheng, "8GHz, 10W Solid-State Power amplifier for microwave digital radio", Electronic Letters, 31st. Jan. 1985, Vol. 21, No. 3.

[10]. Y. Mitsui, M.Kobiki, M.Wataze, K. Segawa, M. Otsubu, T. Ishii, "10-GHz 10W internally matched GaAs Power FET's", IEEE Trans. on MTT, Vol. MTT-29, No. 4, April 1981.

[11]. D. McQuiddy Jr., J.W. Wassel, J. LaGrange, W. Wisseman, "Monolithic Microwave Integrated Circuits : An Historical Perspective", IEEE Trans. on MTT, Vol. MTT-32, No. 9, Sept. 1984.

[12]. J.S. Kilby, "Invention of the Integrated circuits", IEEE Trans. on Electron Devices, Vol. Ed-23, No. 7, pp. 648-654, July 1976.

[13]. W. Shockley, "The Path to the conception of the Bipolar Junction Transistor", IEEE Trans. on Electron Devices, Vol. Ed-23, 1976, July, pp 597-620.

[14]. J. Archer, "Low-Noise implanted-base microwave transistors", Solid-State Electron, Vol. 17, pp. 387-393, April 1974.

[15]. "Solid-State : An old timer comes of age", Joel. M. Cohen, Electronics, Feb. 19, 1968, p120.

[16]. C.A. Liechti, "Microwave Field-Effect Transistor 1976", IEEE Trans. on MTT, Vol. MTT-24, No. 6, June 1976.

[17]. H.J. Whelker, "Discovery and Development of III-V compounds", IEEE Trans. on Electron Devices, Vol. Ed-23, No. 7, July 1976.

[18]. "TRANSISTORS : A Chapter ends - but the story continues", Electronics, Feb. 19, 1968, p 126.

[19]. C.A. Mead, "Schottky-Barrier Gate Field-Effect Transistor", Proc. IEEE, Vol. 54, pp307-308, Feb. 1966.

[20]. W.W. Hooper and W.I. Lehrer, " An epitaxial GaAs Field-Effect Transistor", Proc. IEEE, Vol. 55, pp. 1237-1238, July 1967.

[21]. K.E. Drangeid, R. Sommerholder and W. Walker, "High-Speed Gallium-Arsenide Schottky-Barrier Field-Effect Transistor", Electronic Letters, Vol. 6, pp. 228-229, April 1970.

[22]. W. Baechtold, "X- and Ku-band amplifier with GaAs Schottky- Barrier FETs", in 1972 ISSCC Dig. Tech. Papers, Feb. 1972, pp. 156-157.

[23]. P.C. Chao et al. , "Quarter-micron gate length microwave high mobility transistor", Electronic Letters, 13 Oct. 1983, Vol. 19, No. 21, pp. 894-895.

[24]. J.V. DiLorenzo and W.R. Wisseman", GaAs Power MESFET's : Design, Fabrication, and Performance", IEEE Trans. on MTT, Vol. MTT-27, No. 5, May 1979.

[25]. H. Howe, Jr., "Microwave Integrated Circuits - An Historical Perspective", IEEE Trans. on MTT, Vol MTT-32, No. 9, Sept. 1984.

[26]. R.M. Barret, "Microwave Printed Circuits - The Early Years", IEEE Trans. on MTT, Vol MTT-32, No. 9, Sept. 1984, p983.

[27]. H.A. Wheeler, " Transmission line properties of a strip on a dielectric sheet on a plane", IEEE Trans., Vol MTT-25, No. 8, Aug. 1977, pp. 631-647.

[28]. J. Lange, "Interdigitated stripline Quadrature Hybrid", IEEE Trans. on MTT, Dec. 1969, pp 1150-1151.

[29]. R.S. Pengelly, "Application of Feedback Techniques to the realisation of Hybrid and Monolithic broadband Low-Noise- and Power GaAs FET Amplifiers", Electronic Letters, 15th Oct. 1981, Vol 17, No. 21.

[30]. R.S. Engelbrecht and K. Kurokawa, "A Wide-band Low-noise L- band Balanced Transistor Amplifier", Proc. IEEE, Vol. 53, pp 237-247, March 1965.

[31]. R.S. Pengelly, "Cryogenic 2-4GHz FET Amplifier", Electronic Letters, 11th Sept. 1980, Vol. 16, No. 19, p 730.

[32]. " " , "Broadband Lumped Element X-band GaAs FET amplifier", Electronic Letters, 6th Feb. 1975, Vol. 11, No. 3.

[33]. G.P. Bava, V. Pisani, V. Pozzolo, " 'Source-Pull' technique at microwave frequencies", Electronics letters, 16th Feb 1984, Vol. 20, No. 4, p.152.

[34]. D. Hirson, "Broadband Pin-Diode Switching and Phase Shifting", M.Sc. Thesis, June 1986, The University of Cape Town.

[35]. J.L. Hutchings, "The Development of a Class-C Solid-State L-Band Power Amplifier", M.Sc. Thesis, Nov. 1985, The University of the Witwatersrand.

[36]. S.Y. Liao, Microwave Devices and Circuits, Prentice-Hall, Inc., New Jersey, 1980.

[37]. H.A. Wheeler, Transmission Line Properties of a Strip on a Dielectric Sheet on a Plane, IEEE Trans. MTT, Vol. MTT-25, No. 8, Aug. 1977.

[38]. S-Parameter Design, HP Aplication Note 154, April 1972.

[39]. IRE standards on Methods of Measuring Noise in Linear Two-ports, 1959, Proc. IRE, 48, 1 (Jan. 1960), pp. 60-68.)

[40]. R.A. Pucel, H.A. Haus and H. Statz, Signal and Noise properties of GaAs MIC FET's, in L. Martin Ed, Advances in Electronics and Electron Physics, vol. 38, Academic, NY, 1975, p195.

[41]. H. Fukui, Optimal Noise-Figure of Microwave GaAs MESFET's, IEEE Trans. on Electron Devices, vol. Ed-26, No. 7 , July 1979.

[42]. J.M. Feldman, The Physics and Circuit properties of Transistors, John Wiley and Sons, Inc. New York, 1972.

- F. Kovacs, High-Frequency Application of Semi-conductor Devices, Elsevier Scientific publishing company, New York, 1981.

[43]. H. Rothe and W. Dahlke, "Theory of Noisy Fourpoles", Proc. IRE, 1956, p. 811.

[44]. J.M. Feldman, The Physics and Circuit Properties of TRANSISTORS, John Wiley and Sons, Inc. New York, 1972.

[45]. Chaffin, R.J. and Leighton, W.H., Large-signal S-parameter characterisation of UHF power transistors, 1973 IEEE G-MTT International Symposium on Microwaves, University of Colorado, June 1973, pp. 155 - 157.

[46]. Leighton, W H, Chaffin, R J and Webb, S G, RF amplifier design with large-signal S-parameters IEEE trans. MTT, vol MTT-21, No 12, Dec 1973, pp 309 - 814.

[47]. Mazumder, S R and van der Puije, P D, Two signal method of measuring the large-signal S-parameters of transistors, IEEE Trans. MTT, vol MTT-26, No 6, June 1978, pp 417 - 420.

[48]. Cusack, J.M. et al, Automatic load contour mapping for microwave power transistors, IEEE Trans. MTT, vol. MTT-22, 1974, pp. 660-668.

[49]. Presser, A., Belohoubek, E.F., 1-2GHz high power linear transistor amplifier, RCA Review, vol. 33, Dec. 1972, pp. 737-751.

[50]. Takayama, Y., A new load-pull characterisation method for microwave power transistors, 1976 Digest, IEEE MTT-S, International microwave symposium, pp. 218-220.

- Poulin, D., Load-pull measurements help you meet your match, Microwaves, Nov. 1980, pp. 61-65.

- Bava, G.P., Pisani, U. and Pozzolo, V., Active load technique for load-pull characterisation at microwave frequencies, Electronic Letters, vol. 18, 1982, pp. 178-180.

- Bradley, P.D. and Tucker, R.S., Computer corrected load-pull characterisation of power MESFET's, 1983 Digest, IEEE MTT-Symposium, pp. 224-226.]